

Prepared for:

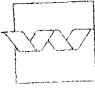

Commission of the European Communities, MAST-OPTICREST
Rijkswaterstaat, Dienst Weg- en Waterbouwkunde

Physical model investigations on coastal structures with shallow foreshores

AFGEHANDELD

2D model tests on the Petten Sea-defence

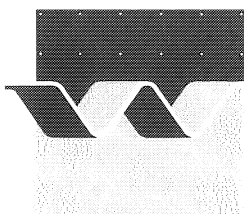
July 1999

	bibliotheek postbus 177 - 2600 MH Delft waterloopkundig laboratorium/WL
BB	68150
WL	#3129
EXPL	 R0007159

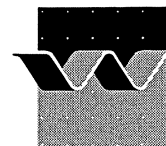
Physical model investigations on coastal structures with shallow foreshores

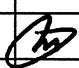
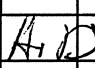

2D model tests on the Petten Sea-defence

M.R.A. van Gent



wl | delft hydraulics



CLIENTS:		Commission of the European Communities; MAST-OPTICREST (MAS3-CT97-0116), Rijkswaterstaat, Dienst Weg- en Waterbouwkunde, WL DELFT HYDRAULICS					
TITLE:		Physical model investigations on coastal structures with shallow foreshores; 2D-model tests on the Petten Sea-defence					
ABSTRACT:		Within the framework of the European MAST-OPTICREST project prototype measurements and physical model investigations have been performed. This report describes the test results of two-dimensional physical model investigations on the Petten Sea-defence ("Pettemer Zeewering"). This site is of special interest since the complex shallow foreshore affects the waves considerably before they reach the toe of the dike. The physical model tests have been performed with a schematised bar in front of the dike. Wave propagation over the shallow foreshore and the resulting wave run-up on the dike were the main topics of these investigations.					
REV.	ORIGINATOR	DATE	REMARKS	REVIEW	APPROVED BY		
0	M.R.A. van Gent	April 1999	Preliminary	G.M. Smith	W.M.K. Tilmans		
1	M.R.A. van Gent 	July 1999	Final	A.R. v. Dongeren 	W.M.K. Tilmans 		
KEYWORDS					STATUS		
Prototype measurements Model tests Wave run-up Dikes Shallow foreshores					<input type="checkbox"/> PRELIMINARY <input type="checkbox"/> DRAFT <input checked="" type="checkbox"/> FINAL		
PROJECT IDENTIFICATION: H3129							

List of Tables

In text:

1. Measured storms in prototype (MP3).
2. Variation of wave height (low water level; constant wave steepness).
3. Variation of wave height (high water level; constant wave steepness).
4. Variation of wave steepness (low water level).
5. Variation of wave steepness (high water level).
6. Variation of wave steepness (high water level; high waves).
7. Variation of water level.
8. Variation of spectral shapes (double-peaked; low water level).
9. Variation of spectral shapes (double-peaked; high water level).
10. Tests for validation of numerical models (regular waves).
11. Comparison between prototype measurements and physical model tests.
12. Influence of using different characteristic wave heights.
13. Influence of using different characteristic wave periods.
14. Influence of using different methods for the characteristic slopes.
15. Examples of wave conditions at the toe of the dike which are expected to lead to wave run-up levels higher than the crest.

In Appendix Tables:

- | | |
|-----|--|
| A1 | Measured wave conditions and wave run-up levels (Tests 1.01-1.06). |
| A2 | Measured wave conditions and wave run-up levels (Tests 2.11-2.15). |
| A3 | Measured wave conditions and wave run-up levels (Tests 2.21-2.24). |
| A4 | Measured wave conditions and wave run-up levels (Tests 2.31-2.34). |
| A5 | Measured wave conditions and wave run-up levels (Tests 2.41-2.44). |
| A6 | Measured wave conditions and wave run-up levels (Tests 2.51-2.54). |
| A7 | Measured wave conditions and wave run-up levels (Tests 2.61-2.65). |
| A8 | Measured wave conditions and wave run-up levels (Tests 2.71-2.73). |
| A9 | Measured wave conditions and wave run-up levels (Tests 2.81-2.83). |
| A10 | Measured wave conditions and wave run-up levels (Tests 3.91-3.94). |

List of Figures

In text:

1. Measured foreshore perpendicular to the Petten Sea-defence.
2. Schematised foreshore for model tests.
3. Model set-up (foreshore).
4. Model set-up (structure).
5. Characteristic slope, used for analysis.
6. Wave energy spectra measured in prototype.
7. Double-peaked wave energy spectra.
8. Comparison between wave energy spectra in prototype and in model tests.
9. Comparison between wave run-up levels measured in prototype and in model tests.
10. Measured 2% wave run-up levels as function of wave height at deep water.
11. Measured 2% wave run-up levels as function of water depth at the toe.
12. Measured 2% wave run-up levels as function of wave steepness at deep water.
13. Measured 2% wave run-up levels as function of surf-similarity parameter based on the peak wave period T_p .
14. Measured 2% wave run-up levels as function of surf-similarity parameter based on the wave period T_m .
15. Measured 2% wave run-up levels as function of surf-similarity parameter based on the wave period $T_{m-1,0}$.
16. Surface elevations on the slope, Tests 3.91-3.94.
17. Measured wave height exceedance curves.
18. Computed wave height exceedance curves.
19. Comparison between measured and computed wave heights ($H_{2\%}$).
20. Comparison between measured and computed wave run-up levels with Equation 6 (based on De Waal and Van der Meer, 1992).
21. Comparison between measured and computed wave run-up levels, using Equation 6 but with the wave steepness s_p at the toe.
22. Comparison between measured and computed wave run-up levels, using the present calibration of Equation 7 (based on Van Gent, 1999).

In Appendix Figures:

- Fxx Measured total wave energy spectra, incident wave energy spectra and wave height evolution (xx denotes the number of the test).

List of Symbols

Roman letters:

B	:	berm width (m)
d	:	water depth during still-water (m)
g	:	gravitational acceleration (m/s^2)
H_{m0}	:	spectral “significant wave height”, $H_{m0} = 4\sqrt{m_0}$ (m)
H_{m0-T}	:	total spectral “significant wave height”, including reflected waves (m)
H_N	:	wave height with an exceedance probability of $1/N$ (m)
H_{rms}	:	root-mean-square wave height (m)
H_s	:	significant wave height (m)
H_{s-T}	:	total significant wave height, including reflected waves (m)
H_{s0}	:	significant wave height in deep water (m)
K_R	:	reflection coefficient, based on spectral analysis (-)
m_n	:	n^{th} moment of the frequency spectrum.
m_0	:	variance of the water surface elevation, i.e. the total wave energy (m^2)
N_w	:	number of waves (-)
S	:	energy density (m^2/Hz)
s_m	:	wave steepness based on the mean wave period, $s_m = 2\pi/g \cdot H_s/T_m^2$ (-)
s_{op}	:	wave steepness based on H_s at the toe and T_p in deep water (-)
s_p	:	wave steepness based on the peak wave period, $s_p = 2\pi/g \cdot H_s/T_p^2$ (-)
s_{-1}	:	wave steepness based on a spectral wave period, $s_{-1} = 2\pi/g \cdot H_s/T_{m-1,0}^2$ (-)
T_m	:	mean wave period (s)
$T_{m0,1}$:	wave period based on zero th and first spectral moment (s)
$T_{m-1,0}$:	wave period based on zero th and first negative spectral moment (s)
T_p	:	peak wave period, defined as the wave period in an arbitrary wave energy spectrum where the spectral density has a global maximum (s)
$T_{p(1)}$:	wave period of the first peak in a double-peaked spectrum (s)
$T_{p(2)}$:	wave period of the second peak in a double-peaked spectrum (s)
x_{CREST}	:	position relative to the crest of the dike (m)
$z_{N\%}$:	wave run-up level relative to the still-water level, unless denoted relative to NAP exceeded by $N\%$ of the incident waves (m)

Greek letters:

α	:	slope of foreshore-section ($^\circ$)
ε	:	root-mean-square error (-)
γ	:	total reduction factor for wave run-up (-)
γ_β	:	reduction factor for wave run-up, due to angular wave attack (-)
γ_b	:	reduction factor for wave run-up, due to a berm (-)
γ_f	:	reduction factor for wave run-up, due to friction (-)
γ_h	:	reduction factor for wave run-up, due to shallow foreshore (-)
φ	:	slope of structure ($^\circ$)
ξ_m	:	surf-similarity parameter at toe of structure, $\xi_m = \tan \varphi / \sqrt{s_m}$ (-)

- ξ_{op} : surf-similarity parameter based on the significant wave height at the toe and the peak wave period at deep water, $\xi_{op} = \tan \varphi / \sqrt{s_{op}}$ (-)
 ξ_p : surf-similarity parameter at toe of structure, $\xi_p = \tan \varphi / \sqrt{s_p}$ (-)
 $\xi_{s,-1}$: surf-similarity parameter at toe of structure, $\xi_{s,-1} = \tan \varphi / \sqrt{s_{,-1}}$ (-)

Abbreviations:

- NAP : Dutch vertical reference level.
 MWL : Mean Water Level, relative to NAP (m)
 SWL : Still Water Level, relative to NAP (m)

I Introduction

I.1 General

Within the framework of the European MAST-OPTICREST project prototype measurements are performed on the Petten Sea-defence ('Pettemer Zeewering'). This dike is of special interest since the complex shallow foreshore affects the waves considerably before they reach the toe of the dike. The effects of such shallow foreshores on wave run-up are not sufficiently known. To increase knowledge on these effects, not only prototype measurements are performed but also physical model tests. The present report describes two-dimensional physical model investigations on the Petten Sea-defence.

Within the Dutch research project 'Wave propagation over shallow foreshores' attention is given to the effects of shallow foreshores on wave run-up and wave overtopping. The present physical model investigations contribute to this research topic. To predict wave run-up and wave overtopping in other situations than the measured conditions for the Petten Sea-defence, the results need to become available in a more generic way such as in predictive models and design formulae.

Recent investigations within this framework have provided a predictive model for the wave height statistics on shallow foreshores, based on a given total wave energy (m_0), a local water depth (d), and a foreshore slope ($\tan \alpha$). A more detailed description of the model, which is an extension of the model in Groenendijk (1998), is given in Groenendijk and Van Gent (1998). The present physical model tests are used to validate this model, developed for straight foreshore slopes, for situations with a complex foreshore. Other recent investigations were focused on predictions of wave run-up and wave overtopping, especially for situations with shallow foreshores, see Van Gent (1999); the present physical model tests are used for comparison with the proposed formulae.

The physical model tests were performed under supervision of dr. M.R.A. van Gent with contributions of ms. S.C. Beck as visiting researcher from Leichtweiss Institut für Wasserbau, dr. A.R. van Dongeren, mr. A. Scheer, mr. L. Tulp and mr. A. ter Veen from WL | DELFT HYDRAULICS, and other partners within the MAST-OPTICREST project.

I.2 Purpose of physical model investigations

The purpose of the two-dimensional physical model tests was to study wave run-up for the situation of the Petten Sea-defence where a complex foreshore considerably affects the wave run-up. The wave conditions tested were performed for the following purposes:

- Comparison of storm conditions measured in prototype with results from physical model tests.
- Analysis of the influence of several parameters on wave run-up (parameter analysis).
- Validation of numerical models.

The actual validation and applications of numerical models is not part of the research presented here. This report does describe validations and applications of mathematical and empirical predictive models and formulae for wave height statistics on shallow foreshores and wave run-up levels.

1.3 Outline

The set-up of the physical model investigations is described in Chapter 2 of this report. In Chapter 3 the test results are described. In Chapter 4 the measured wave height statistics are compared to a predictive model for the probability of exceedance of wave heights, and the measured wave run-up levels are compared to existing formulae for predicting wave run-up. Finally, Chapter 5 provides an overview of the main conclusions with suggestions for further investigations.

2 Model preparation

2.1 Test facility

The physical model tests were performed in the Scheldt-flume of WL | DELFT HYDRAULICS ('De Voorst'). This wave flume has a length of 55 m, a width of 1 m and a height of 1.2 m. The facility is equipped with a wave board for generating regular/monochromatic and irregular/random waves in relatively shallow water by a translatory wave board. Generating combinations of rotational and translatory modes are possible but this was not used in the present tests. The on-line computer facilities for wave board control, data-acquisition and data-processing allow for direct control and computation of relevant wave characteristics. Wave energy spectra can be prescribed by using standard or non-standard spectral shapes or by prescribing specific time-series of wave trains. Second-order wave generation for irregular/random waves is available which produces natural wave trains already directly at the wave board by simultaneously generating bound long waves. This reduces undesirable wave disturbance in the flume. The wave board has active wave absorption which means that waves propagating towards the wave board are measured and that the motion of the wave board accounts for these reflected waves so that the wave board absorbs these waves; thus these reflected waves do not re-reflect against the wave board, thereby not disturbing the measurements. This system prevents the generation of serious undesired long-periodic waves which would affect the measurements. Active-wave absorption is essential for the present tests since the foreshore and the dike result in considerable amounts of reflected energy in the low-frequency range of the wave energy spectra.

2.2 Model set-up and instrumentation

One of the main topics concerning the model set-up was the schematisation of the foreshore. Figure 1 shows the measured foreshore perpendicular to the Petten Sea-defence (provided by RIKZ, see also Wolf, 1998). Between 7 and 3 km offshore the depth gradually decreases from NAP-20 m to NAP-10 m with an average slope of approximately 1:400. Then the foreshore shows an offshore bar with a crest at approximately NAP-6 m ('Pettemer polder'). Landwards of the offshore bar the depth increases again to NAP-12 m at about 1 km from the dike. Seawards of this point the foreshore cannot be modelled in the flume because of limitations of the length of the flume. Figure 2 shows a more detailed graph of the foreshore in the last kilometre which could be modelled in the flume. A second bar with a crest at about NAP-3.5 m is present at about 500 m seaward from the crest of the dike. The toe of the dike is at a level of about NAP-0.5 m. The dike consists of a 1:4.5 lower slope, a berm of about 1:20 from NAP+5.0 m to NAP+5.7 m and a 1:3 upper slope, all modelled as smooth slopes. The crest elevation is NAP+12.9 m.

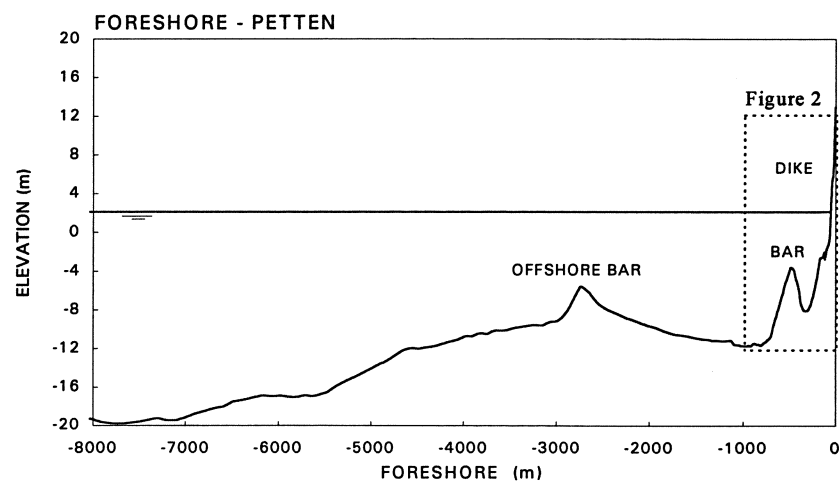


Figure 1 Measured foreshore perpendicular to the Petten Sea-defence.

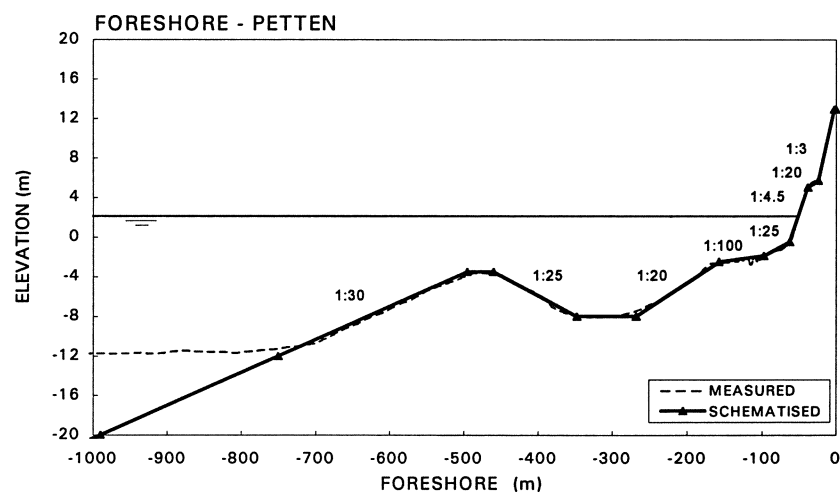


Figure 2 Schematised foreshore for model tests.

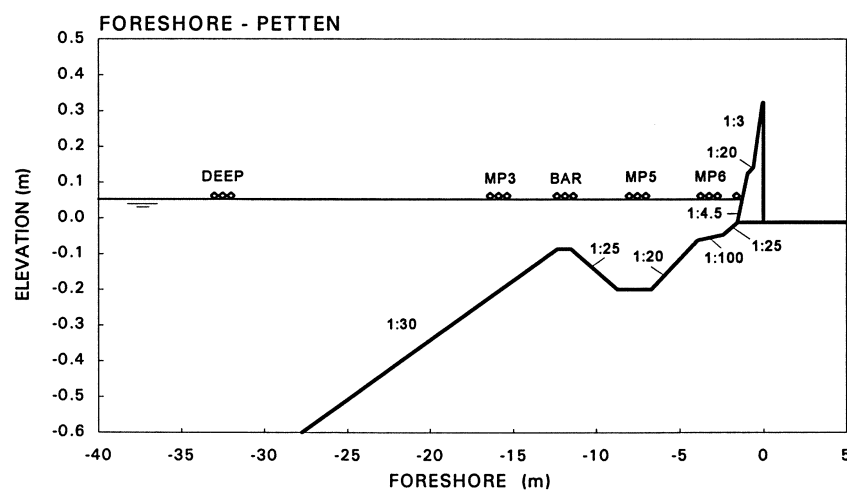


Figure 3 Model set-up (foreshore).

The two bars on the foreshore both cause severe wave breaking under storm conditions. This causes the shapes of the energy density spectra at the toe of the structure to deviate considerably from the deep-water spectral shapes. Since only the most landward bar could be modelled in the tests, the spectral shapes at the corresponding position of the wave board in the prototype situation were affected by wave breaking on the offshore bar. Therefore, for the tests where measured storms were modelled also the measured wave energy spectra were used instead of standard spectral shapes such as Pierson-Moskowitz spectra or JONSWAP-spectra. Because the position of the wave board corresponds to a position in deeper water and because this position was relatively far from the offshore bar where wave breaking occurs, the wave height distribution at the position of the wave board was assumed to have a Rayleigh-distribution.

The model scale for the present tests was chosen at 1:40 which is suitable for accurate wave generation in the flume. For accurate wave generation relatively deep water is desirable, to avoid the need to generate waves that are nearly breaking. Therefore, the water depth at the position of the wave board was increased with respect to the water depth at the corresponding position in the prototype situation; the front slope of the bar was extended to deeper water (see also Figure 2).

Figure 3 shows the foreshore as modelled in the flume (scaled foreshore). At several positions on the foreshore wave conditions were measured; at deep water, at the crest of the bar, at the toe of the structure and at three positions where wave conditions have been measured in the prototype situation: MP3, MP5 and MP6.

Techniques are available to extract both the incident waves and the reflected waves from measured wave height recordings. The method used here (Mansard and Funke, 1980) requires signals from three wave gauges relatively close to each other, consequently leading to a lower accuracy for the energy density in the lower frequencies. These techniques assume linear waves which is a rather rough assumption in positions where severe wave breaking occurs. Common analysis procedures for wave run-up require the wave height of the incident waves at the toe of the dike as input. Since the toe of the dike is in relatively shallow water with breaking waves, these techniques cannot be applied here with sufficient accuracy. Therefore, tests were repeated without the structure in position to obtain the incident waves at the toe of the structure. However, this procedure also introduces undesirable effects since in reality waves reflected by the dike interact with incident waves; these processes are not modelled correctly in tests without the dike in position. Since surfbeat-phenomena (the propagation of wave groups and their associated long wave motion) for which wave reflection is important, are clearly present (see De Haas *et al*, 1999) this method is also expected to introduce inaccuracies.

Besides wave gauges also a step-gauge to measure wave run-up was installed. This step-gauge consists of a beam with a large number of conductive probes. The probes were placed at approximately 2.5 mm (model-scale) above the slope such that water layers thinner than 2.5 mm were not recorded, this is 0.10 m on prototype-scale. The distance between the probes along the slope was 25 mm (model-scale). The step-gauge recorded for each probe the number of times that the probe came into contact with the water surface. Dividing this number by the number of the incident waves yielded the probability of exceedance for each

probe level. From the exceedance probabilities at different probe levels a cumulative exceedance curve was obtained, yielding for instance the wave run-up level that was exceeded by 2% of the incident waves: $z_{2\%}$. In addition to the step-gauge a wave gauge was positioned along the slope which recorded wave run-up levels at a level of approximately 5 mm (model-scale) above the slope, in contrast to the step-gauge which recorded wave run-up levels at a level of 2.5 mm above the slope. Similar to the prototype measurements, the wave run-up levels were measured only on the section above the berm. See Figure 4 for a cross-section of the dike on model scale with the position of the step-gauge.

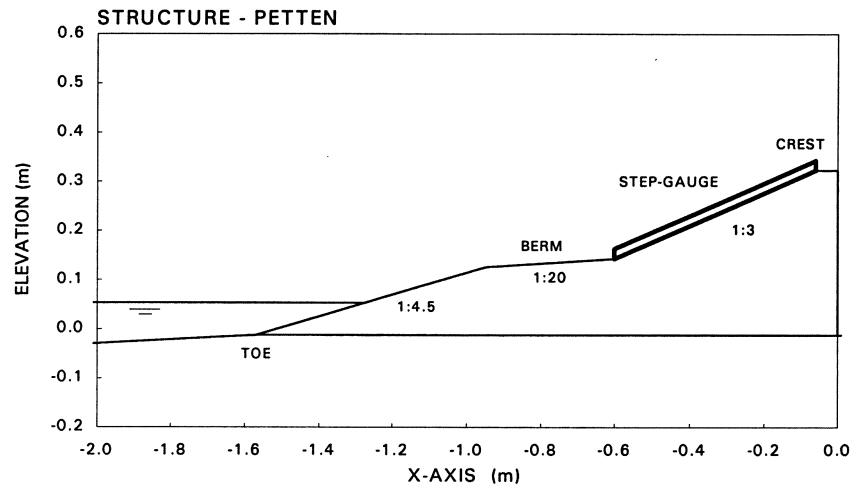


Figure 4 Model set-up (structure).

2.3 Characteristic parameters

To analyse the results use is made of both time-domain analysis and frequency-domain analysis, yielding characteristic parameters for the wave conditions and the wave run-up levels.

For the wave heights of the incident waves the significant wave height H_s (time-domain analysis) and the wave height H_{m0} (spectral analysis) are used. For the total wave heights, including both incident waves and reflected waves, the corresponding wave heights are denoted by H_{s-T} and H_{m0-T} . The reflection coefficient is defined as the ratio of reflected and incident wave heights, using the wave heights H_{m0} from spectral analysis.

For the wave period numerous characteristic wave periods can be used, either based on time-domain analysis (mean wave period T_m) or spectral analysis. Based on spectral analysis wave periods based on moments of the wave energy spectra can be obtained. The spectral moments are based on energy between the cut-off frequencies 0.03 Hz and 0.5 Hz (prototype scale) from the spectra of the incident waves. From the obtained wave energy spectra the spectral moments are computed as follows:

$$m_n = \int_0^\infty f^n \cdot S(f) \cdot df \quad , \quad n = \dots -4, -3, -2, -1, 0, 1, 2, \dots \quad (1)$$

of the three parameters have been used in the analysis. Based on the analysis in Van Gent (1999), use is made of the surf-similarity parameter $\xi_{s,-1}$ where use is made of the significant wave height at the toe of the structure and the wave period $T_{m-1,0}$ at the toe of the structure. For the characteristic slope ϕ use is made here of the average slope angle in the region between $2 H_s$ below the still-water level and $2 H_s$ above the still-water level (see Figure 5). In Section 4.2 the influence of the choice of characteristic parameters is discussed more in detail.

2.4 Test programme

The test programme consisted of three types of measurements:

- Wave conditions corresponding to storms measured in prototype.
- Wave conditions for a parameter analysis.
- Wave conditions for validation of numerical models.

The storms measured in prototype took place on January 1st/2nd, 1995 and January 10th, 1995. Data on these storms were provided by RIKZ and are summarised in Table 1 and Figure 6. The wave conditions in Table 1 and wave energy spectra in Figure 6 were measured at the location MP3. The measured wave run-up levels are based on the number of waves at MP6. Wave run-up in these prototype measurements was measured by sensors in the slope which measure run-up levels of very thin water layers. In contrast to all other types of tests, the wave conditions in Table 1 are based on the total wave signals and not on the incident waves. In the flume spectral shapes were generated such that at MP3 the spectral shapes resemble the measured spectral shapes between the cut-off frequencies 0.03 Hz and 0.3 Hz. The desired wave height in the flume was the measured total significant wave height at MP3 (H_{s-T}). In the prototype measurements the incident waves cannot be extracted from the total wave signals or from the wave energy spectra of the total wave signals. In the model tests these wave energy spectra of the total wave signals were generated as incident waves, a difference between both measurements could therefore not be avoided.

No	Date	Time	MWL (NAP)	H_{s-T}	H_{m0-T}	T_m^*	$T_{m0,1}^*$	$T_{m-1,0}^*$	T_p^*	N_w^*	$z_{2\%}^{**}$ (NAP)
1.01	1-1-1995	15:40	2.10	4.24	4.20	6.8	7.3	8.9	11.1	530	8.33
1.02	1-1-1995	17:00	2.01	4.24	4.23	6.5	7.1	8.6	11.1	551	7.60
1.03	2-1-1995	4:00	2.18	3.84	3.95	6.5	7.5	10.2	16.7	551	8.66
1.04	2-1-1995	5:40	1.64	4.24	4.29	6.9	7.8	10.4	16.7	518	6.89
1.05	2-1-1995	16:20	1.60	3.08	3.10	7.1	7.8	9.8	14.3	503	6.44
1.06	10-1-1995	11:00	2.00	3.70	3.75	6.3	7.0	8.8	10.0	566	7.67

* based on analysis of signals of total waves, including reflected waves ($\Delta f=0.01$ Hz).
 ** based on total number of waves at MP6, including reflected waves.

Table 1 Measured storms in prototype (MP3).

The second type of measurement concerns the analysis of the influence of several wave parameters on wave run-up by varying wave conditions at deep water. The influence of

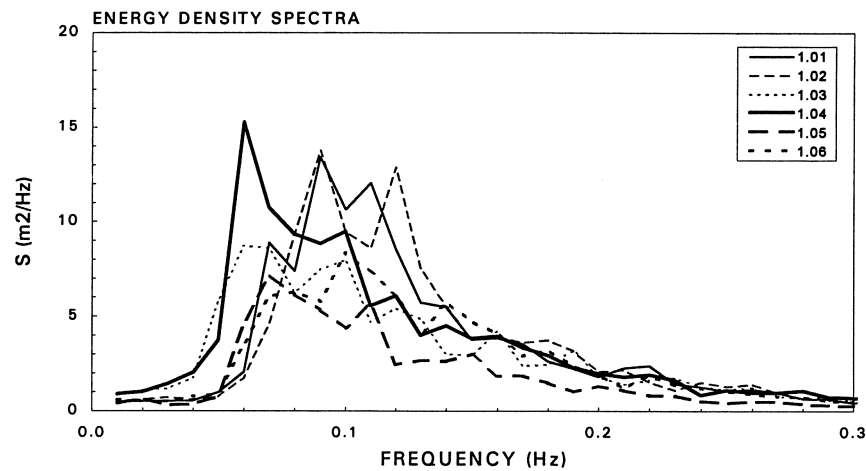


Figure 6 Wave energy spectra measured in prototype.

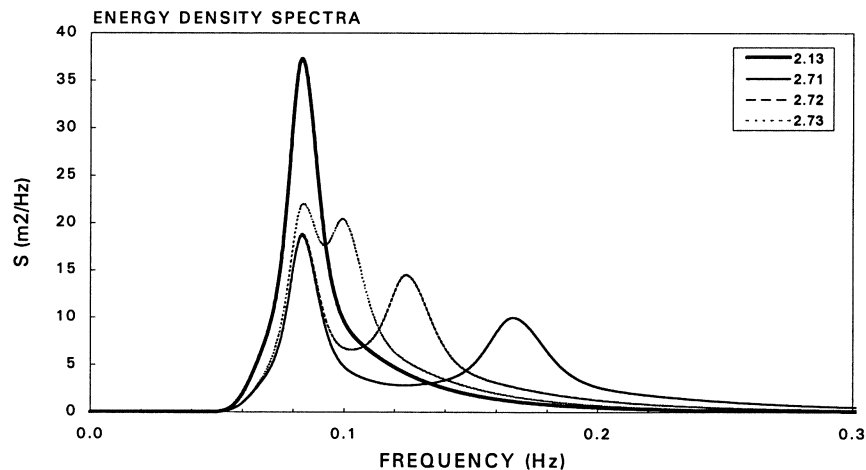


Figure 7 Double-peaked wave energy spectra.

several parameters on wave run-up levels was studied by varying one parameter at deep water per test series. Tables 2 to 9 show the parameters varied in the tests (with target values):

- Variation of wave heights with constant wave steepness and constant still-water level,
- Variation of wave steepnesses with constant wave height and constant still-water level,
- Variation of the still-water levels with constant wave height and wave steepness.

In addition, the spectral shape was varied by prescribing double-peaked wave energy spectra at deep water instead of the standard JONSWAP wave energy spectra as used in the other tests of the parameter analysis. Table 8 and Table 9 show the parameters of the double-peaked wave energy spectra which have been made by superposition of two single peaked JONSWAP spectra with an equal amount of energy in each individual single peaked wave energy spectrum, see also Figure 7. All tests with irregular waves were performed with approximately 1000 waves.

No	SWL (NAP)	H_{s0}	T_p	s_p	Spectral shape
2.11	2.1	2	8.5	0.018	JONSWAP
2.12	2.1	3	10.5	0.018	JONSWAP
2.13	2.1	4	12	0.018	JONSWAP
2.14	2.1	5	13.5	0.018	JONSWAP
2.15	2.1	6	14.5	0.018	JONSWAP

Table 2 Variation of wave height (low water level; constant wave steepness).

No	SWL (NAP)	H_{s0}	T_p	s_p	Spectral shape
2.21	4.7	2	8.5	0.018	JONSWAP
2.22	4.7	3	10.5	0.018	JONSWAP
2.23	4.7	4	12	0.018	JONSWAP
2.24	4.7	5	13.5	0.018	JONSWAP
2.25	4.7	6	14.5	0.018	JONSWAP

Table 3 Variation of wave height (high water level; constant wave steepness).

No	SWL (NAP)	H_{s0}	T_p	s_p	Spectral shape
2.31	2.1	4	7	0.052	JONSWAP
2.32	2.1	4	9	0.032	JONSWAP
2.33/2.13	2.1	4	12	0.018	JONSWAP
2.34	2.1	4	18	0.008	JONSWAP

Table 4 Variation of wave steepness (low water level).

No	SWL (NAP)	H_{s0}	T_p	s_p	Spectral shape
2.41	4.7	4	7	0.052	JONSWAP
2.42	4.7	4	9	0.032	JONSWAP
2.43/2.23	4.7	4	12	0.018	JONSWAP
2.44	4.7	4	18	0.008	JONSWAP

Table 5 Variation of wave steepness (high water level).

No	SWL (NAP)	H_{s0}	T_p	s_p	Spectral shape
2.51	4.7	6	9	0.038	JONSWAP
2.52	4.7	6	12	0.027	JONSWAP
2.53/2.25	4.7	6	14.5	0.018	JONSWAP
2.54	4.7	6	18	0.012	JONSWAP

Table 6 Variation of wave steepness (high water level; high waves).

No	SWL (NAP)	H_{s0}	T_p	s_p	Spectral shape
2.61	1.3	4	12	0.018	JONSWAP
2.62/2.13	2.1	4	12	0.018	JONSWAP
2.63	2.9	4	12	0.018	JONSWAP
2.64	3.8	4	12	0.018	JONSWAP
2.65/2.23	4.7	4	12	0.018	JONSWAP
2.66	5.8	4	12	0.018	JONSWAP

Table 7 Variation of water level.

No	SWL (NAP)	H_{s0}	$T_{p(1)}$	$T_{p(2)}$	Spectral shape
2.71	2.1	4	12	6	DOUBLE-PEAKED
2.72	2.1	4	12	8	DOUBLE-PEAKED
2.73	2.1	4	12	10	DOUBLE-PEAKED

Table 8 Variation of spectral shapes (double-peaked; low water level).

No	SWL (NAP)	H_{s0}	$T_{p(1)}$	$T_{p(2)}$	Spectral shape
2.81	4.7	4	12	6	DOUBLE-PEAKED
2.82	4.7	4	12	8	DOUBLE-PEAKED
2.83	4.7	4	12	10	DOUBLE-PEAKED

Table 9 Variation of spectral shapes (double-peaked; high water level).

<i>No</i>	<i>SWL (NAP)</i>	<i>H₀</i>	<i>T</i>	<i>s₀</i>	<i>Wave type</i>
3.91	4.7	4	6	0.071	REGULAR WAVES
3.92	4.7	4	8	0.040	REGULAR WAVES
3.93	4.7	4	10	0.025	REGULAR WAVES
3.94	4.7	4	12	0.018	REGULAR WAVES

Table 10 Tests for validation of numerical models (regular waves).

Due to the presence of the foreshore the systematic variation of parameters at deep water is not always seen as a systematic variation of parameters at the toe of the structure; for instance, tests with a constant wave steepness at deep water with a systematic variation of the wave height do not result in a constant wave steepness at the toe of the structure.

The third series of tests was performed to validate numerical models. The previous tests can also be used for validation of numerical models but some numerical models require tests with regular/monochromatic waves. Therefore, some tests were performed with regular waves, see Table 10.

The test results are described in Chapter 3 while in Chapter 4 a further analysis of the test results is performed by comparison of results with available mathematical and empirical predictive models and formulae.

3 Analysis of test results

3.1 Test results

In Tables A1-A10 and Figures F 1.01-F 2.83 the results of the model tests are presented. The values of the characteristic parameters discussed in Section 2.3 are listed in these tables while the figures show the total wave energy spectra (including reflected waves), the incident wave energy spectra and the wave height evolution over the foreshore.

Comparison between the test results from the tests with and without the dike in position shows that the wave heights and wave periods of the incident waves at locations such as MP5 and MP6 are not strongly affected by the presence of the dike. Therefore, the wave heights presented in Tables A1-A9 for the position at the toe of the dike have been derived from the tests without the dike in position. Also the wave energy spectra of the incident waves at the position of the toe (TOE in middle graphs) are derived from tests without the dike in position. The data at all other positions are derived from the tests with the dike in position. Not all tests have been repeated without the dike in position. For those tests (15 from a total of 35 tests) the wave heights at the toe of the structure have been obtained from interpolation or extrapolation from tests with similar wave conditions (e.g., wave heights at the toe for Test 2.12 are obtained from interpolation between Test 2.11 and Test 2.13). The results derived from interpolation or extrapolation are presented in Tables A1-A9 in *italics*.

For three tests the 2% wave run-up levels did not reach the slope above the berm: $z_{2\%} < \text{NAP} + 5.7 \text{ m}$ (Tests 2.11, 2.31, 2.61). For four tests with relatively high water levels the 2% wave run-up did exceed the crest level: $z_{2\%} > \text{NAP} + 12.9 \text{ m}$ (Tests 2.25, 2.44, 2.54, 2.66).

The discussion and analysis of results will be presented per type of test series:

- Storms measured in prototype (Section 3.2).
- Parameter analysis (Section 3.3).
- Regular waves (Section 3.4).

Further analysis of the results are performed in the next chapter by comparing results with predictive models and formulae for wave height statistics and wave run-up levels.

3.2 Storms measured in prototype

The first series of tests were performed to compare results from prototype measurements with results from physical model tests. These tests concern six storm periods (within two storms), denoted by Tests 1.01-1.06.

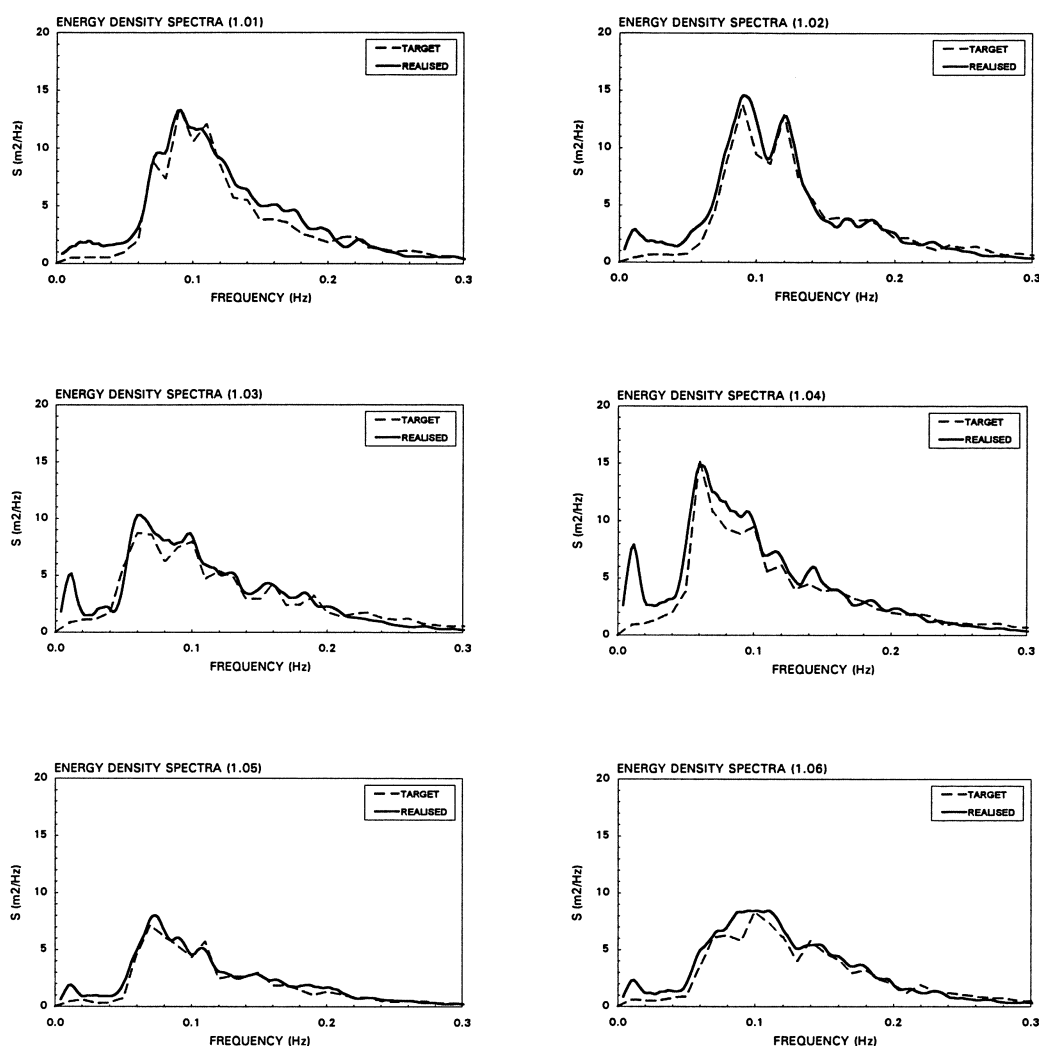


Figure 8 Comparison between wave energy spectra in prototype and in model tests (prototype spectra denoted by 'target', model tests spectra denoted by 'realised').

The shapes of the wave energy spectra at MP3 (including reflected waves) measured in prototype were generated as incident wave energy spectra at MP3 in the model tests. The total wave energy in the spectra at MP3 are such that the total significant wave heights (including reflected waves both in prototype and model tests) after scaling to prototype dimensions are nearly identical in prototype and in model tests. Nevertheless, the incident wave energy spectra in prototype are not known. Therefore, differences between these spectra and the incident wave energy spectra in the model tests cannot be avoided and cannot be analysed. Figure 8 shows comparisons between the measured wave energy spectra of the total waves, including reflected waves, at MP3 in prototype and those in the model tests. The agreement was considered acceptable for the present investigations. The largest differences occur at the lower frequencies. These differences are caused by wave energy in the seaward direction as a result of surfbeat in the shallower part of the foreshore. The differences in these lower frequencies are partly caused by the procedure of analysis and by schematisation effects. The directional spreading of energy in the lower frequencies,

which is in general larger than the directional spreading of the higher frequencies, is not modelled in the flume which might cause more energy in the lower frequencies in the model tests than in prototype circumstances.

Table 11 shows the comparison of the measured wave heights at three locations (MP3, MP5 and MP6). The average difference between the measured significant wave heights in prototype and model tests is at MP3 1.5 %, at MP5 3.4% and at MP6 8.8%.

These differences can be caused by many factors such as a slightly different foreshore during the actual storms than used in the model tests, 3D effects, effects of wind, schematisation-effects, slightly different data acquisition and data analysis procedures and scale effects. Nevertheless, the observed differences are considered acceptable to further investigate wave run-up.

Tests 1.01-1.06: 'Measured storms'														
	MWL		H_{s-T} (MP3)		H_{s-T} (MP5)		H_{s-T} (MP6)		$z_{2\%}$ (NAP)			$z_{2\%}/H_{s-T-MP6}$		differences
Test	P	M	P	M	P	M	P	M	P	M1	M2	P	M2	%
1.01	2.10	2.14	4.24	4.29	2.61	2.69	2.94	2.62	8.3	6.8	7.5	2.1	2.1	-3.3
1.02	2.01	2.01	4.24	4.13	2.65	2.68	2.81	2.56	7.6	6.9	7.4	2.0	2.1	5.1
1.03	2.18	2.21	3.84	3.83	2.61	2.77	2.99	2.69	8.7	7.5	8.4	2.2	2.3	6.0
1.04	1.64	1.62	4.24	4.38	2.39	2.58	2.64	2.53	6.9	6.9	7.1	2.0	2.1	7.9
1.05	1.60	1.59	3.08	3.08	2.37	2.39	2.60	2.30	6.4	5.8	5.8	1.9	1.8	-3.0
1.06	2.00	2.02	3.70	3.76	2.66	2.70	2.78	2.58	7.7	6.8	7.3	2.0	2.0	0.0
P = 'Prototype'; M = 'Model tests'; M1 = 'step-gauge result'; M2 = 'extrapolated to zero water layer'.														

P = 'Prototype'; M = 'Model tests'; M1 = 'step-gauge result'; M2 = 'extrapolated to zero water layer'.

Table 11 Comparison between prototype measurements and physical model tests.

As discussed in Section 2.2 different techniques for measuring wave run-up have been applied. In prototype, thin water layers (between 0.02 m and 0.1 m) were also recorded as wave run-up while in model tests the step-gauge could not record water layers thinner than 0.1 m (prototype scale). Therefore, comparison between the wave run-up levels measured in prototype (indicated by 'P' in Table 11), including thin water layers, and the step-gauge in the model tests (indicated by 'M1' in Table 11), not including thin water layers, is not straightforward. However, based on the results of the wave run-up levels measured in the model tests with a minimum water layer of 0.1 m (step-gauge) and a minimum water layer of 0.2 m (wave-gauge along the slope), extrapolation of these two wave run-up levels can estimate wave run-up levels including thin water layers. These levels are indicated by 'M2' in Table 11. These 'M2'-levels are used for comparison. The comparison is also made for the non-dimensional wave run-up level, where the wave run-up level is the height above the *mean* water level. The wave run-up levels presented in the Appendix Tables, however, are relative to the *still* water level, which causes only minor differences. Wave run-up levels with reference to the *still* water level are given to facility comparisons with results from previous laboratory investigations. The wave heights are the total significant wave heights measured at MP6. The differences in percentage are listed in the last column of Table 11. The average of the differences (absolute values) is 4%. Figure 9 shows the comparison between these wave run-up levels measured in prototype and in model tests.

Although these differences can be caused by many factors such as schematisation and scale effects related to, for instance, the roughness of the slope and the effects of wind on wave

run-up, the observed differences are quite small. The errors introduced by schematisation and scale effects related to roughness and wind are expected to be relatively important for thin water layers on the slope but these are to a large extent avoided by not trying to measure these extremely thin layers, but by extrapolating from thicker layers that are expected to be less influenced by scale effects. This procedure provides at least an estimate of the run-up levels including thin water layers and is considered better than neglecting the presence of these thin water layers. For the purpose of studying the influence of several parameters on wave run-up, this extrapolation is not necessary and has therefore not been applied in the parameter analysis. Nevertheless, it should be kept in mind that neglecting thin water layers, as also done in the derivation of design-formulae discussed in Section 4.2, can provide non-conservative estimates. The tests in Table 11 indicate that the estimates with formulae based on tests neglecting the thin water layers may be in the order of 10% too small compared to reality.

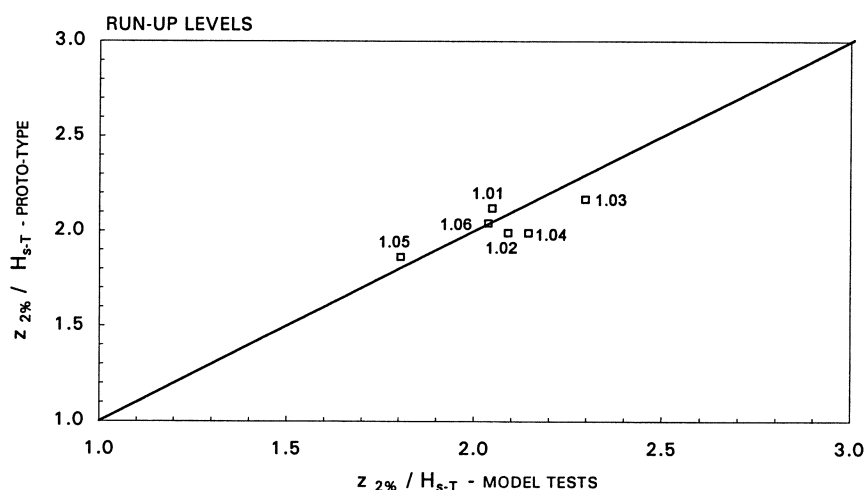


Figure 9 Comparison between wave run-up levels measured in prototype and in model tests.

3.3 Parameter analysis

The test programme discussed in Section 2.4 concerns systematic variations of wave height, wave steepness, water depth and spectral shapes at deep water. It is appropriate to describe the wave run-up as a function of the surf-similarity parameter which accounts for the effects of wave height and wave steepness. Using a suitable characteristic wave height and a characteristic wave period might sufficiently account for the effects of the water depth and the spectral shape. To present the results use is made of the significant wave height of the incident waves at the toe of the structure and the surf-similarity parameter based on various characteristic wave periods.

Figure 10 shows the 2% wave run-up levels as function of the significant wave height at deep water, both made non-dimensional with the significant wave height at the toe of the structure. All tests in Figure 10 have the same deep-water wave steepness, based on the peak wave period. The figure shows a rather clear increase in wave run-up for higher wave heights at deep water.

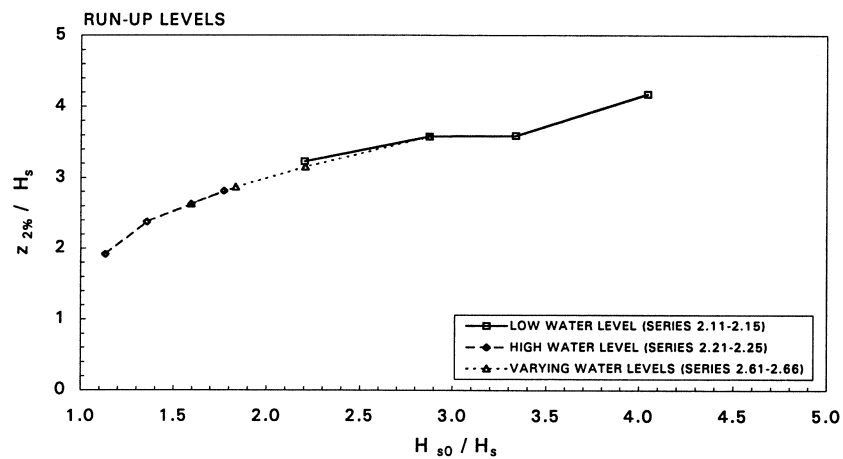


Figure 10 Measured 2% wave run-up levels as function of wave height at deep water.

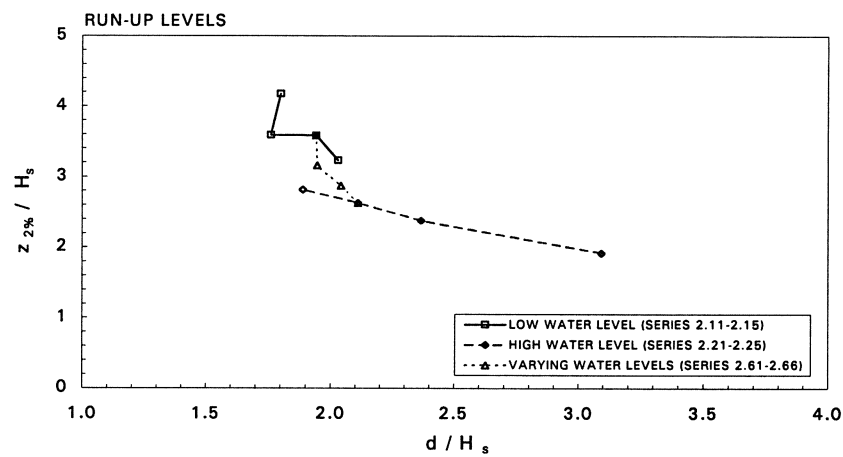


Figure 11 Measured 2% wave run-up levels as function of water depth at the toe.

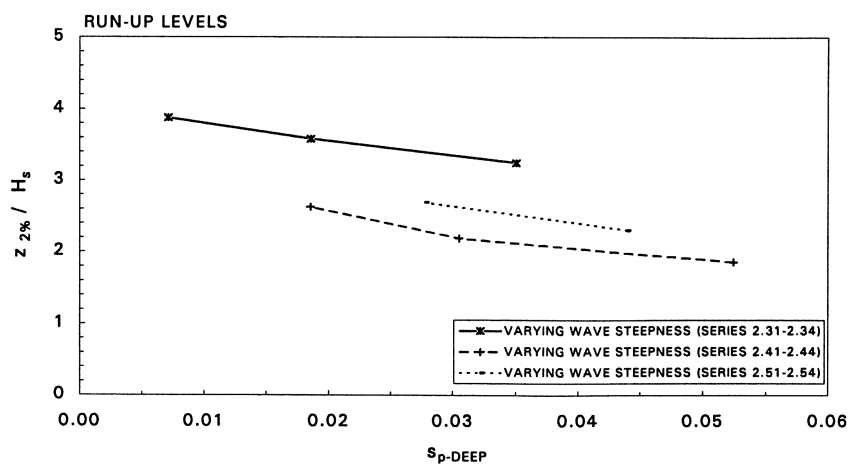


Figure 12 Measured 2% wave run-up levels as function of wave steepness at deep water.

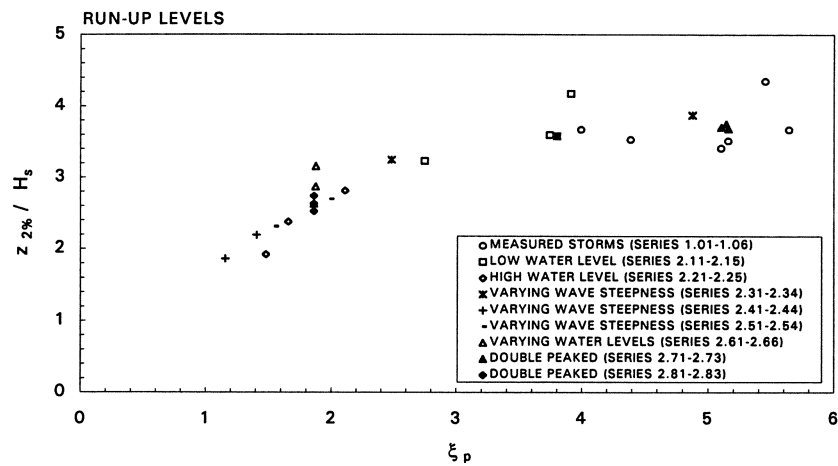


Figure 13 Measured 2% wave run-up levels as function of the surf-similarity parameter based on the peak wave period T_p .

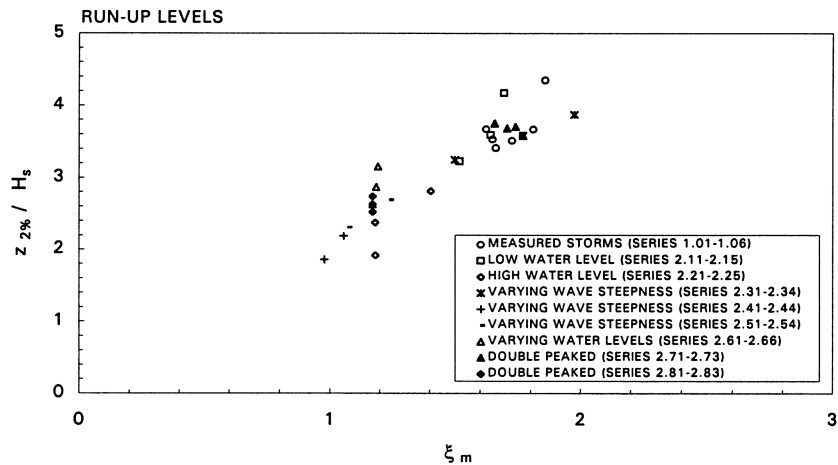


Figure 14 Measured 2% wave run-up levels as function of the surf-similarity parameter based on the wave period T_m .

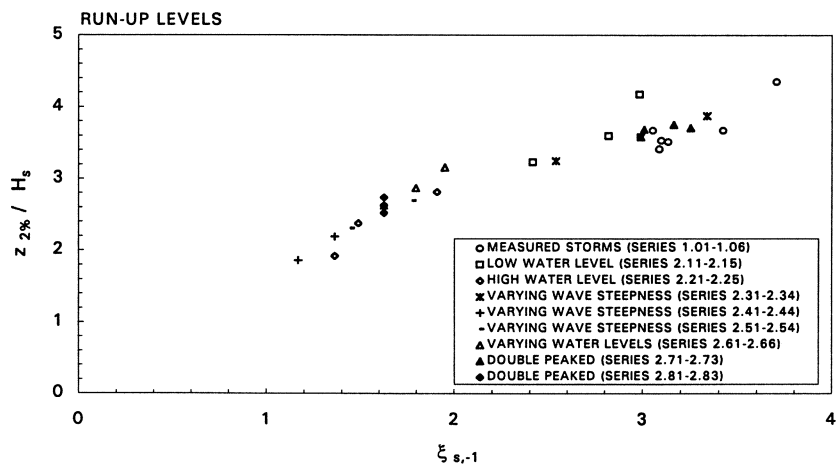


Figure 15 Measured 2% wave run-up levels as function of the surf-similarity parameter based on the wave period $T_{m-1,0}$.

Figure 11 shows the 2%-wave run-up levels as function of the depth at the toe of the structure, both made non-dimensional with the significant wave height at the toe of the structure. Again the tests with the same deep-water wave steepness, based on the peak wave period, are used. The figure shows a clear increase in wave run-up for situations with depth-limited situations at the toe of the structure.

Figure 12 shows the 2%-wave run-up levels as function of the wave steepness at deep water, based on the peak wave period on deep water. Each of the three series concerns conditions having the same water level and the same wave height at deep water. The figure shows a clear dependency of wave run-up on the wave steepness.

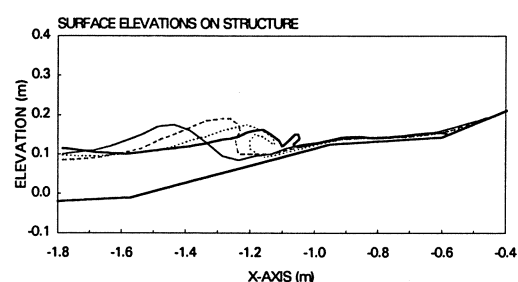
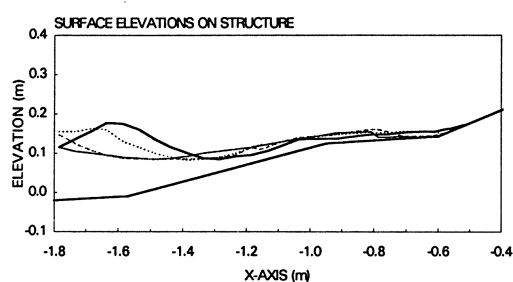
To present the results as a function of the surf-similarity parameter the significant wave height at the toe is used and the characteristic slope as defined in Figure 5. Figures 13-15 show all results as function of the surf-similarity parameter based on the peak wave period T_p (Figure 13), the mean wave period T_m (Figure 14) and the wave period $T_{m-1,0}$ (Figure 15), all based on the incident waves at the toe of the structure. No clear conclusions can be drawn from visual inspection of these three figures; as will also be discussed in Section 4.2 the results using the wave period $T_{m-1,0}$ shows a slightly better trend in the dependency on the surf-similarity parameter than using the other wave periods. This is consistent with results described in Van Gent (1999).

Two tests (Test 1.04 and Test 2.15) clearly contribute the most to the deviation from the main trend. Test 1.04 shows a rather high ratio of $H_{2\%}$ and H_s (1.46). The order of magnitude of the deviations is 10 mm (model scale) in wave run-up level or wave height. Nevertheless, no satisfactory explanation could be found for these deviations. Further analysis in Chapter 4 will therefore be based on all data-points.

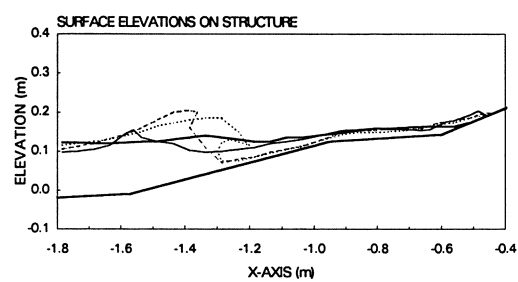
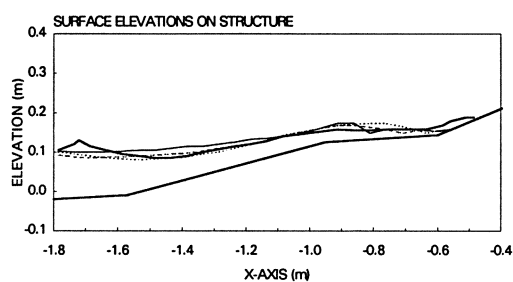
3.4 Regular waves

The tests with regular waves have primarily been done to provide data to verify numerical models. Since the models anticipated to be used simulate the wave motion on the structure, results of observed surface elevations on the slope are presented (Figure 16). The eight surface profiles per test-condition are based on eight equidistant moments in time within a wave period. The figures show plunging waves on the slope for four different wave steepnesses. These surface elevations have been based on an analysis of video recordings. All other data from these tests with regular waves are presented in Table A10.

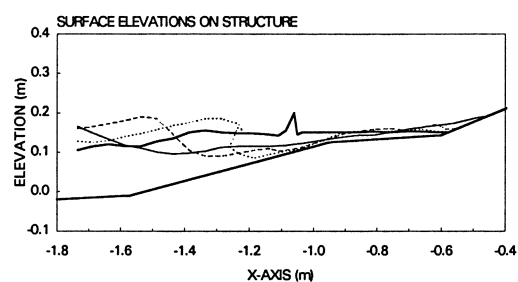
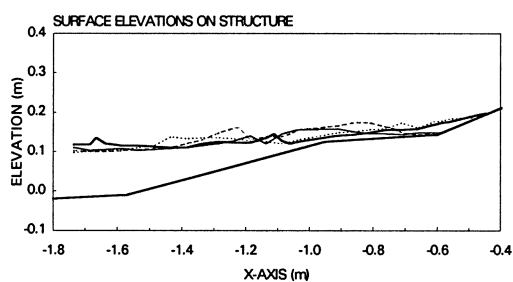
Test 3.91:



Test 3.92:



Test 3.93:



Test 3.94:

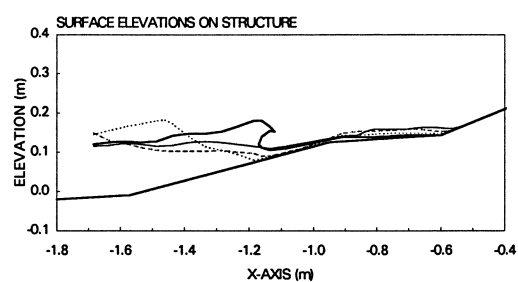
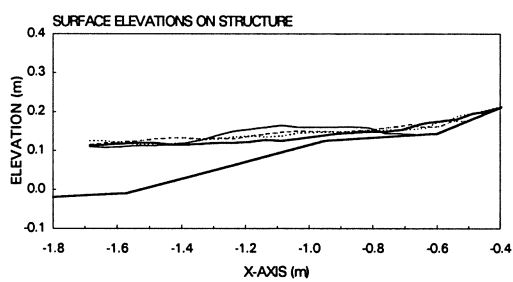


Figure 16 Surface elevations on the slope, Tests 3.91-3.94.

4 Comparison with predictive models

4.1 Wave height statistics on shallow foreshores

In deep water the wave height distribution is accurately described by the Rayleigh distribution. On shallow foreshores the water depth decreases which causes the higher waves in a wave field to break, introducing a change in shape of the wave height distribution. This change in shape is not well described with a formula for a wave height distribution containing only one shape parameter such as in the formula for the Rayleigh distribution. Therefore a Composite Weibull distribution formula is developed which predicts the wave height distribution based on the local total wave energy (m_0), the local water depth (d), and the foreshore slope ($\tan\alpha$). A detailed description of the model, which is an extension of the model in Groenendijk (1998), is given in Groenendijk and Van Gent (1998). The model consists of two Weibull distribution functions, separated by a transitional wave height H_{tr} :

$$F(H) \equiv \Pr\{H \leq H\} = \begin{cases} F_1(H) = 1 - \exp\left(-\left(\frac{H}{H_1}\right)^{k_1}\right) & H \leq H_{tr} \\ F_2(H) = 1 - \exp\left(-\left(\frac{H}{H_2}\right)^{k_2}\right) & H > H_{tr} \end{cases} \quad (4)$$

Waves lower than the transitional wave height are not directly influenced by the depth and obey the first part of the distribution function, $F_1(H)$. Waves higher than the transitional wave height are subject to depth-induced breaking and obey the second part of the distribution function $F_2(H)$. Equation 4 contains five parameters of which three parameters, k_1 , k_2 and H_{tr} , determine the shape of the formula. Calibration based on physical model tests with straight foreshore slopes between 1:250 and 1:20 yielded $k_1=2$ (conform the Rayleigh-distribution) and $k_2=3.6$. The transitional wave height H_{tr} depends on three input values: $H_{tr}=(0.35+5.8 \cdot \tan\alpha) \cdot d$ which is made non-dimensional by using the wave height H_{rms} for which the expression $H_{rms}=(2.69+3.24\sqrt{m_0/d}) \cdot \sqrt{m_0}$ is used. Finally, the two scaling parameters H_1 and H_2 are determined by the continuity condition between both parts, $F_1(H_{tr}) = F_2(H_{tr})$, and the condition that the wave height H_{rms} should satisfy:

$$H_{rms} = \sqrt{\int_0^\infty H^2 F(H) dH} \quad (5)$$

Substitution of Equation 4 in Equation 5 gives a second expression for H_1 and H_2 . Solving this implicit set of equations provides the wave height distribution for a combination of m_0 , d and $\tan\alpha$.

An example of a comparison between measured and predicted wave height distributions is given in Figures 17 and 18. These figures show the measured and computed wave height distributions at six locations for the conditions of Test 2.13 (based on unfiltered wave signals of the incident waves; distributions at the TOE are based on tests without structure).

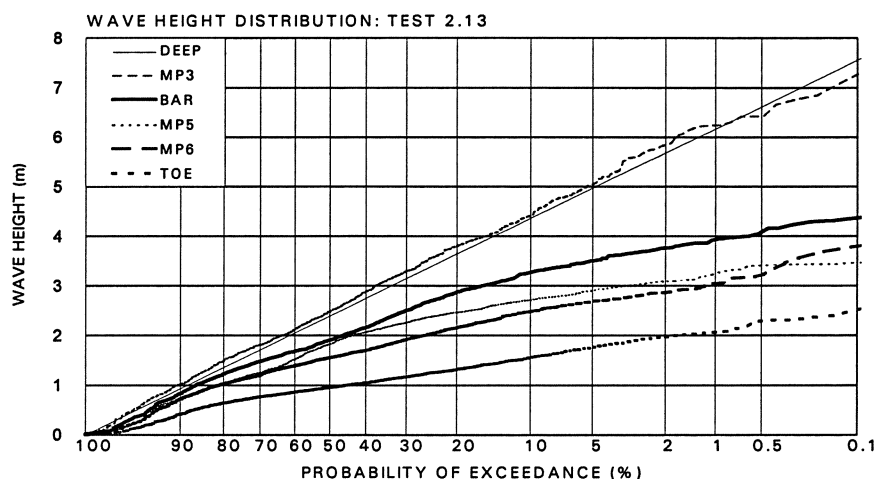


Figure 17 Measured wave height exceedance curves.

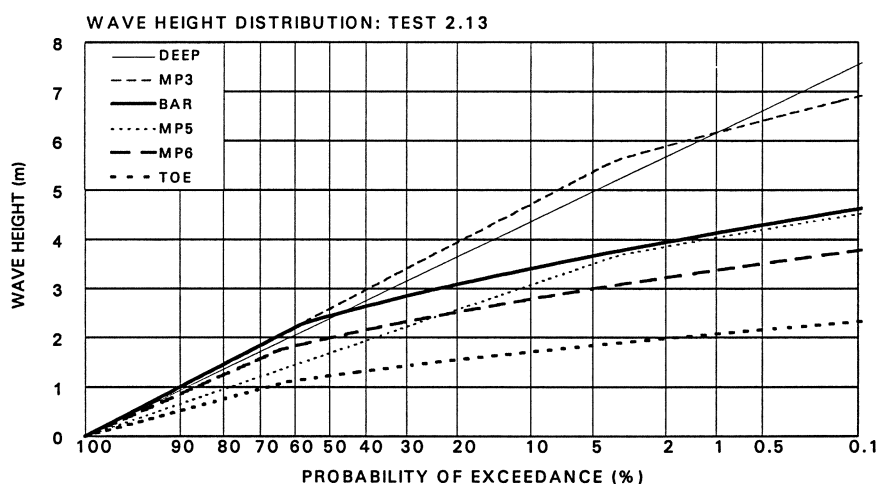


Figure 18 Computed wave height exceedance curves.

These figures show straight lines for the wave height distributions in deep water which means that the distribution follows a Rayleigh distribution. In shallow water the Composite Weibull distribution shows two sections of which the lower waves can be described by a Rayleigh distribution while the higher waves can not. The model based on a Composite Weibull distribution can describe the wave height distribution also for the higher waves in shallow water, see for instance the position BAR in Figures 17 and 18.

As input to the predictive model the measured total wave energy of the incident waves is used (m_0). Since the foreshore is not a straight slope as in the tests used for calibration of the model, characteristic foreshore slopes need to be prescribed per position. Characteristic foreshore slopes are based on slopes between those at the actual position and about a

wavelength seaward of this position because this section of the foreshore largely determines wave breaking at the actual position. For horizontal sections a very gentle slope of 1:400 has been applied. The characteristic foreshore slopes used in the model at the positions DEEP, MP3, BAR, MP5, MP6 and TOE are 1:400, 1:30, 1:100, 1:400, 1:100 and 1:100 respectively.

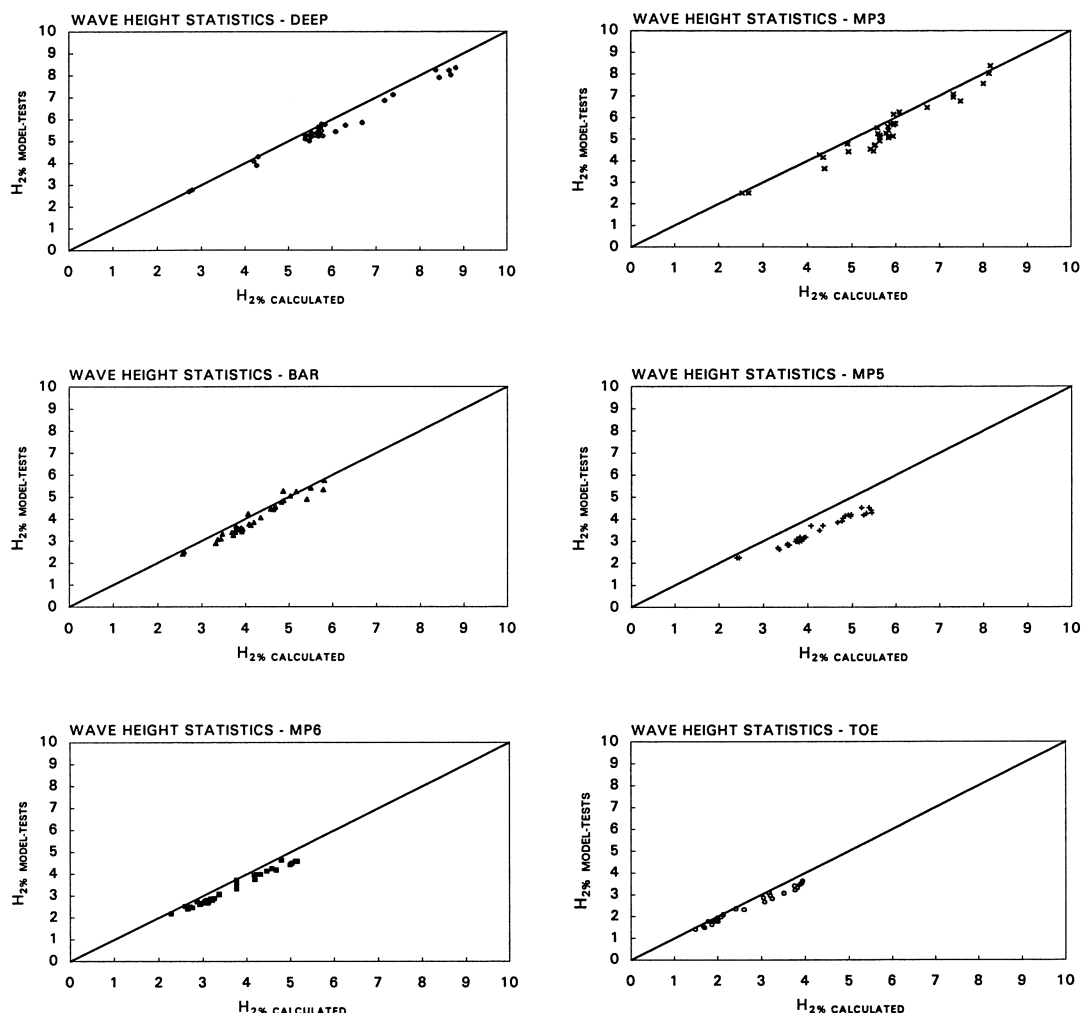


Figure 19 Comparison between measured and computed wave heights ($H_{2\%}$).

Figure 19 shows for each location and all tests a comparison between measured and computed wave heights $H_{2\%}$. The calculated values based on the Composite Weibull distribution provide for most situations rather systematic overestimates of $H_{2\%}$. For the locations DEEP, MP3, BAR, MP5, MP6 and TOE the average differences are 5%, 8%, 7%, 22%, 10% and 10%, respectively. At the location MP5, where broken waves occur in relatively deep water, the Composite Weibull distribution provides the highest overestimates. For this location the model provides distributions which are more close to Rayleigh distributions while in reality the deviations from Rayleigh are larger. For the conditions on this foreshore the Composite Weibull distribution provides less accurate predictions than for the straight foreshore slopes for which it was calibrated and validated.

It is expected that the source of the systematic overestimates by the Composite Weibull distribution can be partly found in the method of calibration of the coefficients in the Composite Weibull distribution. The wave heights used for calibration were based on signals of total waves, including reflected waves. Although the calibration was based on tests without a structure in position, some wave reflection must still have been present, especially reflection of long waves affecting the ratio of for instance $H_{2\%}$ and H_{m0} .

4.2 Wave run-up on dikes

Formulae for wave run-up

Two wave run-up formulae are used for comparison with the measured wave run-up levels; those proposed by De Waal and Van der Meer (1992) and Van Gent (1999). Both are based on the formula by Battjes (1974) where wave run-up was expressed as a function of the surf-similarity parameter. De Waal and Van der Meer (1992) incorporated reduction factors due to the influences of friction, foreshores, angular wave attack and berms. The formula has the following shape:

$$\begin{aligned} z_{2\%} / (\gamma H_s) &= c_0 \xi_{op} & \text{for } \xi_{op} \leq p \\ z_{2\%} / (\gamma H_s) &= c_1 & \text{for } \xi_{op} \geq p \end{aligned} \quad (6)$$

where γ is a reduction factor which takes the effects of friction, foreshores and angular wave attack into account: $\gamma = \gamma_f \gamma_h \gamma_\beta$.

The reduction factor γ_f varies between 0.5 for rock slopes with two or more layers, 0.6 for rock slopes with one layer, 0.95 for grass and 1.0 for smooth impermeable slopes.

The reduction factor γ_h can be approximated by $\gamma_h = H_{2\%} / (1.4 H_s)$. Van der Meer (1997) proposed not to use this reduction factor.

The reduction factor γ_β can be approximated by $\gamma_\beta = 1 - 0.0022 \cdot \beta$ for wave run-up ($\beta \leq 80^\circ$), which was derived from tests with short-crested waves.

Due to the presence of a berm in the seaward slope the slope angle in the surf-similarity parameter is not uniquely defined. De Waal and Van der Meer (1992) proposed to take the influence of a berm into account by replacing $\tan \phi$ in the surf-similarity parameter ξ by:

$\tan \phi = r_{dh} \tan \psi + (1 - r_{dh}) \tan \psi_{eq}$ where the weight factor r_{dh} depends on the position of the berm: $r_{dh} = 0.5 (d_h / H_s)^2$ where d_h is the average depth of the berm with respect to the still-water level ($-1.0 \leq d_h / H_s \leq 1.0$). For $\tan \psi$ an empirical relation for a representative slope angle based on the slope angles below (ψ_{lower}) and above the berm (ψ_{upper}) was proposed: $\cot \psi$ is the average of $(1 - d_h / H_s) \cot \psi_{lower}$ and $(1 + d_h / H_s) \cot \psi_{upper}$. For the equivalent slope around the berm ($\tan \psi_{eq}$) another empirical relation was given, where B is the berm width: $\tan \psi_{eq} = 2 / (\cot \psi_{lower} + \cot \psi_{upper} + B / H_s)$. Use is made of the reduction factor $\gamma_b = \tan \phi / \tan \psi$

($\gamma_b \geq 0.6$). For the structure tested in this study a more simple approach such as defined in Figure 5 can be used to obtain a characteristic slope.

Since limited information is available on combinations of reductions, a maximum total reduction factor $\gamma_b \gamma_f \gamma_h \gamma_\beta = 0.5$ was proposed. See for a more detailed discussion on above-mentioned reduction factors De Waal and Van der Meer (1992) or Van der Meer (1997).

The coefficients c_0 , c_1 and p from Equation 6 were set at 1.5, 3 and 2 based on many physical model tests. For design purposes it was advised to use somewhat safer values: 1.6, 3.2 and 2 respectively. The actual measurement points were best represented by $c_0 = 1.43$.

To account for arbitrary spectral shapes and to derive a formula without a discontinuity at a certain value of the surf-similarity parameter an alternative formula was proposed in Van Gent (1999):

$$\begin{aligned} z_{2\%} / (\gamma H_s) &= c_0 \xi_{s,-1} & \text{for } \xi_{s,-1} \leq p \\ z_{2\%} / (\gamma H_s) &= c_1 - c_2 / \xi_{s,-1} & \text{for } \xi_{s,-1} \geq p \end{aligned} \quad (7)$$

where continuity between both sections and their derivatives determine $c_2 = 0.25 c_1^2 / c_0$ and $p = 0.5 c_1 / c_0$. The wave height and wave period are those at the toe of the structure. The surf-similarity parameter was defined as $\xi_{s,-1} = \tan \phi / \sqrt{(2\pi / g \cdot H_s / T_{m-1,0}^2)}$. The formula allows for incorporation of the reduction factors for berms, foreshore, friction and angular wave attack. The coefficients were not calibrated but a first guess was made based on numerical model computations with the model described in Van Gent (1994, 1995): $c_0 = 1.45$, $c_1 = 3.8$, $c_2 = 2.5$ and $p = 1.3$ (with a standard deviation of 0.11 between the computations and the formula). The computations also indicated that the wave period $T_{m-1,0}$ is the most suitable characteristic wave period for wave run-up in situations where the short-wave energy is distributed in single- or double-peaked wave energy spectra. For situations where at the toe of the structure a single-peaked wave energy spectra is present with a standard spectral shape, the theoretical relation between the peak wave period and the wave period $T_{m-1,0}$ can be used if only the peak wave period is available: $T_p = 1.107 T_{m-1,0}$ for a JONSWAP spectrum and $T_p = 1.167 T_{m-1,0}$ for a Pierson-Moskowitz spectrum.

Comparison of measured wave run-up levels with formulae

The results of the present model tests are compared to the two formulae from Equation 6 and Equation 7. For comparison with Equation 6 the deep-water wave steepness based on the peak wave period is used with the influence of the berm taken into account based on the method described in De Waal and Van der Meer (1992). No reduction factors for friction, foreshores or angular wave attack were applied.

Figure 20 shows rather large differences between the measured wave run-up levels and the formulae by De Waal and Van der Meer (1992). Firstly, the scatter is large and secondly, it is clear that actual wave run-up levels are considerably higher than those predicted by the formula.

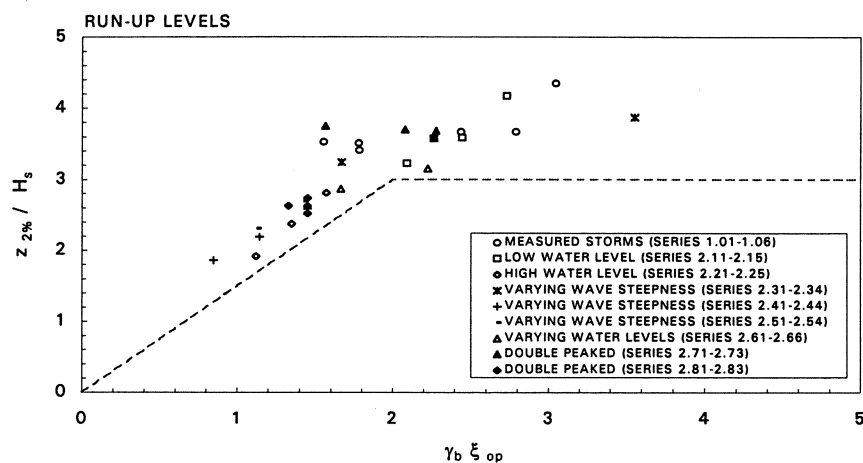


Figure 20 Comparison between measured and computed wave run-up levels, using Equation 6 (based on De Waal and Van der Meer, 1992).

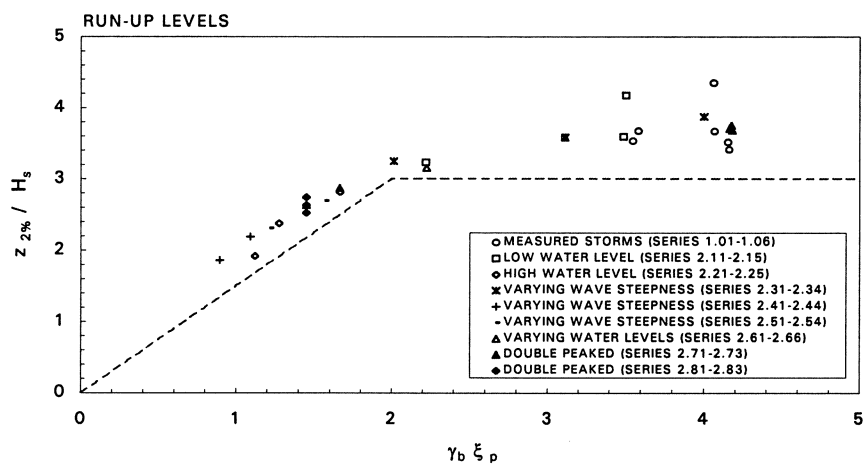


Figure 21 Comparison between measured and computed wave run-up levels, using Equation 6 but with the wave steepness s_p at the toe.

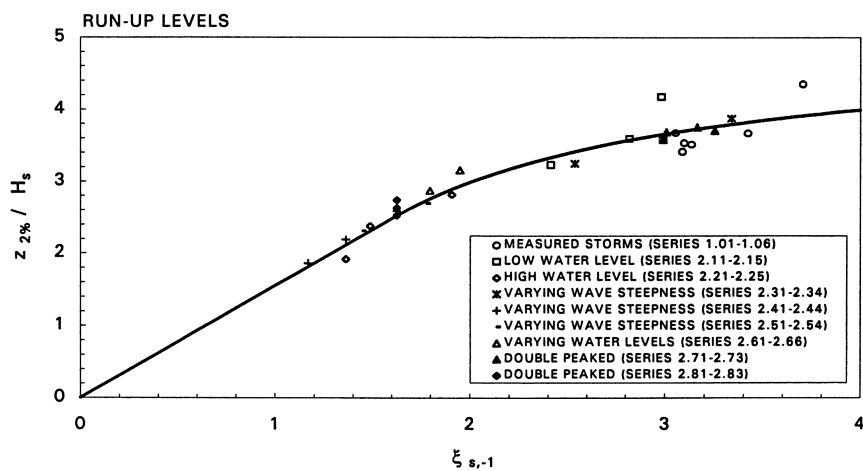


Figure 22 Comparison between measured and computed wave run-up levels, using the present calibration of Equation 7 (based on Van Gent, 1999).

These differences, especially the scatter without a clear trend, are expected to be caused by the use of the deep-water peak wave period in this formula. The foreshore considerably affects the wave conditions, including the peak wave period, between deep-water and the toe of the structure. Figure 21 shows the same results compared to Equation 6 but now with the wave steepness based on the peak wave period at the toe of the structure instead of the peak wave period at deep water (using again the same method for the influence of the berm as described by De Waal and Van der Meer, 1992). This clearly indicates that the use of the deep-water peak wave period is not appropriate.

Figure 21 shows an improvement compared to using Equation 6 as shown in Figure 20. Nevertheless, the wave run-up levels are still underestimated and the trend is not well described by Equation 6. The trend can be described better by using the trend of the formula in Equation 7. However, in Equation 7 also the wave peak period is replaced by the wave period $T_{m-1,0}$. Because in most tests in the present test programme the same peak in the wave energy spectrum becomes dominant, fluctuations in the wave peak period are relatively small. This means that for the tests in the present test programme the use of the wave peak period did not result in the large scatter which in principle can occur when the wave peak period is used.

Figure 22 shows that the dependency on the surf-similarity parameter can be described with Equation 7. In Equation 7 the wave period $T_{m-1,0}$ was used and the characteristic slope was based on the method defined in Figure 5. Since Equation 7 was not calibrated based on physical model tests, the coefficients for c_0 and c_1 have been fitted for the present results, i.e. $c_0=1.55$ and $c_1=5$ (with a standard deviation of 0.18). Including very thin water layers the wave run-up levels might be about 10% higher which means that the values for c_0 and c_1 could also be approximately 10% higher. The present data-set, however, is not considered as very suitable to calibrate Equation 7 since neither the slope angles nor the berm was varied. Nevertheless, comparison between the performance of Equation 6 and Equation 7 in Figure 20 and Figure 22 indicates that Equation 7 is in principle more suitable to describe wave run-up than Equation 6.

Influence of the choice of characteristic parameters

The surf-similarity parameter contains characteristic parameters for the wave height, the wave period and the slope. For each of these parameters several choices can be made. The parameters used in Figure 22 are respectively based on the significant wave height of the incident waves at the toe, the wave period $T_{m-1,0}$ at the toe and the slope angle based on the method defined in Figure 5. The influence of the choice of these three characteristic parameters is studied by using other characteristic parameters and comparison of the performance. Therefore, for combinations of characteristic parameters the coefficients c_0 and c_1 from Equation 7 are calibrated by minimising the root-mean-square error ε between the formula and measured data-points:

$$\varepsilon = \sqrt{\frac{1}{i} \sum_{j=1}^i \left(\frac{(z_{2\%} / \gamma H_s)_{\text{formula}}}{(z_{2\%} / \gamma H_s)_{\text{measured}}} - 1 \right)^2} \quad (8)$$

For the characteristic wave heights in Equation 7 three alternative parameters are used, i.e. the “spectral significant wave height” H_{m0} , the significant wave height H_s and the wave height exceeded by 2% of the incident waves $H_{2\%}$. The wave run-up is also made non-dimensional with the corresponding characteristic wave height. Table 12 shows the results where the wave period $T_{m-1,0}$ is used and the characteristic slopes according Figure 5. Using the significant wave height H_s yields the smallest deviations from the main trend.

Wave height	c_0	c_1	ε
H_{m0}	1.4	4.4	0.066
H_s	1.55	5	0.052
$H_{2\%}$	1.4	3.6	0.056

Table 12 Influence of using different characteristic wave heights (using the wave period $T_{m-1,0}$ and the characteristic slopes according Figure 5).

For the characteristic wave period four parameters are used, i.e. the peak wave period T_p , the wave period $T_{m-1,0}$, the wave period $T_{m0,1}$ and the mean wave period T_m . Table 13 shows the results where the wave height H_s is used and the characteristic slopes according Figure 5. Using the wave period $T_{m-1,0}$ yields the smallest deviations from the main trend. This confirms conclusions drawn from the numerical model investigations described in Van Gent (1999).

Wave period	c_0	c_1	ε
T_p	1.45	4.4	0.068
$T_{m-1,0}$	1.55	5	0.052
$T_{m0,1}$	2	6	0.081
T_m	2.15	6	0.094

Table 13 Influence of using different characteristic wave periods (using the wave height H_s and the characteristic slopes according Figure 5).

For the characteristic slopes three methods are used: A constant slope for all tests (taken equal to the slope of the section below the berm, i.e. $\cot \varphi = 4.5$), the method defined in Figure 5 and the method described in De Waal and Van der Meer (1992). Table 14 shows the results where the wave height H_s is used and the wave period $T_{m-1,0}$. Although the differences are small, the characteristic slopes according the method defined in Figure 5 yields the smallest deviations from the main trend. The method for the characteristic slope by De Waal and Van der Meer (1992) nearly provides the same performance but this method is much more complex without resulting in an improved description of the influence of the berm. Nevertheless, the method defined in Figure 5 needs to be verified based on test results with other types of berms before this simple approach can be used for a wider range of berm-types.

Characteristic slopes	c_0	c_1	ε
$\cot \varphi = 4.5$	1.4	5	0.062
Method from Figure 5	1.55	5	0.052
De Waal and Van der Meer (1992)	2	4.7	0.054

Table 14 Influence of using different methods for the characteristic slopes (using the wave height H_s and the wave period $T_{m-1,0}$).

The results from the above described sensitivity analysis indicate that using the surf-similarity parameter based on the significant wave height H_s , the wave period $T_{m-1,0}$ and the characteristic slopes based on the method defined in Figure 5 results in the best formula for describing wave run-up for the wave conditions in the present tests.

The choice of the procedure of analysis affects the wave heights and wave periods. Using the low-pass and high-pass filtering procedure as applied here, results in lower values (H_s , H_{m0} , $H_{2\%}$, T_m , $T_{m0,1}$, $T_{m-1,0}$, T_p), especially because in the frequencies lower than the lower cut-off frequency an amount of wave energy is present. To provide an impression of the influence of this filtering compared to values obtained if no filtering is applied, the average differences between values obtained with and without filtering are given for the position at the toe of the dike: $\Delta H_s=6\%$, $\Delta H_{m0}=9\%$, $\Delta H_{2\%}=6\%$, $\Delta T_m=2\%$, $\Delta T_{m0,1}=13\%$, $\Delta T_{m-1,0}=34\%$, $\Delta T_p=30\%$. It is clear that these differences are far from negligible. Analysis of the data without filtering however provides the same conclusions, including those concerning the optimal characteristic parameters (see Tables 12, 13 and 14). Also the magnitude of the deviations from the trends are similar (values for ε are similar, expect that the differences between H_{m0} and H_s as characteristic parameters for the wave height become negligibly small). The values for c_0 and c_1 in Equation 7 are however different. Without filtering the optimal values for these coefficients are 1.25 and 4.1 respectively instead of 1.55 and 5 with the applied filtering. The standard deviation of the differences between the formula and the measurements reduces slightly from 0.18 to 0.14. It is not desirable to apply filtering procedures which neglect such a large amount of wave energy of which especially the wave energy in the lower frequencies is considered as contributing to wave run-up. Nevertheless, the data presented in this report concern data based on the described filtering procedure since this was set as the procedure of analysis for mutual comparison of data from the different institutes (prototype measurements and physical model tests) within the framework of the MAST-OPTICREST project.

Crest elevation

Based on the results summarised in Equation 7 with $c_0=1.55$ and $c_1=5$ predictions can be made of situations where the 2% wave run-up levels with water layers thicker than 0.1 m will exceed the crest. Table 15 shows for a few water levels (using $H_{s-toe} = 0.5 d_{toe}$ as a rough approximation for depth-limited situations) examples of wave conditions at the toe of the dike that are expected to cause such overtopping.

SWL	H_s	$T_{m-1,0}$	s_{-1}
NAP+4.2 m	2.4	18.5	0.005
NAP+4.7 m	2.7	13.5	0.009
NAP+5.2 m	2.9	11.1	0.015

Table 15 Examples of wave conditions at the toe of the dike which are expected to lead to wave run-up levels higher than the crest.

For the tests for which the 2% wave run-up levels exceeded the crest elevation Equation 7 also provides wave run-up levels above the crest.

5 Conclusions and recommendations

Based on the investigations described in this report the following conclusions and recommendations are made:

Conclusions:

- Comparisons of storms measured in prototype and storms modelled in physical model tests show good agreement. Wave heights measured at three measurement positions show in average 1.5%, 3.4% and 8.8% differences in the significant wave height. The non-dimensional wave run-up levels differ only 4% on average.
- Considering the observed differences between prototype measurements and model tests it can be concluded that schematisation and scale effects in the model tests are acceptably small.
- Measurement techniques for generating waves in a flume, including the generation of bound long waves, also allow for a rather accurate prescription of specified wave energy spectra at specific locations on the foreshore.
- The formula by De Waal and Van der Meer (1992) using the deep-water wave steepness in the surf-similarity parameter provides poor predictions (scatter and underestimates) of the wave run-up levels in the present tests; this is partly because the foreshore changes the peak wave period considerably.
- The influence of the choice of characteristic parameters in the surf-similarity parameter is studied for the present tests. Of the characteristic parameters studied, the best characteristic parameters for the wave height, wave period and slope are H_s , $T_{m-1,0}$ and the method defined in Figure 5.
- Tests with variations of wave height, wave steepness, water levels and spectral shapes confirm that wave run-up levels can be described by using the surf-similarity parameter $\xi_{s,-1}$ and the equation given in Van Gent (1999):

$$\begin{aligned} z_{2\%} / (\gamma H_s) &= c_0 \xi_{s,-1} & \text{for } \xi_{s,-1} \leq p \\ z_{2\%} / (\gamma H_s) &= c_1 - c_2 / \xi_{s,-1} & \text{for } \xi_{s,-1} \geq p \end{aligned} \quad (9)$$

where the wave height and wave period are those at the toe of the structure, with $\xi_{s,-1} = \tan \phi / \sqrt{(2\pi/g \cdot H_s / T_{m-1,0}^2)}$. The presented data-points are best-described by using $c_0=1.55$, $c_1=5$, $c_2=0.25 c_1^2/c_0$ and $p=0.5 c_1 / c_0$ (with a standard deviation of 0.18). These values depend on the applied filter frequencies (without filtering yielded: $c_0=1.25$ and $c_1=4.1$). These values neglect water layers thinner than approximately 0.1 m. If these thin water layers are to be accounted for, the values for c_0 and c_1 are approximately 10% higher.

- The measurements show considerable amounts of wave energy in the lower frequencies. From examining the wave energy spectra at the toe of the structure, it can be seen that the peak period of the wave energy in the long waves is approximately 7 to 10 times longer than the peak period of the wave energy in the short waves. This indicates that

surfbeat-phenomena, the propagation of wave groups and their associated long wave motions, play a major role on the foreshore of Petten. Detailed analysis of surfbeat-phenomena is however not performed in this report.

Recommendations:

- It is recommended to study the effects of surfbeat-phenomena and their possible contribution to wave run-up levels more in detail.
- A simple method to obtain a characteristic slope angle was successfully applied in this report. It is recommended to study whether this simple approach can be used for a wider range of berm types.
- The data-set forms a basis for numerical analysis and validation of numerical models. It is recommended to study to which extent available numerical models are already able to model the extremely complex conditions on the foreshore and the structure.
- In the present data-set, tests were performed with depth-limited situations at the toe of the structure (the ratio between $H_{2\%}$ and H_s was between 1.18 and 1.46). It is recommended to study the effects of depth-limited situations at the toe of coastal structure on wave run-up and wave overtopping for a wider range of foreshores and structures.

Acknowledgements

This report is part of the EU-MAST project “OPTICREST” (contract MAS3-CT97-0116). The data on the prototype measurements at the Petten Sea-defence were kindly provided by RIKZ. In particular ir. S.R. Holterman is acknowledged for her contribution.

Furthermore, motivation and development of this work have been stimulated in the context of the joint research project “Wave propagation over shallow foreshores” of the Road and Hydraulic Engineering Division (DWW) of the Dutch Department of Public Works (Rijkswaterstaat) and WL | DELFT HYDRAULICS.

Prof. dr. ir. J.A. Battjes of the Delft University of Technology and participants within the “OPTICREST” project, in particular ir. S.R. Holterman, dr.ir. J.W. van der Meer and dipl.-ing. H. Schüttrumpf, are gratefully acknowledged for their comments on a preliminary version of this report.

References

- Battjes, J.A. (1974), *Computation of set-up, longshore currents, runoff and overtopping due to wind-generated waves*, Ph.D.-thesis, Also Comm. On Hydraulics, Dept. of Civil Engineering, Delft University of Technology, Report 74-2.
- De Haas, P.C.A., D.C. Rijks, B.G. Ruessink, J.A. Roelvink, A.J.H.M. Reniers, M.R.A. van Gent (1999), *Onderzoek naar lange golven bij Petten (in Dutch); Investigations on long waves at Petten*, Report by University Utrecht and Delft Hydraulics, Report H3345-January 1999, Delft.
- De Waal, J.P. and J.W. van der Meer (1992), *Wave run-up and overtopping on coastal structures*, Proc. ICCE'92, Vol.2, pp.1758-1771, Venice.
- Groenendijk, H.W. and M.R.A. van Gent (1998), *Shallow foreshore wave height statistics; A predictive model for the probability of exceedance of wave heights*, Delft Hydraulics Report H3351-October 1998, Delft.
- Groenendijk, H.W. (1998), *Shallow foreshore wave height statistics*, M.Sc.-thesis, Delft University of Technology, Also: Delft Hydraulics Report H3245-February 1998, Delft.
- Holterman, S (1998), *Golfploop op dijken met ondiepe voorlanden (in Dutch); Wave run-up at dikes with shallow foreshores*, M.Sc.-thesis, Delft University of Technology.
- Mansard, E. and E. Funke (1980), *The measurement of incident and reflected spectra using a least-square method*, Proc. ICCE'80, Sydney.
- Van der Meer, J.W. (1997), *Golfploop en golfoverslag bij dijken (in Dutch); Wave run-up and wave overtopping at dikes*, Delft Hydraulics Report H2458/H3051-June 1997, Delft.
- Van Gent, M.R.A. (1994), *The modelling of wave action on and in coastal structures*, Coastal Engineering, Vol.22 (3-4), pp.311-339, Elsevier, Amsterdam.
- Van Gent, M.R.A. (1995), *Wave interaction with permeable coastal structures*, Ph.D.-thesis, Delft University of Technology, ISBN 90-407-1182-8, Delft University Press, Delft.
- Van Gent, M.R.A. (1999), *Wave run-up and wave overtopping for double peaked wave energy spectra*, Delft Hydraulics Report H3351-January 1999, Delft.
- Wolf, F.C.J. (1998), *Description of field sites for the measurement of wave run-up*, RIKZ Report 98.138x-November 1998.

Tables

Tests 1.01-1.06: 'Measured storms'															
1.01	<i>x-crest</i>	<i>d</i>	<i>SWL</i>	<i>H_s</i>	<i>H_{m0}</i>	<i>H_{2%}</i>	<i>T_m</i>	<i>T_{m 0,1}</i>	<i>T_{m-1,0}</i>	<i>T_p</i>	<i>K_R</i>	<i>z_{2%}</i> (NAP)	<i>z_{10%}</i> (SWL)	<i>z_{2%}</i> (SWL)	<i>z_{1%}</i> (SWL)
DEEP	-1300	26.10	2.10	4.5	4.8	5.9	6.9	7.3	8.2	9.3	0.27	6.8	3.9	4.7	5.1
MP3	-635	10.30	2.10	3.9	4.1	5.1	7.6	8.1	9.4	10.8	0.33				
BAR	-475	5.60	2.10	2.8	3.1	3.4	7.2	7.6	10.0	11.8	0.50				
MP5	-300	10.10	2.10	2.5	2.7	3.0	7.0	7.4	9.4	10.8	0.44				
MP6	-130	4.34	2.10	2.2	2.5	2.8	6.8	7.3	10.9	13.0	0.61				
TOE*	-65	2.72	2.10	1.4	1.6	1.8	7.0	8.1	13.1	21.6					
1.02	<i>x-crest</i>	<i>d</i>	<i>SWL</i>	<i>H_s</i>	<i>H_{m0}</i>	<i>H_{2%}</i>	<i>T_m</i>	<i>T_{m 0,1}</i>	<i>T_{m-1,0}</i>	<i>T_p</i>	<i>K_R</i>	<i>z_{2%}</i> (NAP)	<i>z_{10%}</i> (SWL)	<i>z_{2%}</i> (SWL)	<i>z_{1%}</i> (SWL)
DEEP	-1300	26.04	2.04	4.3	4.5	5.7	7.2	7.8	8.7	8.1	0.26	6.9	3.9	4.8	5.4
MP3	-635	10.24	2.04	3.9	4.1	5.2	7.7	8.3	9.5	10.8	0.33				
BAR	-475	5.54	2.04	2.8	3.2	3.5	7.1	7.7	10.1	10.8	0.51				
MP5	-300	10.04	2.04	2.5	2.7	3.1	7.1	7.7	9.7	10.8	0.44				
MP6	-130	4.28	2.04	2.2	2.5	2.7	6.7	7.5	11.0	14.4	0.63				
TOE*	-65	2.66	2.04	1.4	1.6	1.9	7.0	8.0	13.1	18.5					
1.03	<i>x-crest</i>	<i>d</i>	<i>SWL</i>	<i>H_s</i>	<i>H_{m0}</i>	<i>H_{2%}</i>	<i>T_m</i>	<i>T_{m 0,1}</i>	<i>T_{m-1,0}</i>	<i>T_p</i>	<i>K_R</i>	<i>z_{2%}</i> (NAP)	<i>z_{10%}</i> (SWL)	<i>z_{2%}</i> (SWL)	<i>z_{1%}</i> (SWL)
DEEP	-1300	26.24	2.24	3.7	3.9	5.0	7.2	8.0	9.7	14.4	0.30	7.5	4.2	5.3	5.6
MP3	-635	10.44	2.24	3.5	3.7	4.7	7.9	8.7	10.7	14.4	0.35				
BAR	-475	5.74	2.24	2.8	3.1	3.5	7.3	8.1	11.1	16.2	0.52				
MP5	-300	10.24	2.24	2.5	2.7	3.1	7.3	7.9	10.4	16.2	0.47				
MP6	-130	4.48	2.24	2.2	2.5	2.7	7.1	8.0	12.1	16.2	0.64				
TOE*	-65	2.86	2.24	1.4	1.7	2.0	7.5	8.7	14.2	18.5					
1.04	<i>x-crest</i>	<i>d</i>	<i>SWL</i>	<i>H_s</i>	<i>H_{m0}</i>	<i>H_{2%}</i>	<i>T_m</i>	<i>T_{m 0,1}</i>	<i>T_{m-1,0}</i>	<i>T_p</i>	<i>K_R</i>	<i>z_{2%}</i> (NAP)	<i>z_{10%}</i> (SWL)	<i>z_{2%}</i> (SWL)	<i>z_{1%}</i> (SWL)
DEEP	-1300	25.66	1.66	4.1	4.4	5.4	7.9	8.8	10.7	16.2	0.29	6.9	4.1	5.3	5.8
MP3	-635	9.86	1.66	3.9	4.2	5.1	8.4	9.3	11.5	16.2	0.34				
BAR	-475	5.16	1.66	2.7	3.0	3.4	7.9	8.6	12.0	16.2	0.53				
MP5	-300	9.66	1.66	2.3	2.5	2.9	7.0	7.8	10.4	7.2	0.50				
MP6	-130	3.90	1.66	2.0	2.3	2.7	7.2	8.1	12.4	18.5	0.68				
TOE*	-65	2.28	1.66	1.2	1.4	1.8	7.4	9.0	14.7	21.6					
1.05	<i>x-crest</i>	<i>d</i>	<i>SWL</i>	<i>H_s</i>	<i>H_{m0}</i>	<i>H_{2%}</i>	<i>T_m</i>	<i>T_{m 0,1}</i>	<i>T_{m-1,0}</i>	<i>T_p</i>	<i>K_R</i>	<i>z_{2%}</i> (NAP)	<i>z_{10%}</i> (SWL)	<i>z_{2%}</i> (SWL)	<i>z_{1%}</i> (SWL)
DEEP	-1300	25.60	1.60	2.9	3.1	3.9	7.1	7.8	9.4	13.0	0.29	5.7	4.1	4.5	
MP3	-635	9.80	1.60	2.8	3.0	3.6	7.6	8.5	10.3	13.0	0.35				
BAR	-475	5.10	1.60	2.4	2.7	3.1	7.1	7.7	10.4	14.4	0.50				
MP5	-300	9.60	1.60	2.2	2.3	2.7	7.0	7.6	9.8	14.4	0.44				
MP6	-130	3.84	1.60	1.9	2.2	2.5	6.9	7.5	11.1	13.0	0.64				
TOE*	-65	2.22	1.60	1.1	1.3	1.5	6.9	8.1	13.1	21.6					
1.06	<i>x-crest</i>	<i>d</i>	<i>SWL</i>	<i>H_s</i>	<i>H_{m0}</i>	<i>H_{2%}</i>	<i>T_m</i>	<i>T_{m 0,1}</i>	<i>T_{m-1,0}</i>	<i>T_p</i>	<i>K_R</i>	<i>z_{2%}</i> (NAP)	<i>z_{10%}</i> (SWL)	<i>z_{2%}</i> (SWL)	<i>z_{1%}</i> (SWL)
DEEP	-1300	26.04	2.04	3.7	4.0	5.2	6.9	7.4	8.6	9.3	0.27	6.8	4.7	4.9	
MP3	-635	10.24	2.04	3.5	3.7	4.5	7.6	8.1	9.5	9.3	0.34				
BAR	-475	5.54	2.04	2.7	3.0	3.4	7.3	7.7	10.2	11.8	0.51				
MP5	-300	10.04	2.04	2.4	2.6	3.0	7.2	7.6	9.7	7.6	0.44				
MP6	-130	4.28	2.04	2.1	2.4	2.7	6.9	7.7	11.4	16.2	0.61				
TOE*	-65	2.66	2.04	1.4	1.6	1.8	7.2	8.2	13.1	21.6					
* data are based on tests without dike.															

* data are based on tests without dike.

Table A1 Measured wave conditions and wave run-up levels (Tests 1.01-1.06).

Tests 2.11-2.15: 'Variation of wave height (low water level; constant wave steepness)'															
2.11	<i>x-crest</i>	<i>d</i>	<i>SWL</i>	<i>H_s</i>	<i>H_{m0}</i>	<i>H_{2%}</i>	<i>T_m</i>	<i>T_{m 0,1}</i>	<i>T_{m-1,0}</i>	<i>T_p</i>	<i>K_R</i>	<i>z_{2%}</i> (NAP)	<i>z_{10%}</i> (SWL)	<i>z_{2%}</i> (SWL)	<i>z_{1%}</i> (SWL)
DEEP	-1300	26.10	2.10	2.0	2.0	2.8	7.0	7.2	7.7	8.6	0.26				
MP3	-635	10.30	2.10	1.9	1.9	2.5	7.0	7.4	7.8	8.6	0.31				
BAR	-475	5.60	2.10	1.8	1.9	2.4	6.7	7.0	7.8	8.6	0.40				
MP5	-300	10.10	2.10	1.7	1.8	2.2	6.9	7.4	8.1	8.6	0.34				
MP6	-130	4.34	2.10	1.7	1.8	2.2	6.2	6.6	7.7	8.6	0.50				
TOE*	-65	2.72	2.10	1.2	1.4	1.5	5.4	5.9	7.8	8.6					
2.12	<i>x-crest</i>	<i>d</i>	<i>SWL</i>	<i>H_s</i>	<i>H_{m0}</i>	<i>H_{2%}</i>	<i>T_m</i>	<i>T_{m 0,1}</i>	<i>T_{m-1,0}</i>	<i>T_p</i>	<i>K_R</i>	<i>z_{2%}</i> (NAP)	<i>z_{10%}</i> (SWL)	<i>z_{2%}</i> (SWL)	<i>z_{1%}</i> (SWL)
DEEP	-1300	26.10	2.10	3.0	3.1	4.1	8.4	8.9	9.5	10.8	0.25				
MP3	-635	10.30	2.10	3.0	3.0	4.2	8.7	9.1	9.7	10.8	0.30				
BAR	-475	5.60	2.10	2.6	2.8	3.3	7.4	7.8	9.2	10.8	0.45				
MP5	-300	10.10	2.10	2.4	2.5	2.8	7.6	8.2	9.4	10.8	0.37				
MP6	-130	4.34	2.10	2.1	2.4	2.6	6.6	7.0	9.3	10.8	0.57				
TOE*	-65	2.72	2.10	1.3	1.5	1.8	6.3	6.7	10.1	11.5					
												6.4		4.3	4.5
2.13	<i>x-crest</i>	<i>d</i>	<i>SWL</i>	<i>H_s</i>	<i>H_{m0}</i>	<i>H_{2%}</i>	<i>T_m</i>	<i>T_{m 0,1}</i>	<i>T_{m-1,0}</i>	<i>T_p</i>	<i>K_R</i>	<i>z_{2%}</i> (NAP)	<i>z_{10%}</i> (SWL)	<i>z_{2%}</i> (SWL)	<i>z_{1%}</i> (SWL)
DEEP	-1300	26.10	2.10	4.0	4.1	5.6	9.8	10.3	10.9	11.8	0.24				
MP3	-635	10.30	2.10	4.1	4.1	5.7	9.6	9.8	10.8	11.8	0.31				
BAR	-475	5.60	2.10	2.9	3.2	3.5	8.0	8.6	10.6	11.8	0.51				
MP5	-300	10.10	2.10	2.6	2.8	3.1	7.4	8.2	9.9	11.8	0.44				
MP6	-130	4.34	2.10	2.3	2.6	2.8	7.1	7.8	11.1	14.4	0.62				
TOE*	-65	2.72	2.10	1.4	1.6	1.9	7.5	8.4	12.8	16.2					
												7.1	4.1	5.0	5.4
2.14	<i>x-crest</i>	<i>d</i>	<i>SWL</i>	<i>H_s</i>	<i>H_{m0}</i>	<i>H_{2%}</i>	<i>T_m</i>	<i>T_{m 0,1}</i>	<i>T_{m-1,0}</i>	<i>T_p</i>	<i>K_R</i>	<i>z_{2%}</i> (NAP)	<i>z_{10%}</i> (SWL)	<i>z_{2%}</i> (SWL)	<i>z_{1%}</i> (SWL)
DEEP	-1300	26.10	2.10	5.2	5.2	7.1	11.0	11.4	12.3	13.0	0.21				
MP3	-635	10.30	2.10	5.1	5.0	6.5	10.4	10.4	11.9	13.0	0.31				
BAR	-475	5.60	2.10	3.1	3.3	3.7	9.0	9.4	11.9	14.4	0.52				
MP5	-300	10.10	2.10	2.6	2.8	3.1	7.5	8.2	10.3	14.4	0.47				
MP6	-130	4.34	2.10	2.4	2.7	3.1	7.4	8.1	11.6	14.4	0.63				
TOE*	-65	2.72	2.10	1.5	1.7	2.1	8.1	9.1	13.9	18.5					
												7.6	4.4	5.5	6.1
2.15	<i>x-crest</i>	<i>d</i>	<i>SWL</i>	<i>H_s</i>	<i>H_{m0}</i>	<i>H_{2%}</i>	<i>T_m</i>	<i>T_{m 0,1}</i>	<i>T_{m-1,0}</i>	<i>T_p</i>	<i>K_R</i>	<i>z_{2%}</i> (NAP)	<i>z_{10%}</i> (SWL)	<i>z_{2%}</i> (SWL)	<i>z_{1%}</i> (SWL)
DEEP	-1300	26.10	2.10	6.1	6.2	8.4	11.7	12.2	13.1	14.4	0.19				
MP3	-635	10.30	2.10	5.6	5.5	6.9	10.9	10.6	12.5	14.4	0.31				
BAR	-475	5.60	2.10	3.2	3.4	3.8	9.8	9.9	12.7	14.4	0.50				
MP5	-300	10.10	2.10	2.6	2.9	3.2	7.6	8.2	10.6	16.2	0.47				
MP6	-130	4.34	2.10	2.4	2.7	3.0	7.3	8.1	11.7	14.4	0.63				
TOE*	-65	2.72	2.10	1.5	1.7	2.1	8.0	9.3	14.1	18.5					
												8.4	4.8	6.3	7.0
* data are based on tests without dike.															

* data are based on tests without dike.

Table A2 Measured wave conditions and wave run-up levels (Tests 2.11-2.15).

Tests 2.21-2.25: 'Variation of wave height (high water level; constant wave steepness)'															
2.21	<i>x-crest</i>	<i>d</i>	<i>SWL</i>	<i>H_s</i>	<i>H_{m0}</i>	<i>H_{2%}</i>	<i>T_m</i>	<i>T_{m 0,1}</i>	<i>T_{m-1,0}</i>	<i>T_p</i>	<i>K_R</i>	<i>z_{2%}</i> (NAP)	<i>z_{10%}</i> (SWL)	<i>z_{2%}</i> (SWL)	<i>z_{1%}</i> (SWL)
DEEP	-1300	28.70	4.70	1.9	2.0	2.7	7.0	7.2	7.6	8.6	0.33				
MP3	-635	12.90	4.70	1.8	1.8	2.5	7.0	7.4	7.8	8.6	0.37				
BAR	-475	8.20	4.70	1.8	1.8	2.5	6.9	7.3	7.9	8.6	0.40				
MP5	-300	12.70	4.70	1.7	1.7	2.2	7.1	7.4	7.9	8.6	0.41				
MP6	-130	6.94	4.70	1.8	1.8	2.5	7.0	7.2	7.8	8.6	0.44				
TOE*	-65	5.32	4.70	1.7	1.8	2.4	6.9	7.2	7.9	8.6					
2.22	<i>x-crest</i>	<i>d</i>	<i>SWL</i>	<i>H_s</i>	<i>H_{m0}</i>	<i>H_{2%}</i>	<i>T_m</i>	<i>T_{m 0,1}</i>	<i>T_{m-1,0}</i>	<i>T_p</i>	<i>K_R</i>	<i>z_{2%}</i> (NAP)	<i>z_{10%}</i> (SWL)	<i>z_{2%}</i> (SWL)	<i>z_{1%}</i> (SWL)
DEEP	-1300	28.70	4.70	3.0	3.1	4.3	8.5	8.9	9.5	10.8	0.30				
MP3	-635	12.90	4.70	3.0	3.0	4.3	8.7	9.1	9.7	10.8	0.34				
BAR	-475	8.20	4.70	3.1	3.1	4.2	8.4	8.5	9.5	10.8	0.38				
MP5	-300	12.70	4.70	2.8	2.9	3.7	8.6	9.1	10.0	10.8	0.38				
MP6	-130	6.94	4.70	2.9	3.0	3.7	7.7	8.0	9.3	10.8	0.44				
TOE*	-65	5.32	4.70	2.2	2.4	2.9	7.3	7.6	9.1	10.2					
2.23	<i>x-crest</i>	<i>d</i>	<i>SWL</i>	<i>H_s</i>	<i>H_{m0}</i>	<i>H_{2%}</i>	<i>T_m</i>	<i>T_{m 0,1}</i>	<i>T_{m-1,0}</i>	<i>T_p</i>	<i>K_R</i>	<i>z_{2%}</i> (NAP)	<i>z_{10%}</i> (SWL)	<i>z_{2%}</i> (SWL)	<i>z_{1%}</i> (SWL)
DEEP	-1300	28.70	4.70	4.0	4.1	5.7	9.7	10.3	11.0	11.8	0.23				
MP3	-635	12.90	4.70	4.1	4.1	5.7	10.1	10.2	11.0	11.8	0.27				
BAR	-475	8.20	4.70	3.9	3.9	4.8	9.4	9.1	10.6	11.8	0.36				
MP5	-300	12.70	4.70	3.5	3.6	4.2	9.0	9.7	10.9	11.8	0.31				
MP6	-130	6.94	4.70	3.4	3.7	4.2	8.0	8.5	10.6	13.0	0.42				
TOE*	-65	5.32	4.70	2.5	2.8	3.1	7.4	7.9	10.3	11.8					
2.24	<i>x-crest</i>	<i>d</i>	<i>SWL</i>	<i>H_s</i>	<i>H_{m0}</i>	<i>H_{2%}</i>	<i>T_m</i>	<i>T_{m 0,1}</i>	<i>T_{m-1,0}</i>	<i>T_p</i>	<i>K_R</i>	<i>z_{2%}</i> (NAP)	<i>z_{10%}</i> (SWL)	<i>z_{2%}</i> (SWL)	<i>z_{1%}</i> (SWL)
DEEP	-1300	28.70	4.70	5.0	5.1	6.9	10.9	11.5	12.3	13.0	0.21				
MP3	-635	12.90	4.70	5.2	5.1	7.1	10.9	10.9	12.1	13.0	0.26				
BAR	-475	8.20	4.70	4.4	4.4	5.2	9.8	9.6	11.6	13.0	0.37				
MP5	-300	12.70	4.70	3.7	4.0	4.3	8.8	9.4	11.0	13.0	0.32				
MP6	-130	6.94	4.70	3.8	4.0	4.4	8.9	9.4	12.1	14.4	0.42				
TOE*	-65	5.32	4.70	2.8	3.1	3.3	9.1	9.4	12.4	13.7					
2.25	<i>x-crest</i>	<i>d</i>	<i>SWL</i>	<i>H_s</i>	<i>H_{m0}</i>	<i>H_{2%}</i>	<i>T_m</i>	<i>T_{m 0,1}</i>	<i>T_{m-1,0}</i>	<i>T_p</i>	<i>K_R</i>	<i>z_{2%}</i> (NAP)	<i>z_{10%}</i> (SWL)	<i>z_{2%}</i> (SWL)	<i>z_{1%}</i> (SWL)
DEEP	-1300	28.70	4.70	6.0	6.1	8.2	11.8	12.2	13.2	14.4	0.20				
MP3	-635	12.90	4.70	6.1	5.9	8.0	11.2	11.1	12.6	14.4	0.26				
BAR	-475	8.20	4.70	4.4	4.7	5.4	9.5	9.7	12.0	14.4	0.39				
MP5	-300	12.70	4.70	3.8	4.1	4.4	8.9	9.3	11.2	14.4	0.35				
MP6	-130	6.94	4.70	3.9	4.1	4.6	9.0	9.5	12.5	16.2	0.45				
TOE*	-65	5.32	4.70	2.9	3.1	3.5	9.2	9.6	13.0	16.2					
* data are based on tests without dike.															

Table A3 Measured wave conditions and wave run-up levels (Tests 2.21-2.25).

Tests 2.31-2.34: 'Variation of wave steepness (low water level)'															
2.31	<i>x-crest</i>	<i>d</i>	<i>SWL</i>	<i>H_s</i>	<i>H_{m0}</i>	<i>H_{2%}</i>	<i>T_m</i>	<i>T_{m 0,1}</i>	<i>T_{m-1,0}</i>	<i>T_p</i>	<i>K_R</i>	<i>z_{2%}</i> (<i>NAP</i>)	<i>z_{10%}</i> (<i>SWL</i>)	<i>z_{2%}</i> (<i>SWL</i>)	<i>z_{1%}</i> (<i>SWL</i>)
DEEP	-1300	26.10	2.10	3.9	4.0	5.3	10.3	6.5	6.7	6.8	0.22				
MP3	-635	10.30	2.10	3.3	3.4	4.4	11.1	6.7	7.1	7.2	0.28				
BAR	-475	5.60	2.10	2.4	2.6	2.9	12.4	6.3	7.4	7.2	0.46				
MP5	-300	10.10	2.10	2.3	2.5	2.8	13.5	6.7	7.5	7.6	0.31				
MP6	-130	4.34	2.10	2.0	2.2	2.5	5.9	6.2	7.9	7.2	0.53				
TOE*	-65	2.72	2.10	1.3	1.5	1.6	5.6	6.0	9.0	6.8					
2.32	<i>x-crest</i>	<i>d</i>	<i>SWL</i>	<i>H_s</i>	<i>H_{m0}</i>	<i>H_{2%}</i>	<i>T_m</i>	<i>T_{m 0,1}</i>	<i>T_{m-1,0}</i>	<i>T_p</i>	<i>K_R</i>	<i>z_{2%}</i> (<i>NAP</i>)	<i>z_{10%}</i> (<i>SWL</i>)	<i>z_{2%}</i> (<i>SWL</i>)	<i>z_{1%}</i> (<i>SWL</i>)
DEEP	-1300	26.10	2.10	4.1	4.2	5.8	7.4	7.8	8.2	8.6	0.22				
MP3	-635	10.30	2.10	3.8	3.8	5.2	7.5	7.9	8.5	8.6	0.29				
BAR	-475	5.60	2.10	2.7	3.0	3.3	6.7	7.1	8.6	9.3	0.47				
MP5	-300	10.10	2.10	2.4	2.6	3.0	7.1	7.4	8.7	9.3	0.37				
MP6	-130	4.34	2.10	2.1	2.4	2.7	6.3	6.8	9.3	10.0	0.59				
TOE*	-65	2.72	2.10	1.4	1.5	1.8	6.3	7.0	10.6	10.4					
2.33	<i>x-crest</i>	<i>d</i>	<i>SWL</i>	<i>H_s</i>	<i>H_{m0}</i>	<i>H_{2%}</i>	<i>T_m</i>	<i>T_{m 0,1}</i>	<i>T_{m-1,0}</i>	<i>T_p</i>	<i>K_R</i>	<i>z_{2%}</i> (<i>NAP</i>)	<i>z_{10%}</i> (<i>SWL</i>)	<i>z_{2%}</i> (<i>SWL</i>)	<i>z_{1%}</i> (<i>SWL</i>)
DEEP	-1300	26.10	2.10	4.0	4.1	5.6	9.8	10.3	10.9	11.8	0.24				
MP3	-635	10.30	2.10	4.1	4.1	5.7	9.6	9.8	10.8	11.8	0.31				
BAR	-475	5.60	2.10	2.9	3.2	3.5	8.0	8.6	10.6	11.8	0.51				
MP5	-300	10.10	2.10	2.6	2.8	3.1	7.4	8.2	9.9	11.8	0.44				
MP6	-130	4.34	2.10	2.3	2.6	2.8	7.1	7.8	11.1	14.4	0.62				
TOE*	-65	2.72	2.10	1.4	1.6	1.9	7.5	8.4	12.8	16.2					
2.34	<i>x-crest</i>	<i>d</i>	<i>SWL</i>	<i>H_s</i>	<i>H_{m0}</i>	<i>H_{2%}</i>	<i>T_m</i>	<i>T_{m 0,1}</i>	<i>T_{m-1,0}</i>	<i>T_p</i>	<i>K_R</i>	<i>z_{2%}</i> (<i>NAP</i>)	<i>z_{10%}</i> (<i>SWL</i>)	<i>z_{2%}</i> (<i>SWL</i>)	<i>z_{1%}</i> (<i>SWL</i>)
DEEP	-1300	26.10	2.10	3.8	3.9	5.3	14.3	15.1	16.3	18.5	0.26				
MP3	-635	10.30	2.10	4.4	4.2	6.2	13.3	12.1	14.4	18.5	0.31				
BAR	-475	5.60	2.10	2.8	3.0	3.7	9.6	10.1	13.5	18.5	0.53				
MP5	-300	10.10	2.10	2.5	2.7	3.0	7.7	8.5	11.0	18.5	0.48				
MP6	-130	4.34	2.10	2.3	2.6	2.9	7.7	8.7	12.4	18.5	0.65				
TOE*	-65	2.72	2.10	1.4	1.6	1.9	8.4	9.3	14.2	20.8					
* data are based on tests without dike.															

* data are based on tests without dike.

Table A4 Measured wave conditions and wave run-up levels (Tests 2.31-2.34).

Tests 2.41-2.44: 'Variation of wave steepness (high water level)'															
2.41	<i>x-crest</i>	<i>d</i>	<i>SWL</i>	<i>H_s</i>	<i>H_{m0}</i>	<i>H_{2%}</i>	<i>T_m</i>	<i>T_{m 0,1}</i>	<i>T_{m-1,0}</i>	<i>T_p</i>	<i>K_R</i>	<i>z_{2%}</i> (<i>NAP</i>)	<i>z_{10%}</i> (<i>SWL</i>)	<i>z_{2%}</i> (<i>SWL</i>)	<i>z_{1%}</i> (<i>SWL</i>)
DEEP	-1300	28.70	4.70	3.8	3.9	5.1	6.1	6.4	6.7	6.8	0.26				
MP3	-635	12.90	4.70	3.4	3.4	4.8	6.4	6.7	6.9	7.2	0.28				
BAR	-475	8.20	4.70	3.0	3.1	3.8	6.3	6.6	7.1	7.2	0.37				
MP5	-300	12.70	4.70	2.9	3.0	3.7	6.7	6.8	7.2	7.2	0.31				
MP6	-130	6.94	4.70	2.8	2.9	3.6	6.4	6.7	7.3	7.2	0.41				
TOE*	-65	5.32	4.70	2.3	2.6	2.8	6.1	6.3	7.3	7.2					
2.42	<i>x-crest</i>	<i>d</i>	<i>SWL</i>	<i>H_s</i>	<i>H_{m0}</i>	<i>H_{2%}</i>	<i>T_m</i>	<i>T_{m 0,1}</i>	<i>T_{m-1,0}</i>	<i>T_p</i>	<i>K_R</i>	<i>z_{2%}</i> (<i>NAP</i>)	<i>z_{10%}</i> (<i>SWL</i>)	<i>z_{2%}</i> (<i>SWL</i>)	<i>z_{1%}</i> (<i>SWL</i>)
DEEP	-1300	28.70	4.70	4.1	4.2	5.8	7.4	7.7	8.2	9.3	0.26				
MP3	-635	12.90	4.70	3.8	3.9	5.3	7.6	7.9	8.4	9.3	0.31				
BAR	-475	8.20	4.70	3.6	3.6	4.5	7.4	7.6	8.5	9.3	0.38				
MP5	-300	12.70	4.70	3.2	3.4	3.9	7.6	7.9	8.7	9.3	0.35				
MP6	-130	6.94	4.70	3.1	3.3	3.9	7.1	7.5	8.7	9.3	0.44				
TOE*	-65	5.32	4.70	2.4	2.7	3.0	6.6	7.0	8.5	8.8					
2.43	<i>x-crest</i>	<i>d</i>	<i>SWL</i>	<i>H_s</i>	<i>H_{m0}</i>	<i>H_{2%}</i>	<i>T_m</i>	<i>T_{m 0,1}</i>	<i>T_{m-1,0}</i>	<i>T_p</i>	<i>K_R</i>	<i>z_{2%}</i> (<i>NAP</i>)	<i>z_{10%}</i> (<i>SWL</i>)	<i>z_{2%}</i> (<i>SWL</i>)	<i>z_{1%}</i> (<i>SWL</i>)
DEEP	-1300	28.70	4.70	4.0	4.1	5.7	9.7	10.3	11.0	11.8	0.23				
MP3	-635	12.90	4.70	4.1	4.1	5.7	10.1	10.2	11.0	11.8	0.27				
BAR	-475	8.20	4.70	3.9	3.9	4.8	9.4	9.1	10.6	11.8	0.36				
MP5	-300	12.70	4.70	3.5	3.6	4.2	9.0	9.7	10.9	11.8	0.31				
MP6	-130	6.94	4.70	3.4	3.7	4.2	8.0	8.5	10.6	13.0	0.42				
TOE*	-65	5.32	4.70	2.5	2.8	3.1	7.4	7.9	10.3	11.8					
2.44	<i>x-crest</i>	<i>d</i>	<i>SWL</i>	<i>H_s</i>	<i>H_{m0}</i>	<i>H_{2%}</i>	<i>T_m</i>	<i>T_{m 0,1}</i>	<i>T_{m-1,0}</i>	<i>T_p</i>	<i>K_R</i>	<i>z_{2%}</i> (<i>NAP</i>)	<i>z_{10%}</i> (<i>SWL</i>)	<i>z_{2%}</i> (<i>SWL</i>)	<i>z_{1%}</i> (<i>SWL</i>)
DEEP	-1300	28.70	4.70	3.8	3.9	5.1	14.3	15.2	16.4	18.5	0.31				
MP3	-635	12.90	4.70	4.4	4.2	6.3	14.5	13.4	15.3	18.5	0.32				
BAR	-475	8.20	4.70	3.9	3.9	5.3	11.6	10.9	13.7	18.5	0.44				
MP5	-300	12.70	4.70	3.5	3.5	4.2	9.6	9.9	12.1	18.5	0.41				
MP6	-130	6.94	4.70	3.5	3.7	4.3	9.7	10.2	13.5	18.5	0.49				
TOE*	-65	5.32	4.70	2.5	2.8	3.1	8.7	9.4	13.1	16.2					
* data are based on tests without dike.															

Table A5 Measured wave conditions and wave run-up levels (Tests 2.41-2.44).

Tests 2.51-2.54: 'Variation of wave steepness (high water level, high waves)'															
2.51	<i>x-crest</i>	<i>d</i>	<i>SWL</i>	<i>H_s</i>	<i>H_{m0}</i>	<i>H_{2%}</i>	<i>T_m</i>	<i>T_{m 0.1}</i>	<i>T_{m-1.0}</i>	<i>T_p</i>	<i>K_R</i>	<i>z_{2%}</i> (<i>NAP</i>)	<i>z_{10%}</i> (<i>SWL</i>)	<i>z_{2%}</i> (<i>SWL</i>)	<i>z_{1%}</i> (<i>SWL</i>)
DEEP	-1300	28.70	4.70	5.9	6.0	7.9	7.6	8.0	8.4	9.3	0.23				
MP3	-635	12.90	4.70	5.2	5.2	6.8	8.0	8.3	8.8	9.3	0.27				
BAR	-475	8.20	4.70	4.1	4.3	4.9	7.6	7.8	8.8	9.3	0.37				
MP5	-300	12.70	4.70	3.6	3.9	4.2	8.1	8.1	9.0	9.3	0.32				
MP6	-130	6.94	4.70	3.5	3.8	4.2	7.4	7.7	9.2	10.0	0.44				
TOE*	-65	5.32	4.70	2.7	3.0	3.2	6.9	7.2	9.3	10.0					
2.52	<i>x-crest</i>	<i>d</i>	<i>SWL</i>	<i>H_s</i>	<i>H_{m0}</i>	<i>H_{2%}</i>	<i>T_m</i>	<i>T_{m 0.1}</i>	<i>T_{m-1.0}</i>	<i>T_p</i>	<i>K_R</i>	<i>z_{2%}</i> (<i>NAP</i>)	<i>z_{10%}</i> (<i>SWL</i>)	<i>z_{2%}</i> (<i>SWL</i>)	<i>z_{1%}</i> (<i>SWL</i>)
DEEP	-1300	28.70	4.70	6.0	6.2	8.0	9.8	10.2	10.9	11.8	0.20				
MP3	-635	12.90	4.70	5.9	5.8	7.6	9.8	9.9	11.0	11.8	0.27				
BAR	-475	8.20	4.70	4.5	4.6	5.3	9.2	9.1	10.9	11.8	0.37				
MP5	-300	12.70	4.70	3.8	4.1	4.3	8.7	9.0	10.6	11.8	0.32				
MP6	-130	6.94	4.70	3.7	4.0	4.5	8.2	8.7	11.3	13.0	0.44				
TOE*	-65	5.32	4.70	2.8	3.1	3.5	8.1	8.5	11.6	13.0					
2.53	<i>x-crest</i>	<i>d</i>	<i>SWL</i>	<i>H_s</i>	<i>H_{m0}</i>	<i>H_{2%}</i>	<i>T_m</i>	<i>T_{m 0.1}</i>	<i>T_{m-1.0}</i>	<i>T_p</i>	<i>K_R</i>	<i>z_{2%}</i> (<i>NAP</i>)	<i>z_{10%}</i> (<i>SWL</i>)	<i>z_{2%}</i> (<i>SWL</i>)	<i>z_{1%}</i> (<i>SWL</i>)
DEEP	-1300	28.70	4.70	6.0	6.1	8.2	11.8	12.2	13.2	14.4	0.20				
MP3	-635	12.90	4.70	6.1	5.9	8.0	11.2	11.1	12.6	14.4	0.26				
BAR	-475	8.20	4.70	4.4	4.7	5.4	9.5	9.7	12.0	14.4	0.39				
MP5	-300	12.70	4.70	3.8	4.1	4.4	8.9	9.3	11.2	14.4	0.35				
MP6	-130	6.94	4.70	3.9	4.1	4.6	9.0	9.5	12.5	16.2	0.45				
TOE*	-65	5.32	4.70	2.9	3.1	3.5	9.2	9.6	13.0	16.2					
2.54	<i>x-crest</i>	<i>d</i>	<i>SWL</i>	<i>H_s</i>	<i>H_{m0}</i>	<i>H_{2%}</i>	<i>T_m</i>	<i>T_{m 0.1}</i>	<i>T_{m-1.0}</i>	<i>T_p</i>	<i>K_R</i>	<i>z_{2%}</i> (<i>NAP</i>)	<i>z_{10%}</i> (<i>SWL</i>)	<i>z_{2%}</i> (<i>SWL</i>)	<i>z_{1%}</i> (<i>SWL</i>)
DEEP	-1300	28.70	4.70	5.9	5.9	8.3	14.4	14.7	16.1	18.5	0.22				
MP3	-635	12.90	4.70	6.3	6.0	8.4	13.5	12.2	14.6	18.5	0.29				
BAR	-475	8.20	4.70	4.6	4.7	5.7	10.7	10.6	13.8	18.5	0.43				
MP5	-300	12.70	4.70	3.8	4.1	4.5	9.4	9.6	12.0	18.5	0.40				
MP6	-130	6.94	4.70	3.8	4.1	4.6	9.2	10.0	13.2	18.5	0.50				
TOE*	-65	5.32	4.70	2.9	3.2	3.6	9.2	10.0	13.8	18.8					
* data are based on tests without dike.															

Table A6 Measured wave conditions and wave run-up levels (Tests 2.51-2.54).

Tests 2.61-2.66: 'Variation of water level'															
2.61	<i>x-crest</i>	<i>d</i>	<i>SWL</i>	<i>H_s</i>	<i>H_{m0}</i>	<i>H_{2%}</i>	<i>T_m</i>	<i>T_{m 0,1}</i>	<i>T_{m-1,0}</i>	<i>T_p</i>	<i>K_R</i>	<i>z_{2%}</i> (NAP)	<i>z_{10%}</i> (SWL)	<i>z_{2%}</i> (SWL)	<i>z_{1%}</i> (SWL)
DEEP	-1300	25.30	1.30	3.9	4.0	5.4	9.8	10.2	10.9	11.8	0.21				
MP3	-635	9.50	1.30	4.0	3.9	5.5	9.6	9.6	10.7	11.8	0.29				
BAR	-475	4.80	1.30	2.6	2.8	3.1	7.9	8.5	10.8	11.8	0.52				
MP5	-300	9.30	1.30	2.2	2.3	2.6	6.9	7.6	9.5	11.8	0.44				
MP6	-130	3.54	1.30	1.9	2.1	2.4	6.9	7.6	11.2	14.1	0.67				
TOE*	-65	1.92	1.30	1.0	1.2	1.4	7.4	8.7	13.8	18.5					
2.62	<i>x-crest</i>	<i>d</i>	<i>SWL</i>	<i>H_s</i>	<i>H_{m0}</i>	<i>H_{2%}</i>	<i>T_m</i>	<i>T_{m 0,1}</i>	<i>T_{m-1,0}</i>	<i>T_p</i>	<i>K_R</i>	<i>z_{2%}</i> (NAP)	<i>z_{10%}</i> (SWL)	<i>z_{2%}</i> (SWL)	<i>z_{1%}</i> (SWL)
DEEP	-1300	26.10	2.10	4.0	4.1	5.6	9.8	10.3	10.9	11.8	0.24				
MP3	-635	10.30	2.10	4.1	4.1	5.7	9.6	9.8	10.8	11.8	0.31				
BAR	-475	5.60	2.10	2.9	3.2	3.5	8.0	8.6	10.6	11.8	0.51				
MP5	-300	10.10	2.10	2.6	2.8	3.1	7.4	8.2	9.9	11.8	0.44				
MP6	-130	4.34	2.10	2.3	2.6	2.8	7.1	7.8	11.1	14.4	0.62				
TOE*	-65	2.72	2.10	1.4	1.6	1.9	7.5	8.4	12.8	16.2					
2.63	<i>x-crest</i>	<i>d</i>	<i>SWL</i>	<i>H_s</i>	<i>H_{m0}</i>	<i>H_{2%}</i>	<i>T_m</i>	<i>T_{m 0,1}</i>	<i>T_{m-1,0}</i>	<i>T_p</i>	<i>K_R</i>	<i>z_{2%}</i> (NAP)	<i>z_{10%}</i> (SWL)	<i>z_{2%}</i> (SWL)	<i>z_{1%}</i> (SWL)
DEEP	-1300	26.90	2.90	4.0	4.1	5.4	9.8	10.3	11.0	11.8	0.26				
MP3	-635	11.10	2.90	4.1	4.1	5.7	9.7	9.9	10.9	11.8	0.31				
BAR	-475	6.40	2.90	3.3	3.5	4.1	8.3	8.7	10.5	11.8	0.47				
MP5	-300	10.90	2.90	2.9	3.1	3.5	7.8	8.6	10.2	11.8	0.41				
MP6	-130	5.14	2.90	2.7	3.0	3.3	7.5	8.1	11.0	13.0	0.55				
TOE*	-65	3.52	2.90	1.8	2.1	2.3	7.5	8.1	12.2	11.8					
2.64	<i>x-crest</i>	<i>d</i>	<i>SWL</i>	<i>H_s</i>	<i>H_{m0}</i>	<i>H_{2%}</i>	<i>T_m</i>	<i>T_{m 0,1}</i>	<i>T_{m-1,0}</i>	<i>T_p</i>	<i>K_R</i>	<i>z_{2%}</i> (NAP)	<i>z_{10%}</i> (SWL)	<i>z_{2%}</i> (SWL)	<i>z_{1%}</i> (SWL)
DEEP	-1300	27.80	3.80	4.0	4.1	5.4	9.8	10.3	10.9	11.8	0.24				
MP3	-635	12.00	3.80	4.1	4.1	5.7	9.9	10.1	11.0	11.8	0.29				
BAR	-475	7.30	3.80	3.6	3.7	4.5	8.6	8.9	10.5	11.8	0.41				
MP5	-300	11.80	3.80	3.3	3.4	3.8	8.5	9.1	10.5	11.8	0.35				
MP6	-130	6.04	3.80	3.1	3.4	3.8	7.8	8.3	10.8	13.0	0.49				
TOE*	-65	4.42	3.80	2.2	2.5	2.7	7.4	8.0	11.3	11.8					
2.65	<i>x-crest</i>	<i>d</i>	<i>SWL</i>	<i>H_s</i>	<i>H_{m0}</i>	<i>H_{2%}</i>	<i>T_m</i>	<i>T_{m 0,1}</i>	<i>T_{m-1,0}</i>	<i>T_p</i>	<i>K_R</i>	<i>z_{2%}</i> (NAP)	<i>z_{10%}</i> (SWL)	<i>z_{2%}</i> (SWL)	<i>z_{1%}</i> (SWL)
DEEP	-1300	28.70	4.70	4.0	4.1	5.7	9.7	10.3	11.0	11.8	0.23				
MP3	-635	12.90	4.70	4.1	4.1	5.7	10.1	10.2	11.0	11.8	0.27				
BAR	-475	8.20	4.70	3.9	3.9	4.8	9.4	9.1	10.6	11.8	0.36				
MP5	-300	12.70	4.70	3.5	3.6	4.2	9.0	9.7	10.9	11.8	0.31				
MP6	-130	6.94	4.70	3.4	3.7	4.2	8.0	8.5	10.6	13.0	0.42				
TOE*	-65	5.32	4.70	2.5	2.8	3.1	7.4	7.9	10.3	11.8					
2.66	<i>x-crest</i>	<i>d</i>	<i>SWL</i>	<i>H_s</i>	<i>H_{m0}</i>	<i>H_{2%}</i>	<i>T_m</i>	<i>T_{m 0,1}</i>	<i>T_{m-1,0}</i>	<i>T_p</i>	<i>K_R</i>	<i>z_{2%}</i> (NAP)	<i>z_{10%}</i> (SWL)	<i>z_{2%}</i> (SWL)	<i>z_{1%}</i> (SWL)
DEEP	-1300	29.60	5.60	4.0	4.1	5.6	9.9	10.3	11.0	11.8	0.26				
MP3	-635	13.80	5.60	4.0	4.0	5.6	9.9	10.3	11.1	11.8	0.29				
BAR	-475	9.10	5.60	4.0	4.0	5.0	9.6	9.5	10.8	11.8	0.35				
MP5	-300	13.60	5.60	3.7	3.7	4.5	9.2	9.9	11.0	11.8	0.33				
MP6	-130	7.84	5.60	3.6	3.8	4.6	8.3	8.7	10.6	13.0	0.41				
TOE*	-65	6.22	5.60	2.7	3.0	3.4	7.4	7.6	10.5	11.8					
* data are based on tests without dike.															

* data are based on tests without dike.

Table A7 Measured wave conditions and wave run-up levels (Tests 2.61-2.66).

<i>Tests 2.71-2.73: 'Variation of spectral shapes (double-peaked; low water level)'</i>															
2.71	<i>x-crest</i>	<i>d</i>	<i>SWL</i>	<i>H_s</i>	<i>H_{m0}</i>	<i>H_{2%}</i>	<i>T_m</i>	<i>T_{m 0,1}</i>	<i>T_{m-1,0}</i>	<i>T_p</i>	<i>K_R</i>	<i>z_{2%}</i> (NAP)	<i>z_{10%}</i> (SWL)	<i>z_{2%}</i> (SWL)	<i>z_{1%}</i> (SWL)
DEEP	-1300	26.10	2.10	3.8	4.1	5.2	6.8	7.4	8.5	11.8	0.28	7.1	4.0	5.0	5.5
MP3	-635	10.30	2.10	3.5	3.7	4.5	7.6	8.1	9.4	11.8	0.34				
BAR	-475	5.60	2.10	2.7	3.0	3.4	7.2	7.7	9.9	11.8	0.50				
MP5	-300	10.10	2.10	2.5	2.6	3.1	7.0	7.6	9.4	11.8	0.44				
MP6	-130	4.34	2.10	2.2	2.5	2.8	6.9	7.5	10.8	14.4	0.63				
TOE*	-65	2.72	2.10	1.4	1.6	1.8	7.1	8.0	12.6	21.6					
2.72	<i>x-crest</i>	<i>d</i>	<i>SWL</i>	<i>H_s</i>	<i>H_{m0}</i>	<i>H_{2%}</i>	<i>T_m</i>	<i>T_{m 0,1}</i>	<i>T_{m-1,0}</i>	<i>T_p</i>	<i>K_R</i>	<i>z_{2%}</i> (NAP)	<i>z_{10%}</i> (SWL)	<i>z_{2%}</i> (SWL)	<i>z_{1%}</i> (SWL)
DEEP	-1300	26.10	2.10	3.9	4.1	5.3	7.6	8.2	9.1	8.1	0.28	7.2	4.1	5.1	5.5
MP3	-635	10.30	2.10	3.7	3.8	4.9	7.9	8.5	9.6	10.8	0.34				
BAR	-475	5.60	2.10	2.8	3.1	3.6	7.3	7.8	10.0	11.8	0.52				
MP5	-300	10.10	2.10	2.5	2.7	3.0	7.2	7.7	9.7	11.8	0.46				
MP6	-130	4.34	2.10	2.1	2.4	2.7	6.8	7.6	11.3	14.4	0.65				
TOE*	-65	2.72	2.10	1.4	1.6	1.9	7.0	8.2	13.3	21.6					
2.73	<i>x-crest</i>	<i>d</i>	<i>SWL</i>	<i>H_s</i>	<i>H_{m0}</i>	<i>H_{2%}</i>	<i>T_m</i>	<i>T_{m 0,1}</i>	<i>T_{m-1,0}</i>	<i>T_p</i>	<i>K_R</i>	<i>z_{2%}</i> (NAP)	<i>z_{10%}</i> (SWL)	<i>z_{2%}</i> (SWL)	<i>z_{1%}</i> (SWL)
DEEP	-1300	26.10	2.10	3.9	4.1	5.4	8.7	9.2	10.0	10.8	0.26	7.2	4.1	5.1	5.6
MP3	-635	10.30	2.10	4.0	4.0	5.3	8.7	9.0	10.0	10.8	0.32				
BAR	-475	5.60	2.10	2.9	3.1	3.6	7.7	8.2	10.2	10.8	0.51				
MP5	-300	10.10	2.10	2.6	2.7	3.2	7.4	7.9	9.6	11.8	0.45				
MP6	-130	4.34	2.10	2.3	2.5	2.9	7.2	7.7	11.0	14.4	0.63				
TOE*	-65	2.72	2.10	1.4	1.6	1.9	7.4	8.4	13.8	21.6					

* data are based on tests without dike.

Table A8 Measured wave conditions and wave run-up levels (Tests 2.71-2.73).

Tests 2.81-2.83: 'Variation of spectral shapes (double-peaked; high water level)'															
2.81	<i>x-crest</i>	<i>d</i>	<i>SWL</i>	<i>H_s</i>	<i>H_{m0}</i>	<i>H_{2%}</i>	<i>T_m</i>	<i>T_{m 0,1}</i>	<i>T_{m-1,0}</i>	<i>T_p</i>	<i>K_R</i>	<i>z_{2%}</i> (<i>NAP</i>)	<i>z_{10%}</i> (<i>SWL</i>)	<i>z_{2%}</i> (<i>SWL</i>)	<i>z_{1%}</i> (<i>SWL</i>)
DEEP	-1300	28.70	4.70	3.9	4.2	5.3	6.8	7.4	8.6	11.8	0.27				
MP3	-635	12.90	4.70	3.6	3.8	4.7	7.5	8.1	9.3	11.8	0.30				
BAR	-475	8.20	4.70	3.4	3.7	4.4	7.6	8.1	9.7	11.8	0.37				
MP5	-300	12.70	4.70	3.2	3.4	4.0	7.6	8.2	9.6	11.8	0.33				
MP6	-130	6.94	4.70	3.1	3.4	4.0	7.4	7.9	10.0	11.8	0.42				
TOE*	-65	5.32	4.70	2.5	2.8	3.1	7.4	7.9	10.3	11.8					
2.82	<i>x-crest</i>	<i>d</i>	<i>SWL</i>	<i>H_s</i>	<i>H_{m0}</i>	<i>H_{2%}</i>	<i>T_m</i>	<i>T_{m 0,1}</i>	<i>T_{m-1,0}</i>	<i>T_p</i>	<i>K_R</i>	<i>z_{2%}</i> (<i>NAP</i>)	<i>z_{10%}</i> (<i>SWL</i>)	<i>z_{2%}</i> (<i>SWL</i>)	<i>z_{1%}</i> (<i>SWL</i>)
DEEP	-1300	28.70	4.70	3.9	4.0	5.3	7.9	8.3	9.3	11.8	0.27				
MP3	-635	12.90	4.70	3.8	3.9	5.1	8.0	8.6	9.7	11.8	0.31				
BAR	-475	8.20	4.70	3.5	3.7	4.5	7.6	8.3	9.9	11.8	0.39				
MP5	-300	12.70	4.70	3.3	3.5	4.1	8.1	8.7	10.2	11.8	0.35				
MP6	-130	6.94	4.70	3.1	3.4	4.0	7.5	7.9	10.2	11.8	0.44				
TOE*	-65	5.32	4.70	2.5	2.8	3.1	7.4	7.9	10.3	11.8					
2.83	<i>x-crest</i>	<i>d</i>	<i>SWL</i>	<i>H_s</i>	<i>H_{m0}</i>	<i>H_{2%}</i>	<i>T_m</i>	<i>T_{m 0,1}</i>	<i>T_{m-1,0}</i>	<i>T_p</i>	<i>K_R</i>	<i>z_{2%}</i> (<i>NAP</i>)	<i>z_{10%}</i> (<i>SWL</i>)	<i>z_{2%}</i> (<i>SWL</i>)	<i>z_{1%}</i> (<i>SWL</i>)
DEEP	-1300	28.70	4.70	4.0	4.1	5.5	8.6	9.1	9.9	10.8	0.25				
MP3	-635	12.90	4.70	4.0	4.0	5.4	8.8	9.3	10.1	10.8	0.29				
BAR	-475	8.20	4.70	3.8	3.8	4.8	8.2	8.5	9.9	10.8	0.38				
MP5	-300	12.70	4.70	3.5	3.6	4.1	8.5	8.9	10.2	11.8	0.33				
MP6	-130	6.94	4.70	3.3	3.6	4.1	7.6	8.0	10.1	11.8	0.43				
TOE*	-65	5.32	4.70	2.5	2.8	3.1	7.4	7.9	10.3	11.8					
* data are based on tests without dike.															

Table A9 Measured wave conditions and wave run-up levels (Tests 2.81-2.83).

<i>Tests 3.91-3.94: 'Tests for validation of numerical models (regular waves)'</i>								
3.91	<i>x-crest</i>	<i>d</i>	<i>SWL</i>	<i>H</i>	<i>T</i>	<i>K_R</i>	<i>z (NAP)</i>	<i>z (SWL)</i>
DEEP	-1300	28.70	4.70	4.4	6.0	0.11	8.0	3.3
MP3	-635	12.90	4.70	3.6	6.0	0.07		
BAR	-475	8.20	4.70	3.3	6.0	0.07		
MP5	-300	12.70	4.70	3.4	6.0	0.07		
MP6	-130	6.94	4.70	2.7	6.0	0.10		
3.92	<i>x-crest</i>	<i>d</i>	<i>SWL</i>	<i>H</i>	<i>T</i>	<i>K_R</i>	<i>z (NAP)</i>	<i>z (SWL)</i>
DEEP	-1300	28.70	4.70	4.3	8.0	0.14	8.3	3.6
MP3	-635	12.90	4.70	3.8	8.0	0.19		
BAR	-475	8.20	4.70	3.8	8.0	0.11		
MP5	-300	12.70	4.70	3.5	8.0	0.25		
MP6	-130	6.94	4.70	2.9	8.0	0.27		
3.93	<i>x-crest</i>	<i>d</i>	<i>SWL</i>	<i>H</i>	<i>T</i>	<i>K_R</i>	<i>z (NAP)</i>	<i>z (SWL)</i>
DEEP	-1300	28.70	4.70	4.1	10.0	0.12	8.0	3.3
MP3	-635	12.90	4.70	3.9	10.0	0.10		
BAR	-475	8.20	4.70	3.5	10.0	0.18		
MP5	-300	12.70	4.70	3.7	10.0	0.12		
MP6	-130	6.94	4.70	2.7	10.0	0.43		
3.94	<i>x-crest</i>	<i>d</i>	<i>SWL</i>	<i>H</i>	<i>T</i>	<i>K_R</i>	<i>z (NAP)</i>	<i>z (SWL)</i>
DEEP	-1300	28.70	4.70	4.1	12.0	0.06	8.6	3.9
MP3	-635	12.90	4.70	4.0	12.0	0.08		
BAR	-475	8.20	4.70	3.5	12.0	0.15		
MP5	-300	12.70	4.70	3.2	12.0	0.14		
MP6	-130	6.94	4.70	2.4	12.0	0.16		

Table A10 Measured wave conditions and wave run-up levels (Tests 3.91-3.94).

Figures

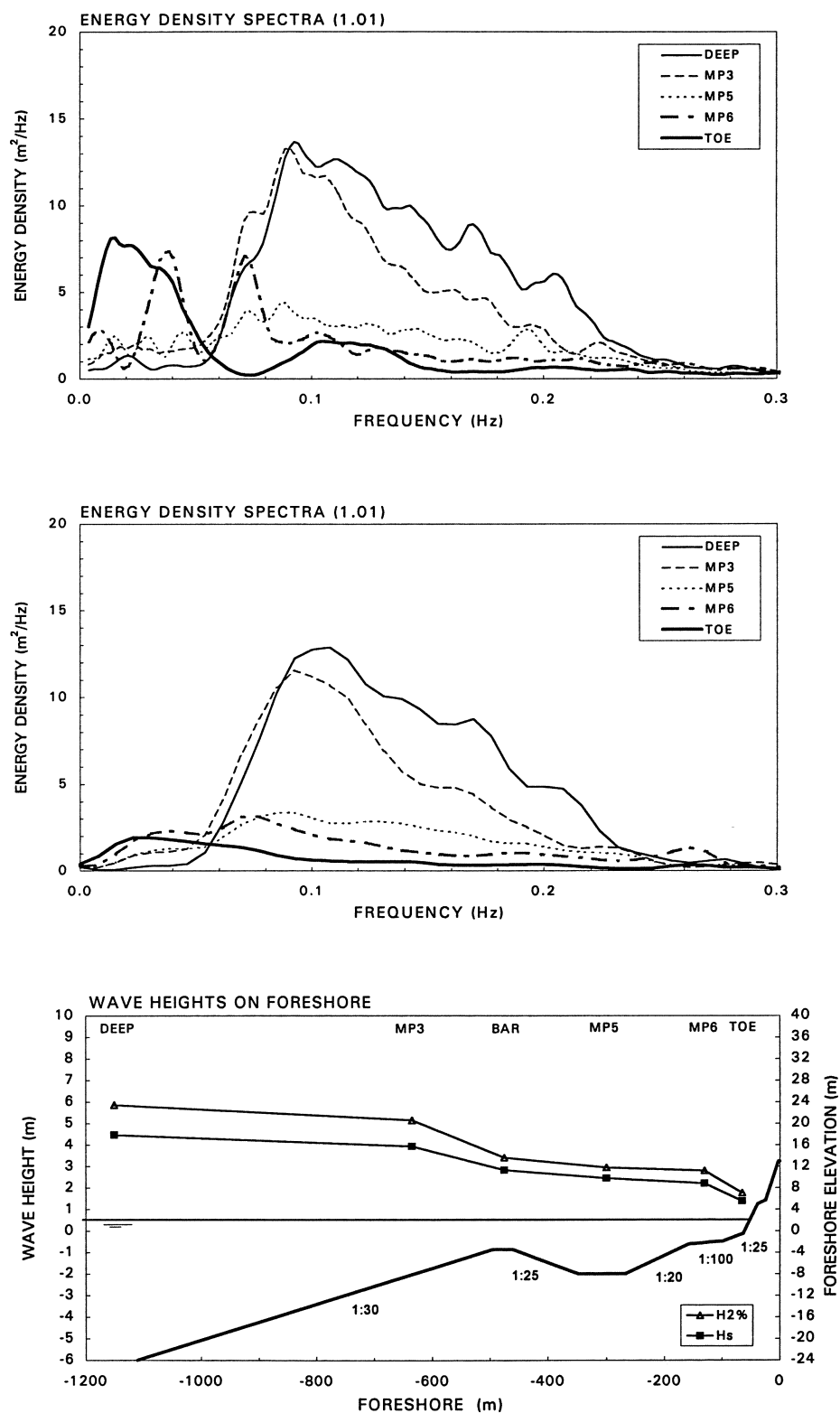


Figure F 1.01 Measured total wave energy spectra (upper), incident wave energy spectra (middle) and wave height evolution (lower).

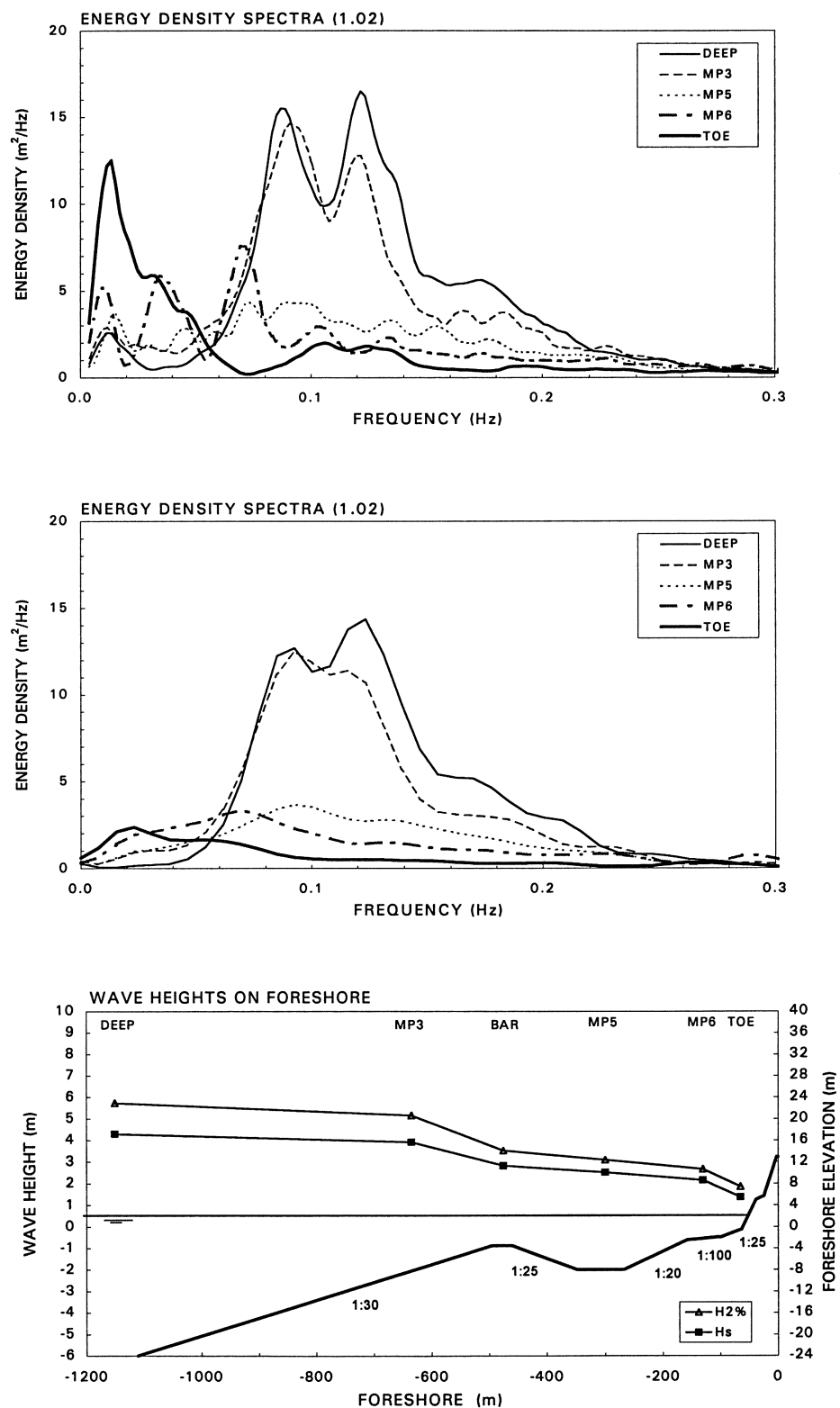


Figure F.1.02 Measured total wave energy spectra (upper), incident wave energy spectra (middle) and wave height evolution (lower).

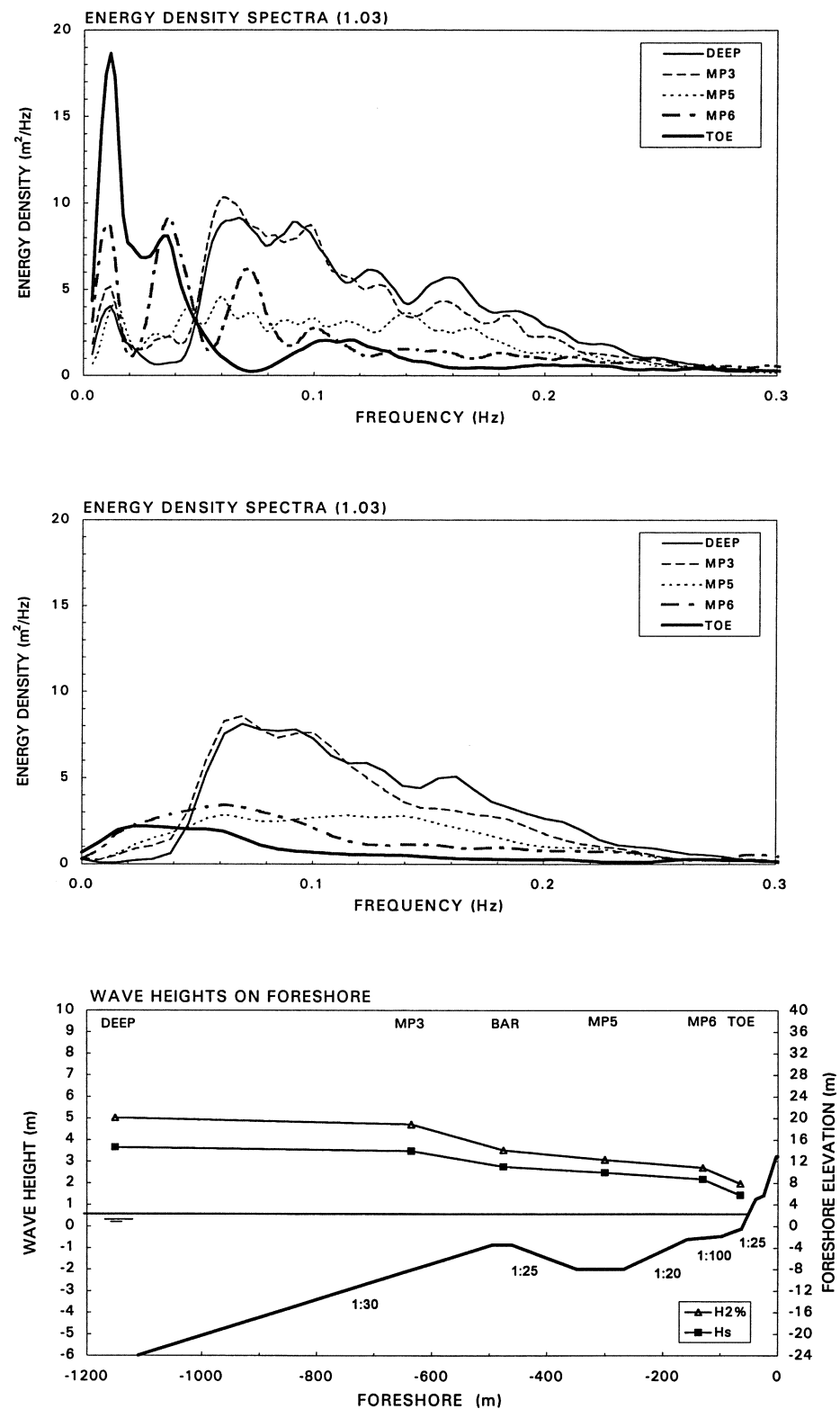


Figure F 1.03 Measured total wave energy spectra (upper), incident wave energy spectra (middle) and wave height evolution (lower).

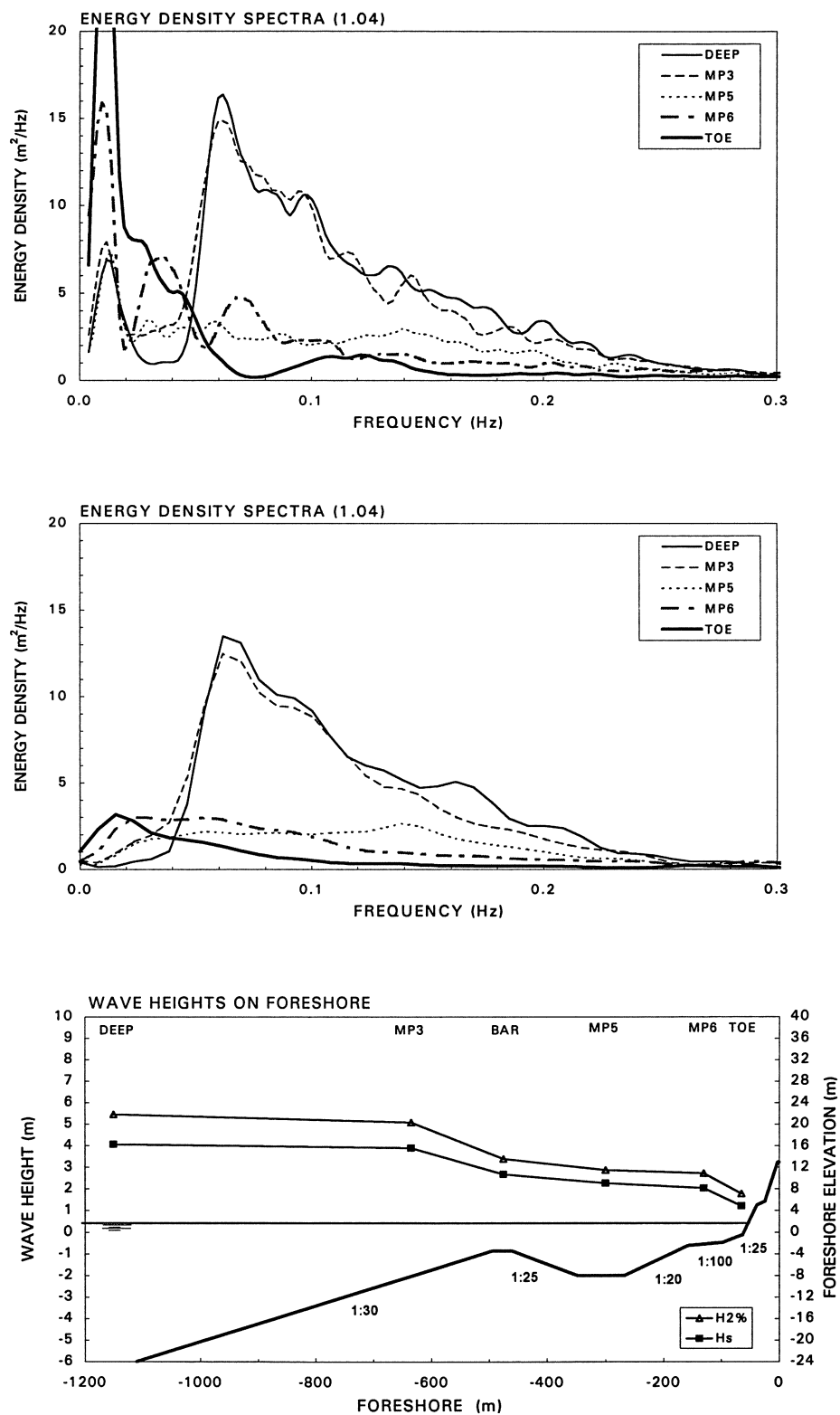


Figure F.1.04 Measured total wave energy spectra (upper), incident wave energy spectra (middle) and wave height evolution (lower).

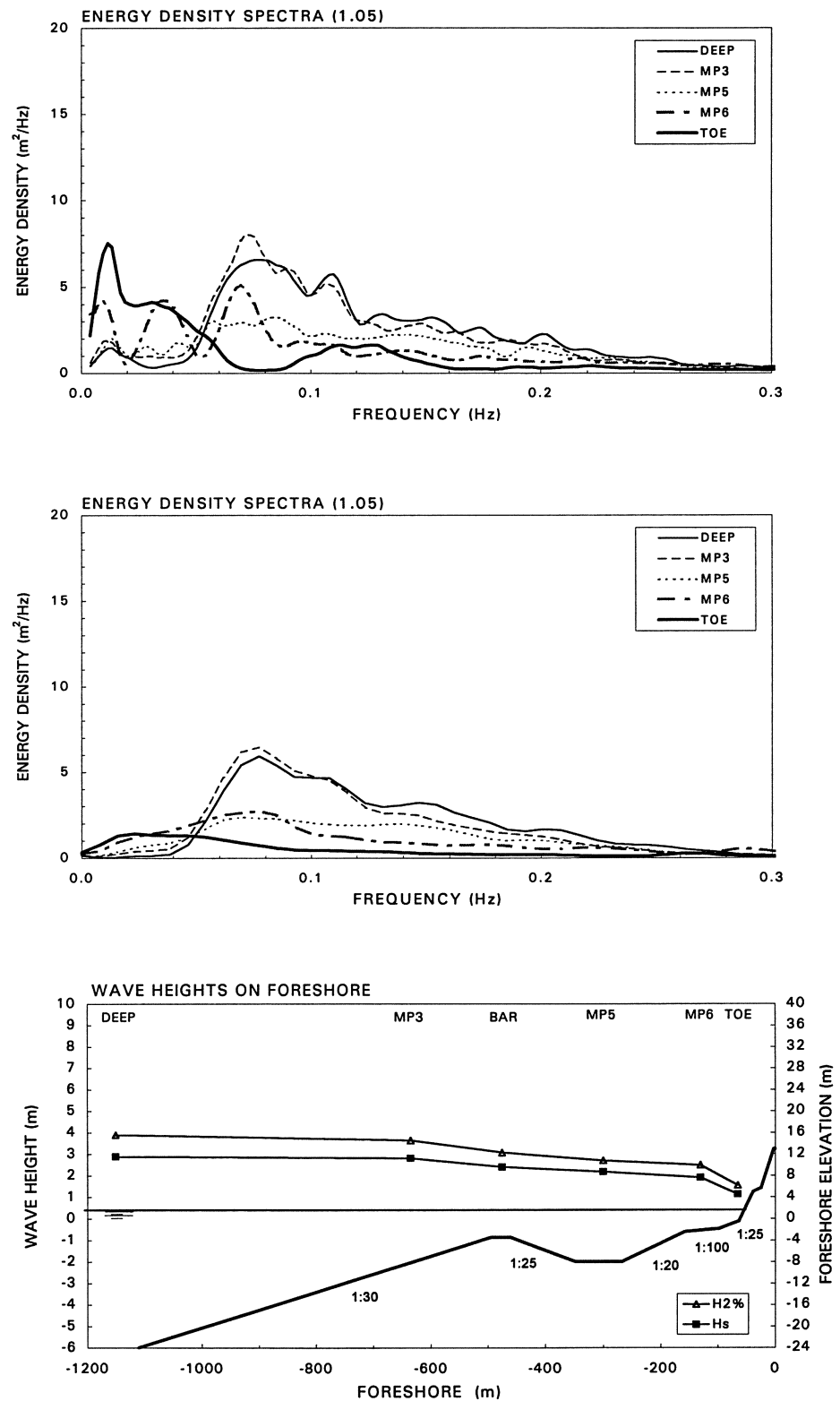


Figure F 1.05 Measured total wave energy spectra (upper), incident wave energy spectra (middle) and wave height evolution (lower).

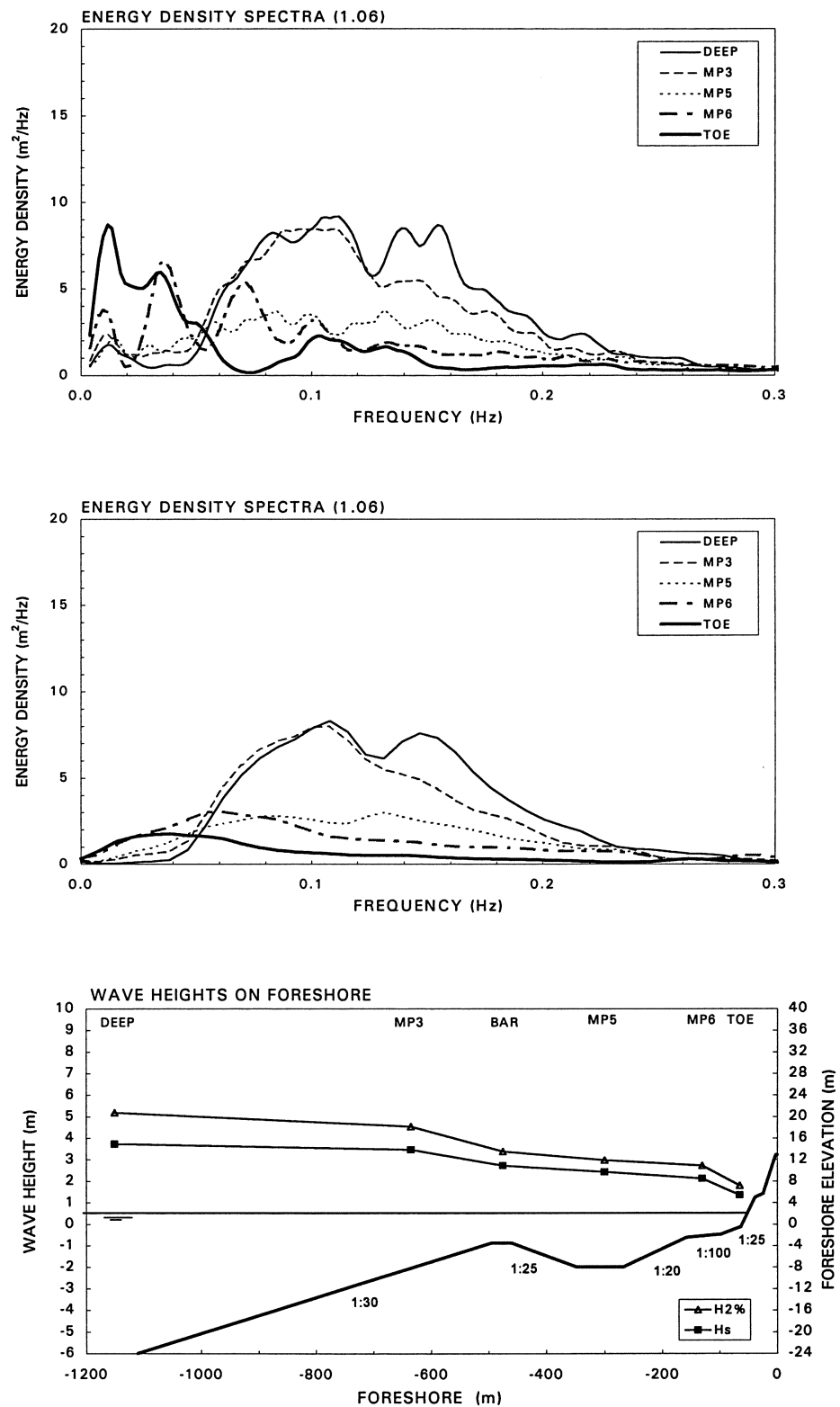


Figure F 1.06 Measured total wave energy spectra (upper), incident wave energy spectra (middle) and wave height evolution (lower).

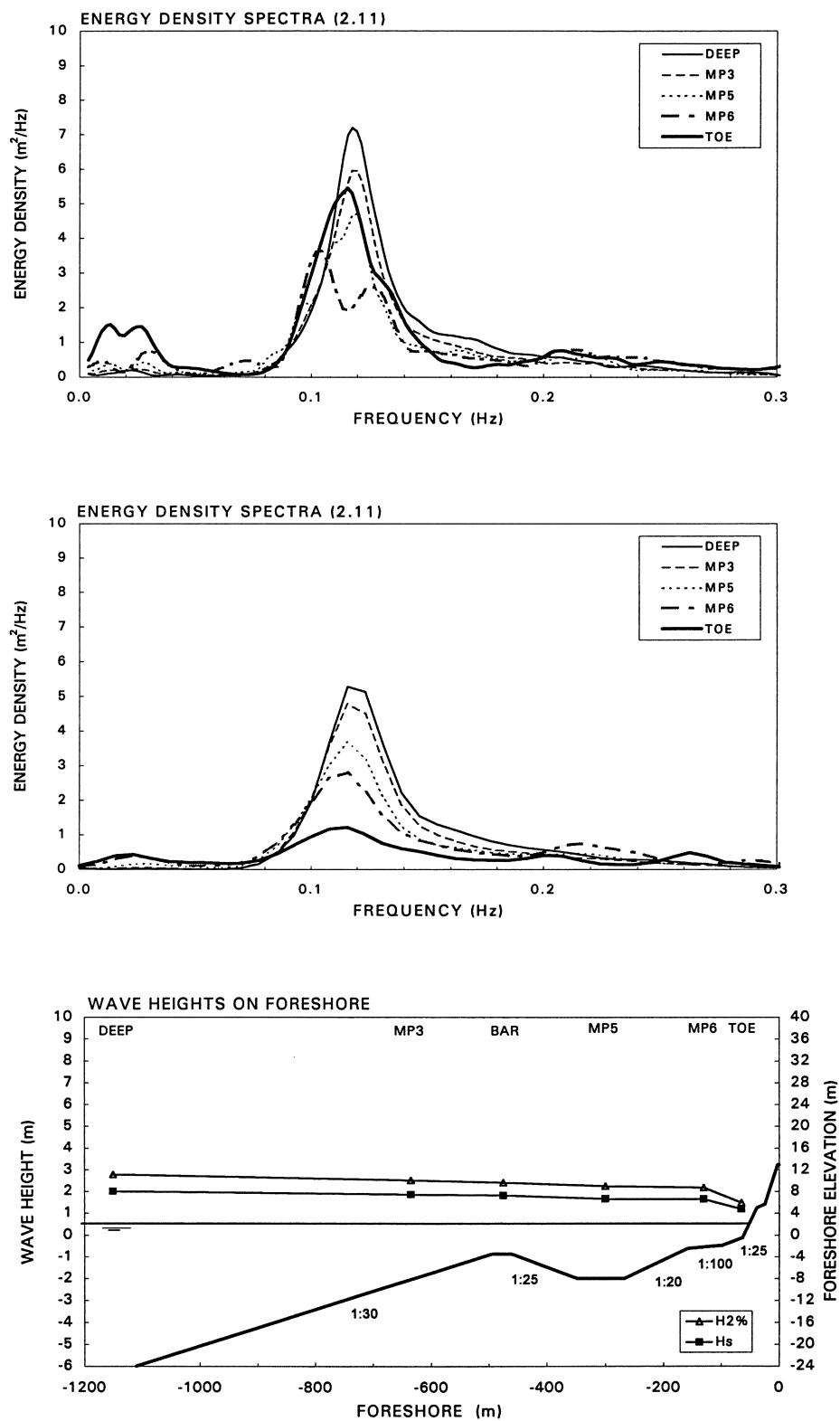


Figure F 2.11 Measured total wave energy spectra (upper), incident wave energy spectra (middle) and wave height evolution (lower).

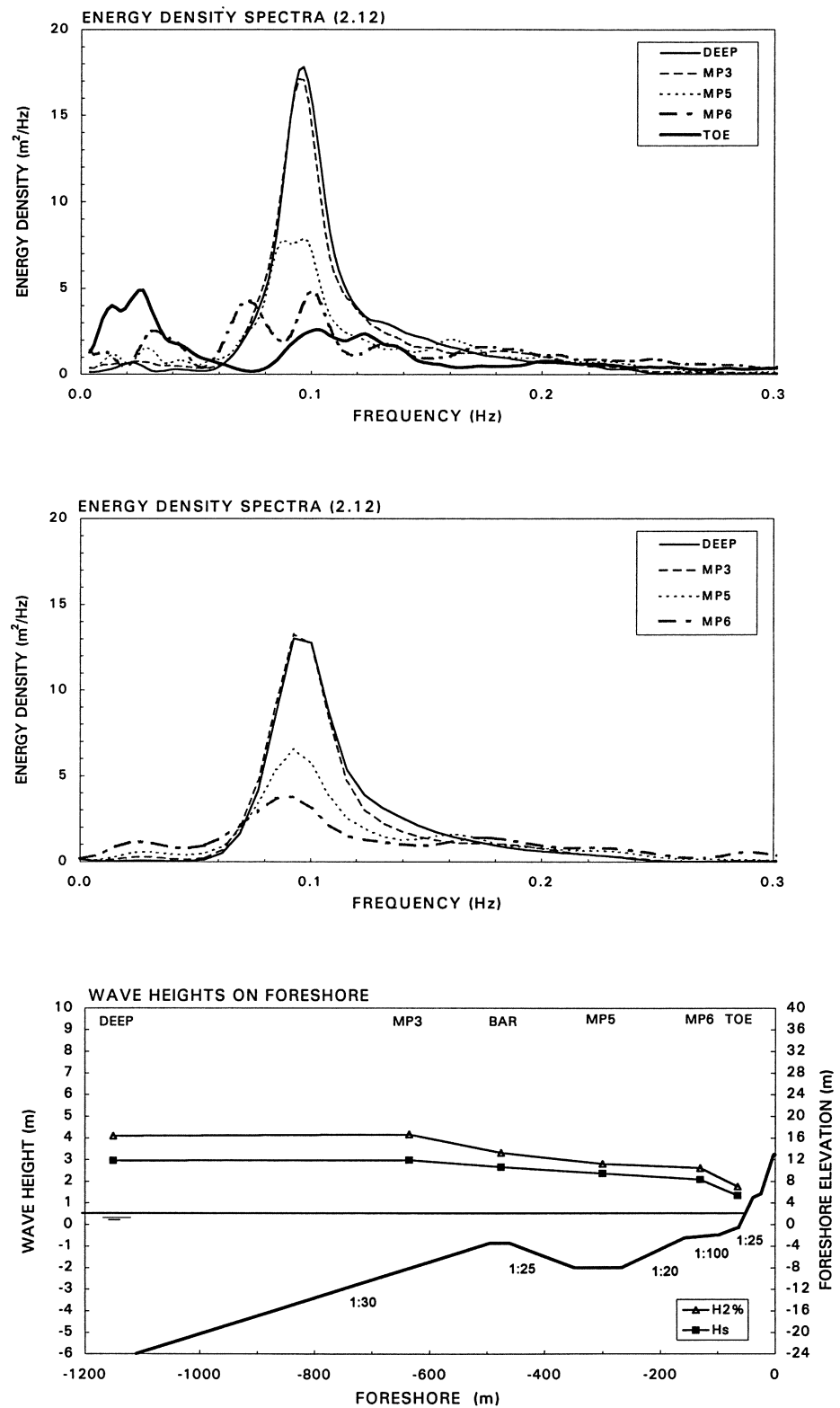


Figure F 2.12 Measured total wave energy spectra (upper), incident wave energy spectra (middle) and wave height evolution (lower).

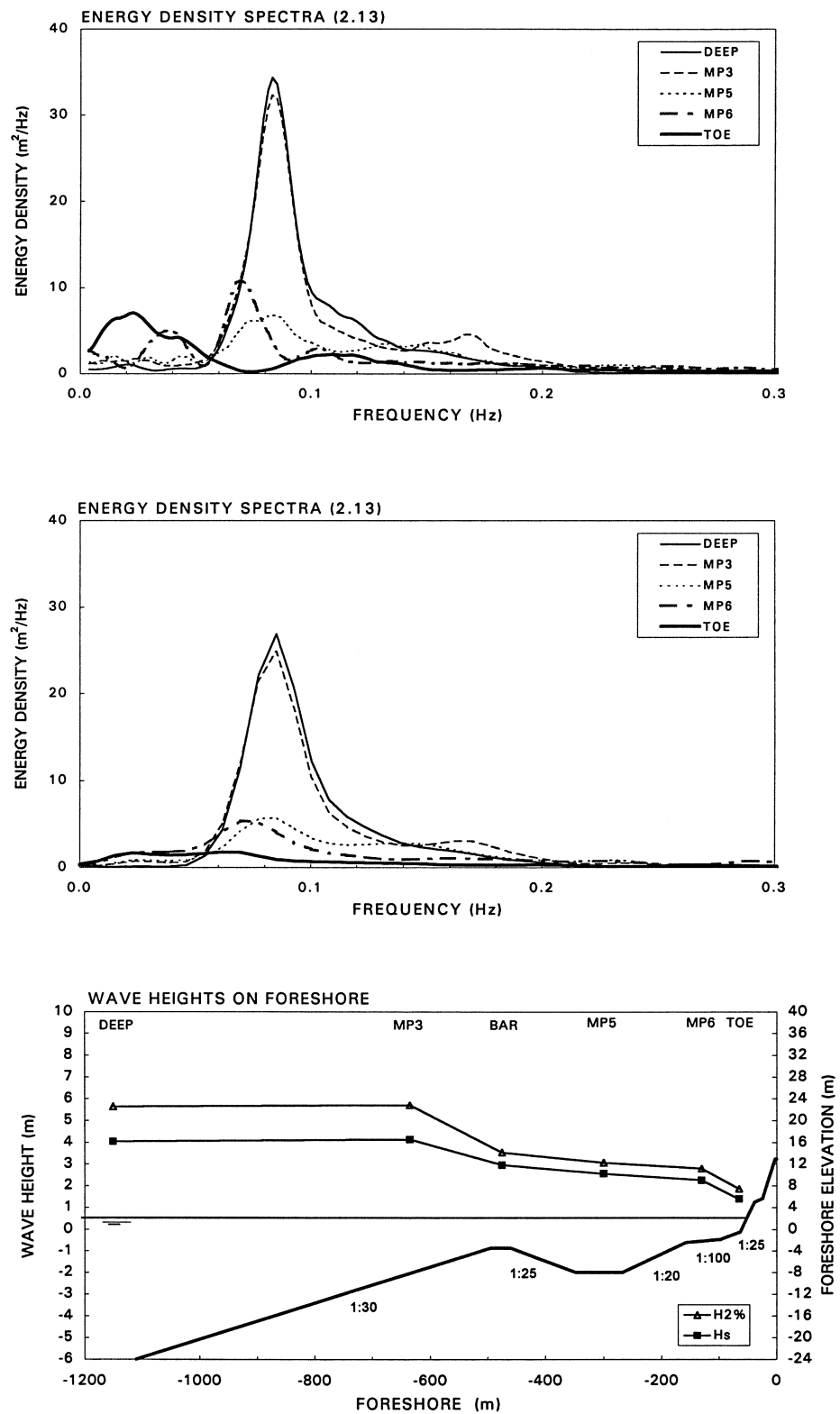


Figure F 2.13 Measured total wave energy spectra (upper), incident wave energy spectra (middle) and wave height evolution (lower).

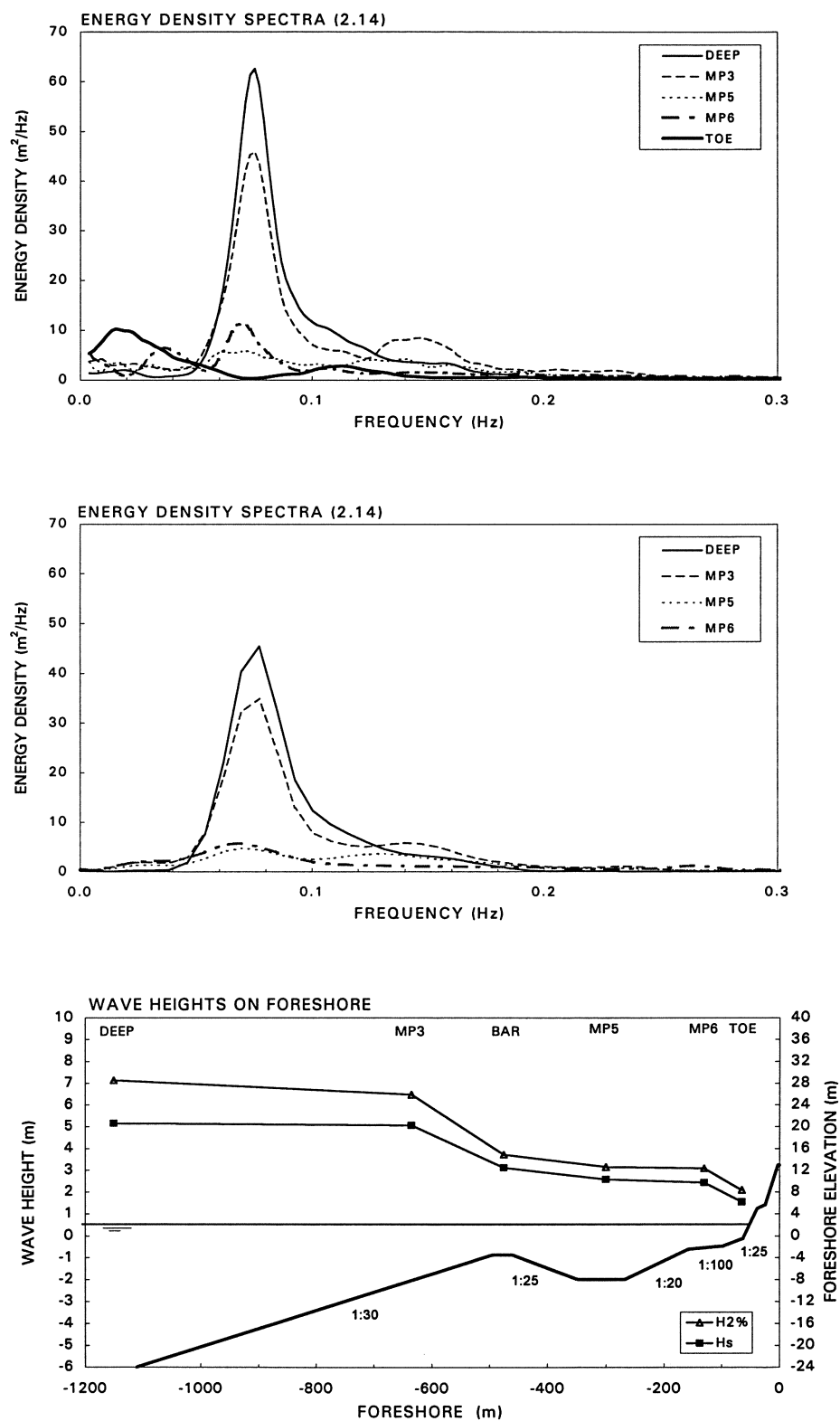


Figure F 2.14 Measured total wave energy spectra (upper), incident wave energy spectra (middle) and wave height evolution (lower).

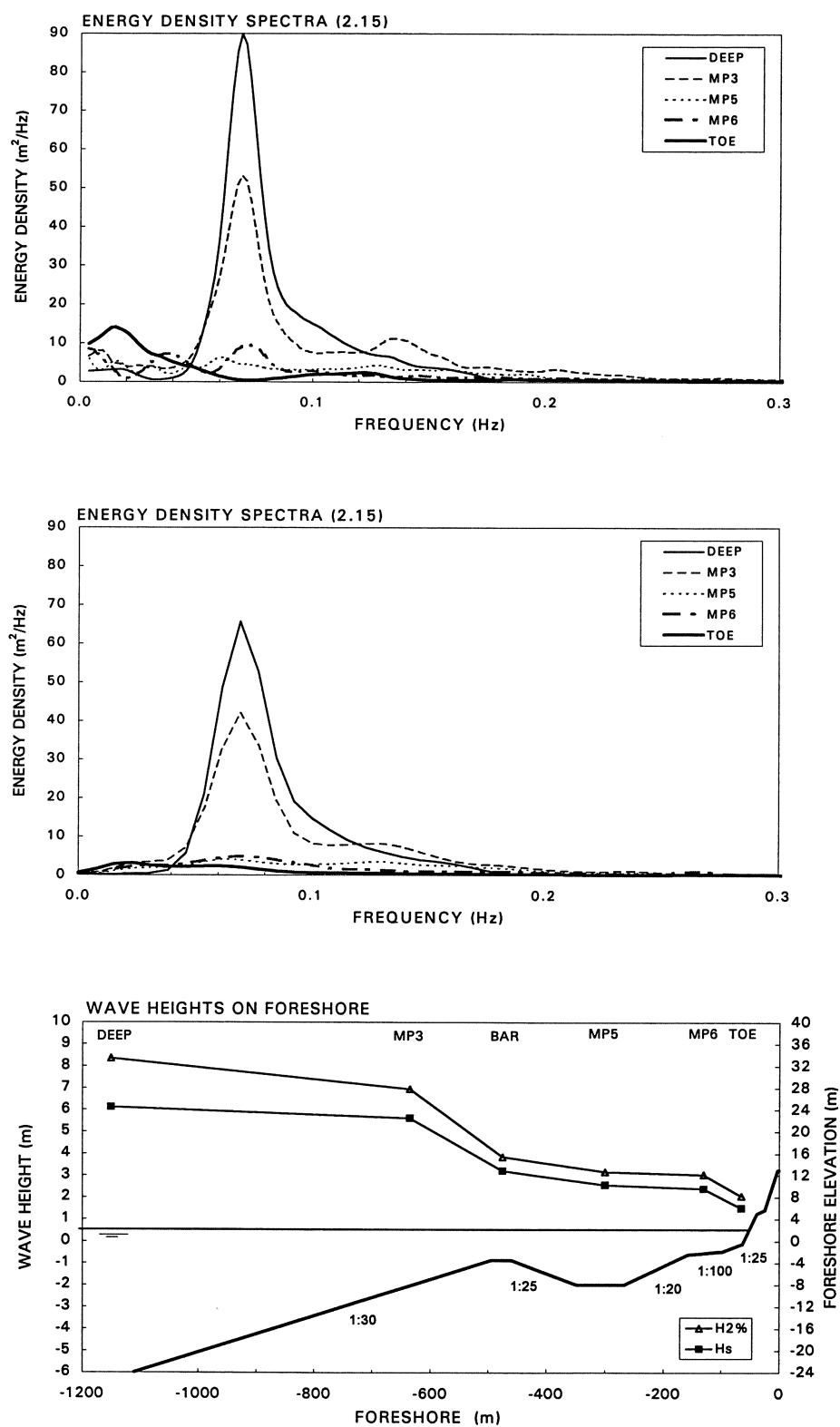


Figure F 2.15 Measured total wave energy spectra (upper), incident wave energy spectra (middle) and wave height evolution (lower).

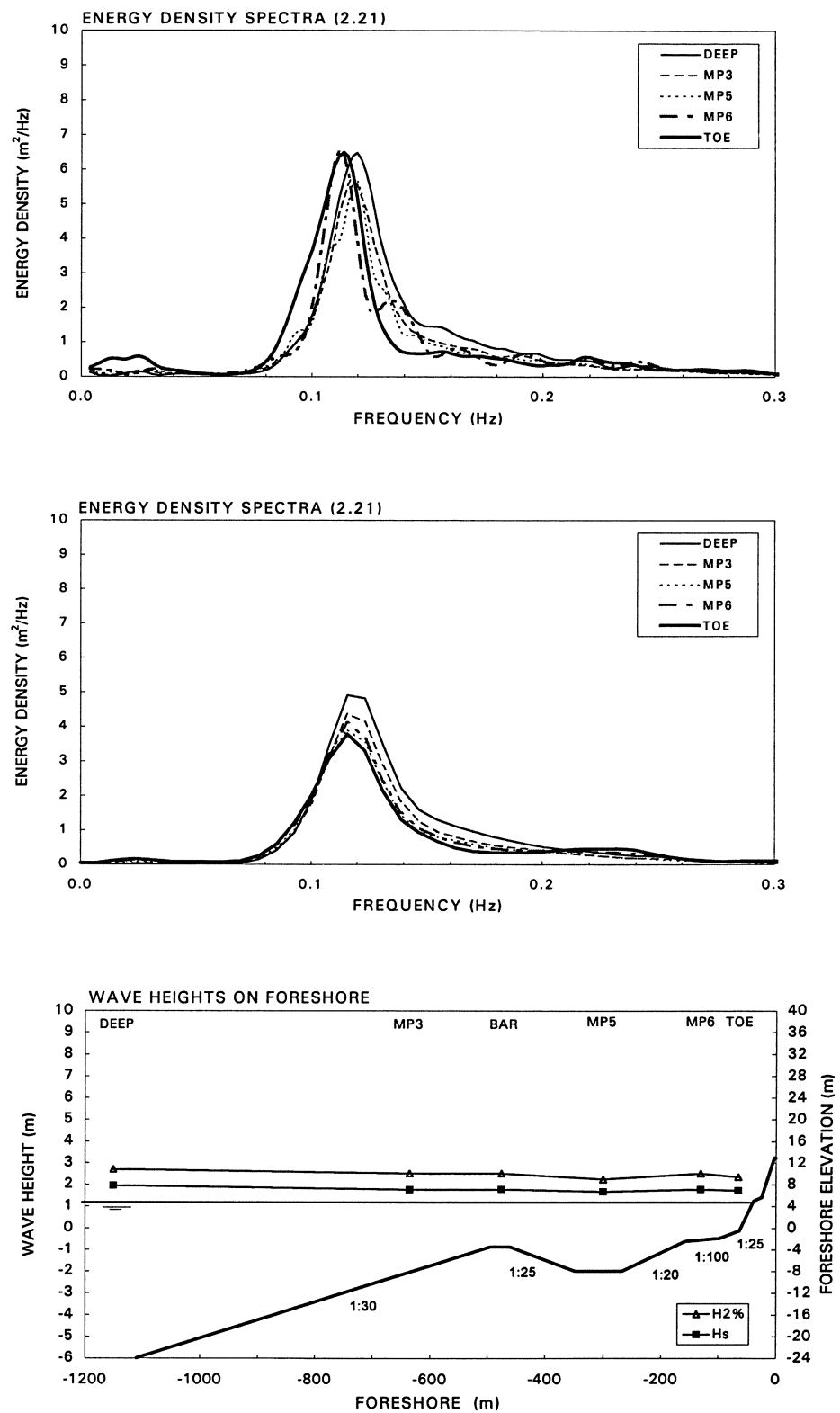


Figure F.2.21 Measured total wave energy spectra (upper), incident wave energy spectra (middle) and wave height evolution (lower).

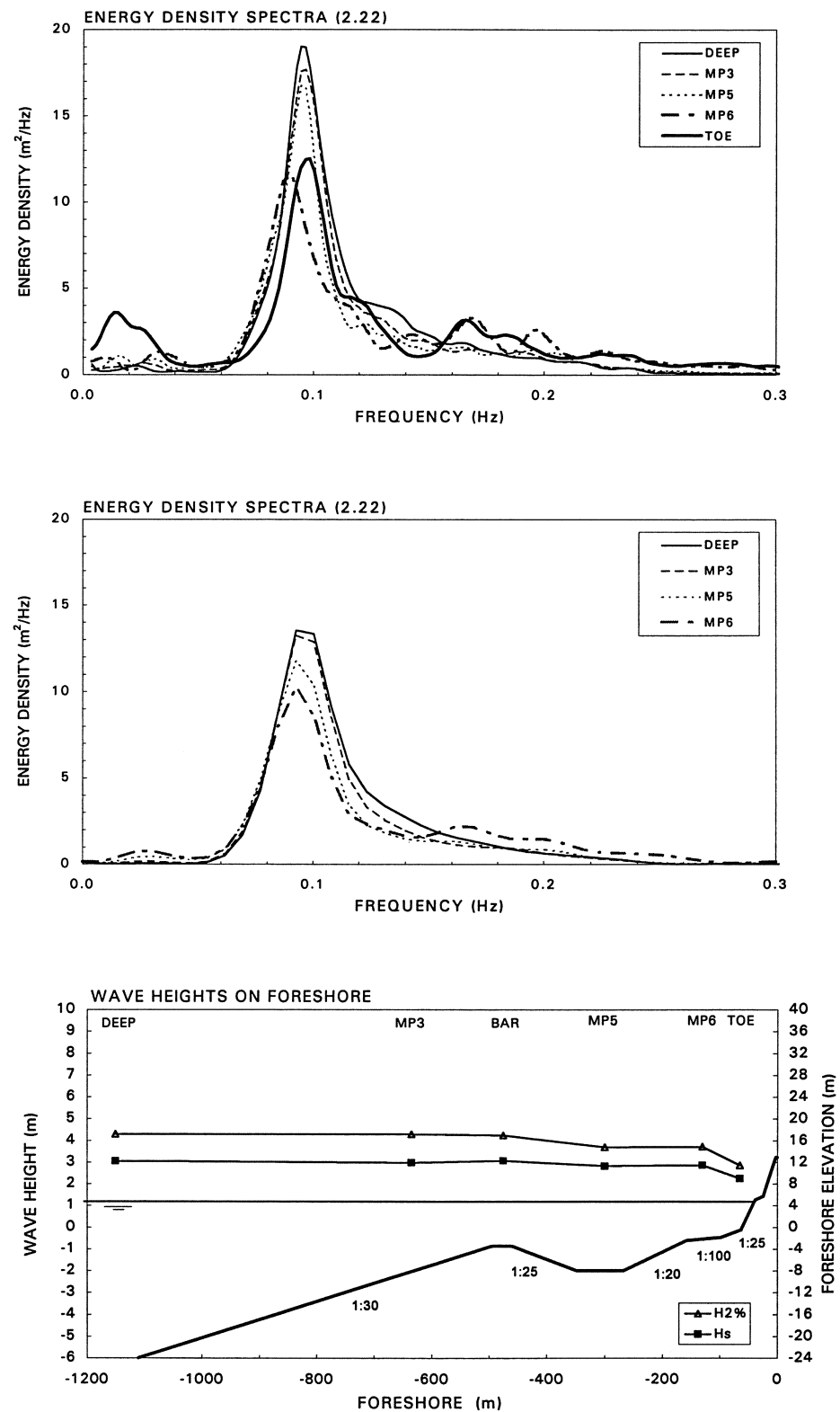


Figure F 2.22 Measured total wave energy spectra (upper), incident wave energy spectra (middle) and wave height evolution (lower).

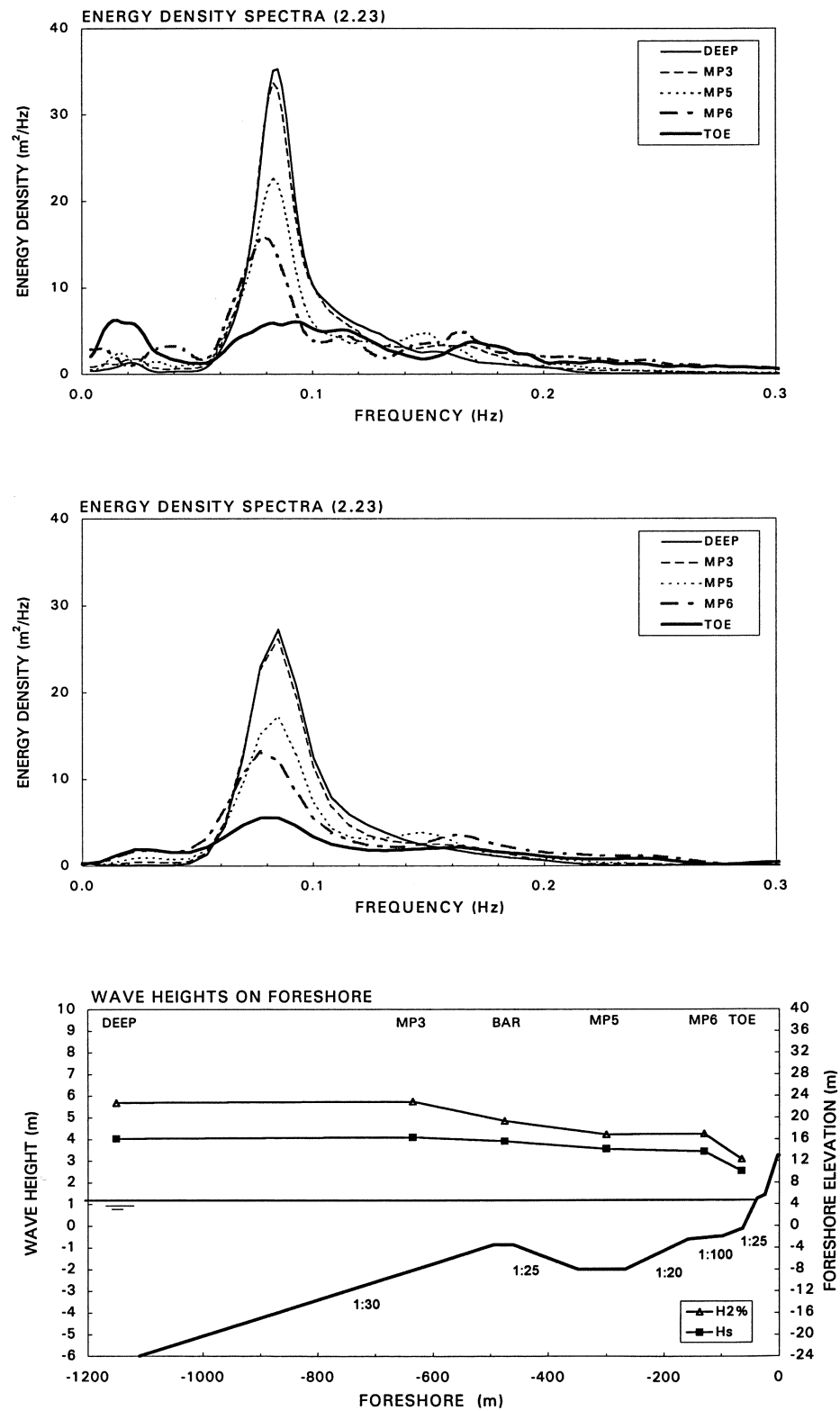


Figure F.2.23 Measured total wave energy spectra (upper), incident wave energy spectra (middle) and wave height evolution (lower).

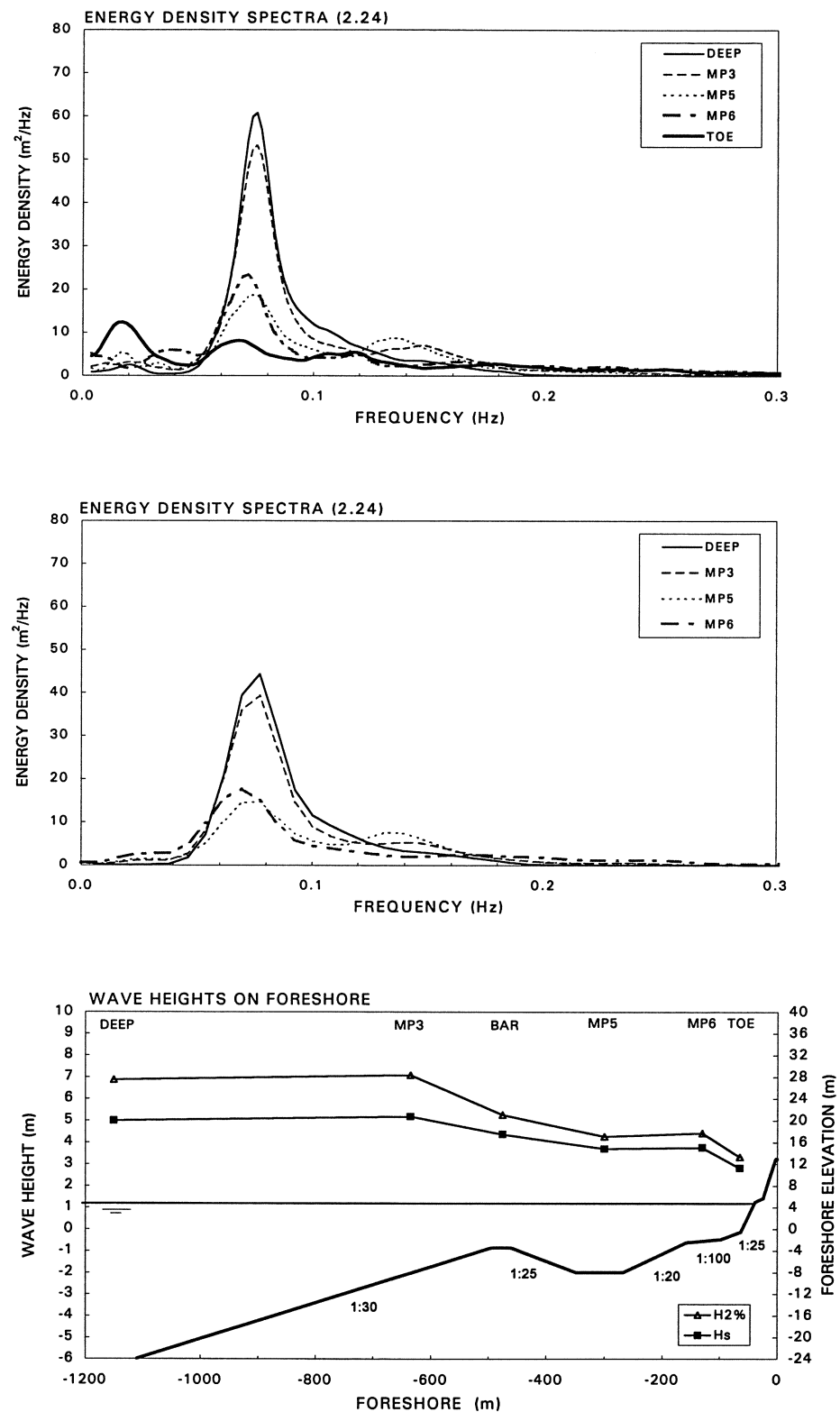


Figure F 2.24 Measured total wave energy spectra (upper), incident wave energy spectra (middle) and wave height evolution (lower).

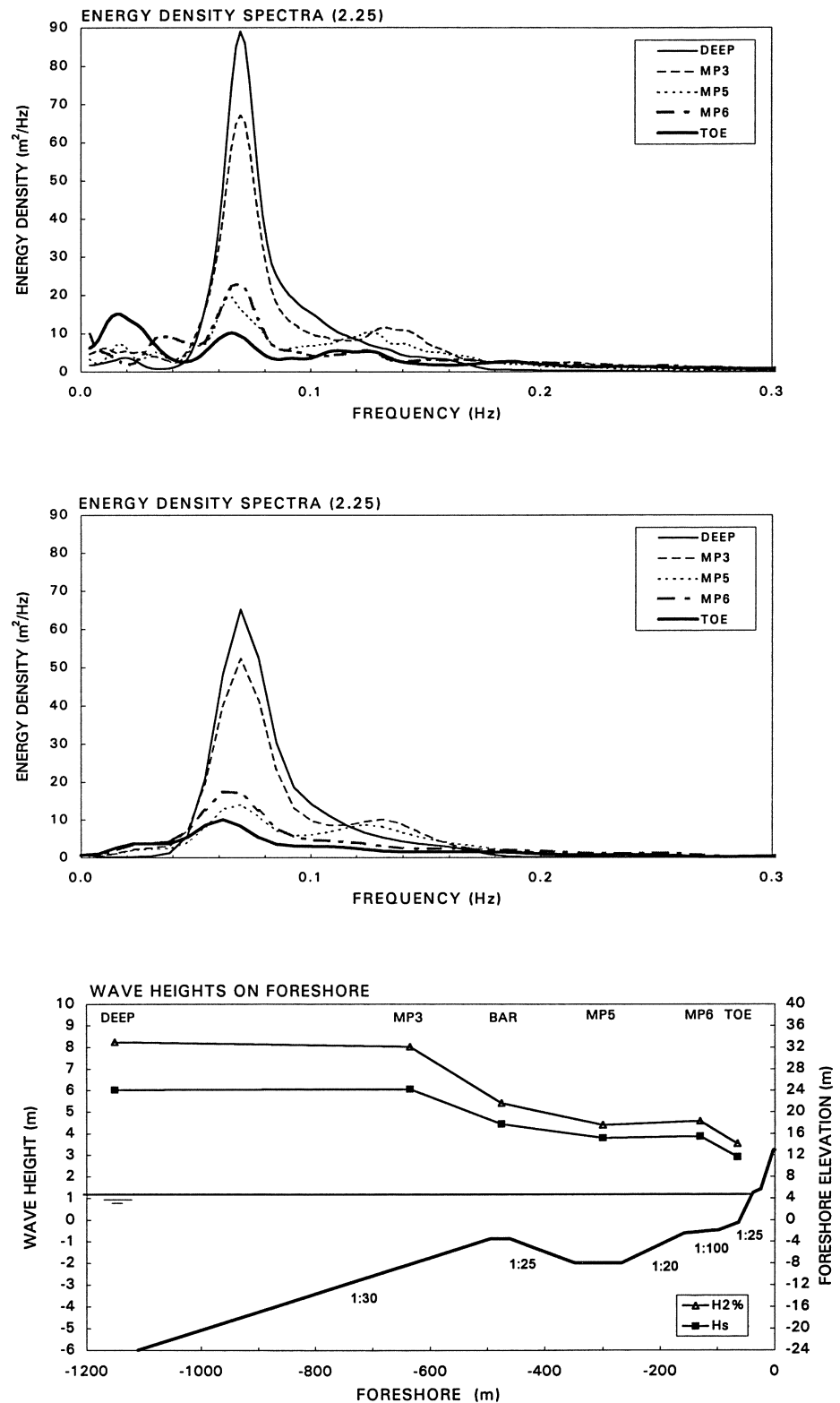


Figure F.2.25 Measured total wave energy spectra (upper), incident wave energy spectra (middle) and wave height evolution (lower).

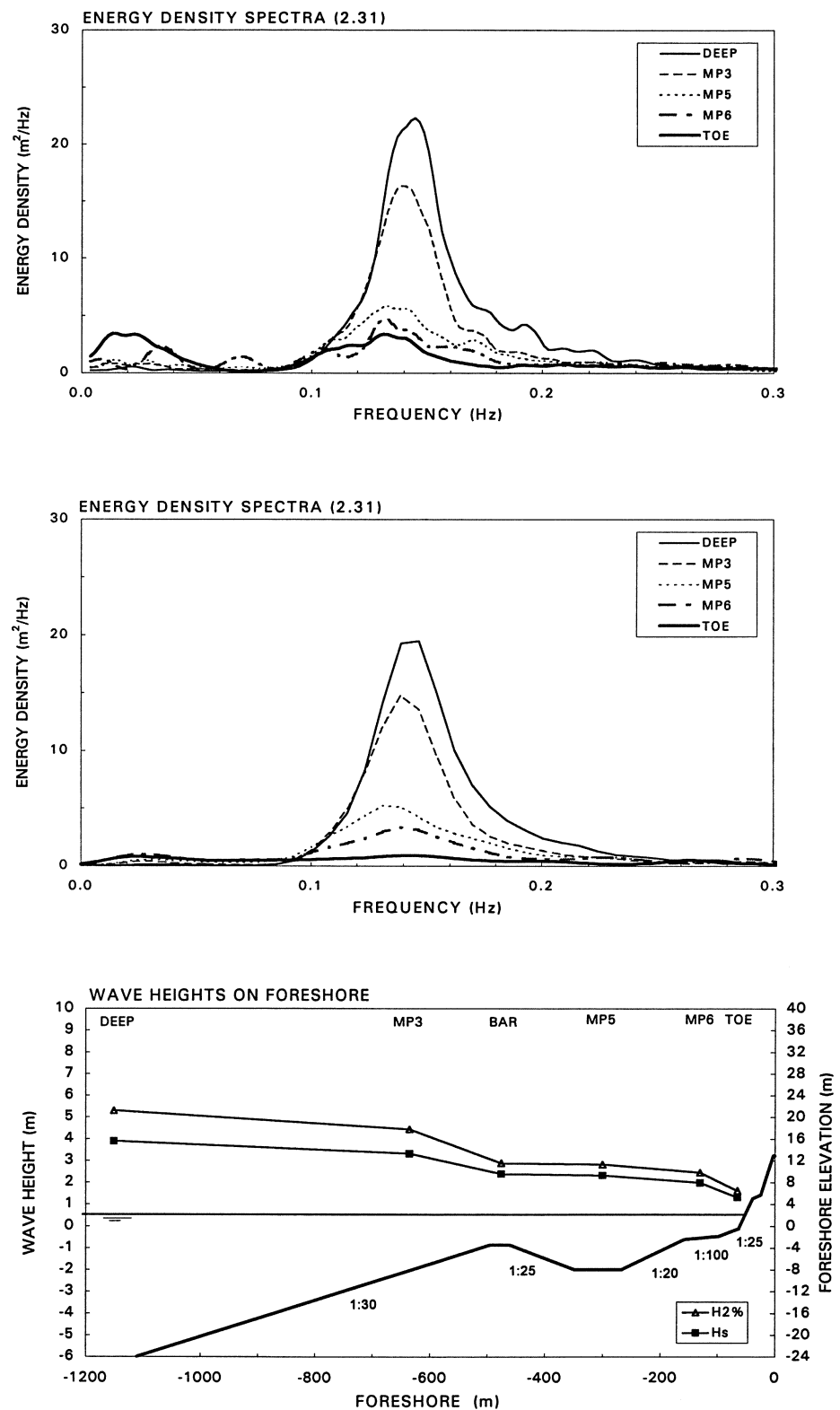


Figure F 2.31 Measured total wave energy spectra (upper), incident wave energy spectra (middle) and wave height evolution (lower).

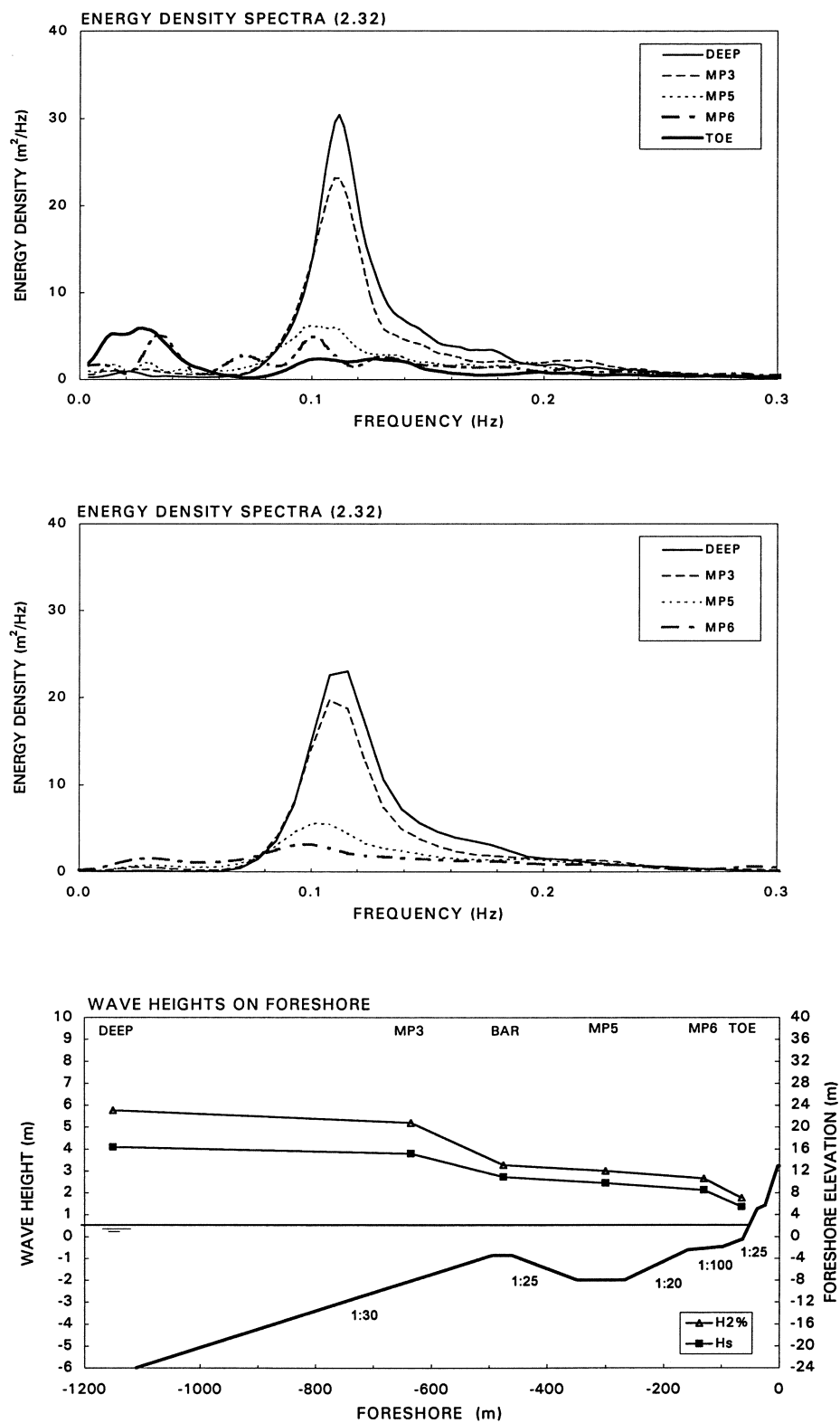


Figure F 2.32 Measured total wave energy spectra (upper), incident wave energy spectra (middle) and wave height evolution (lower).

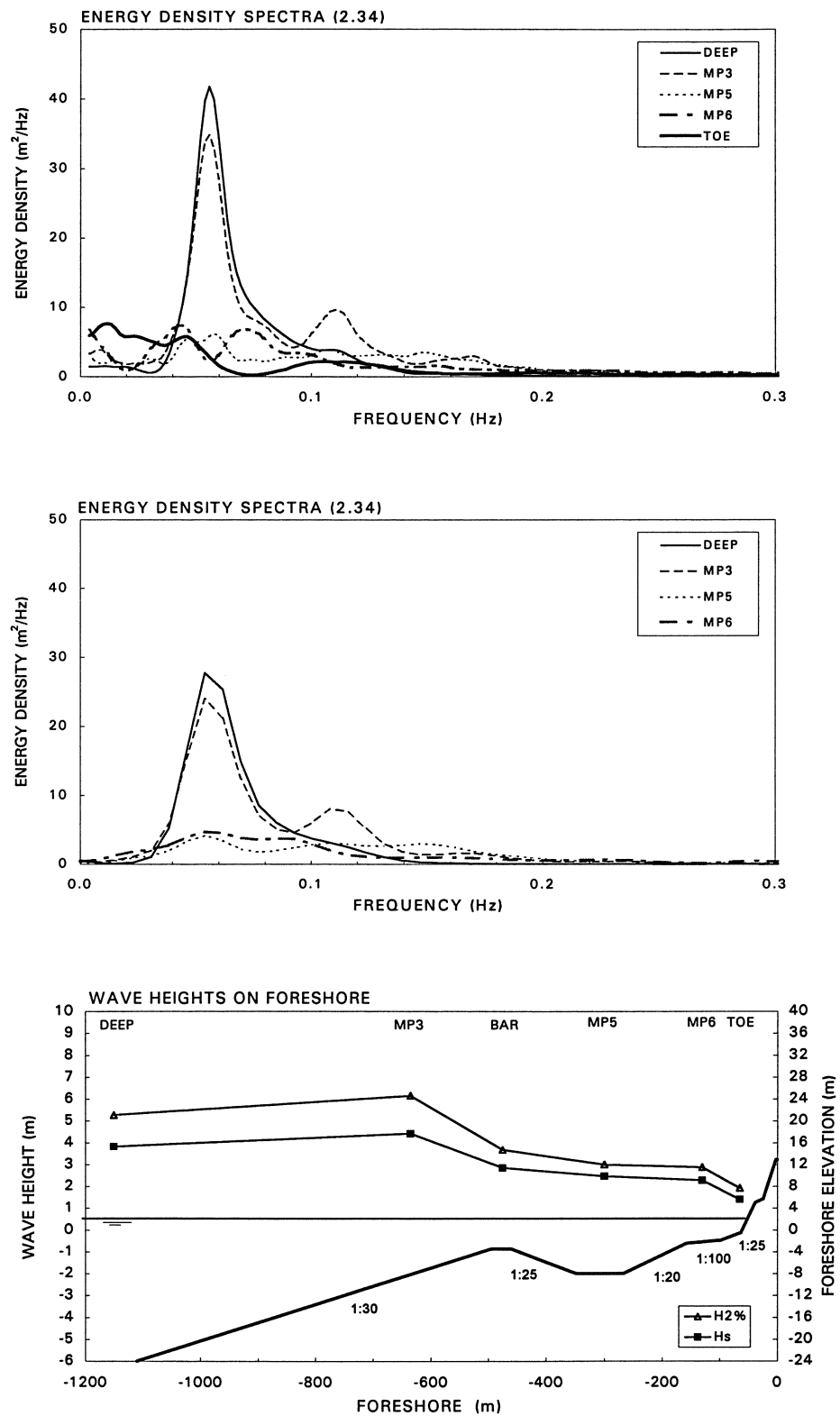


Figure F 2.34 Measured total wave energy spectra (upper), incident wave energy spectra (middle) and wave height evolution (lower).

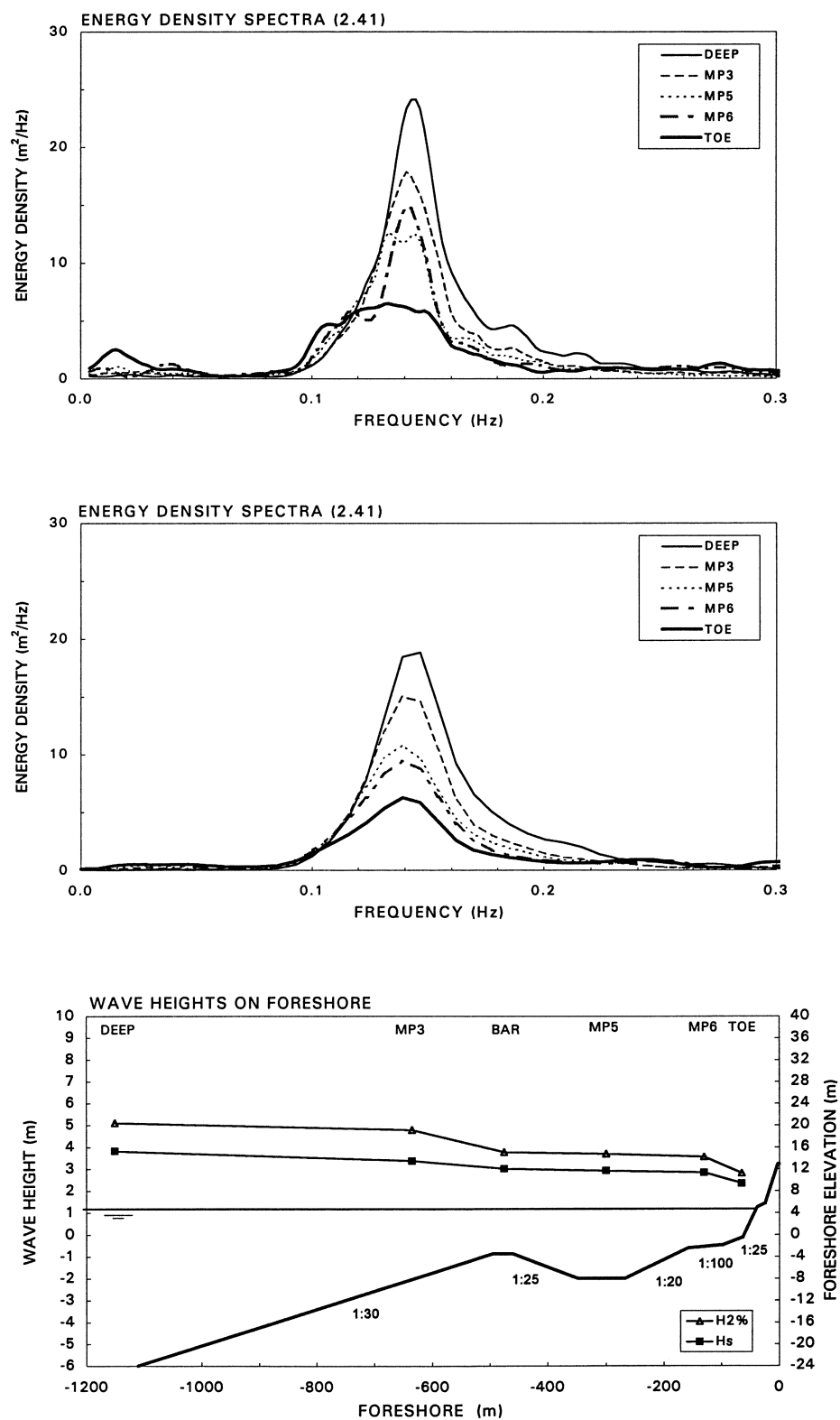


Figure F 2.41 Measured total wave energy spectra (upper), incident wave energy spectra (middle) and wave height evolution (lower).

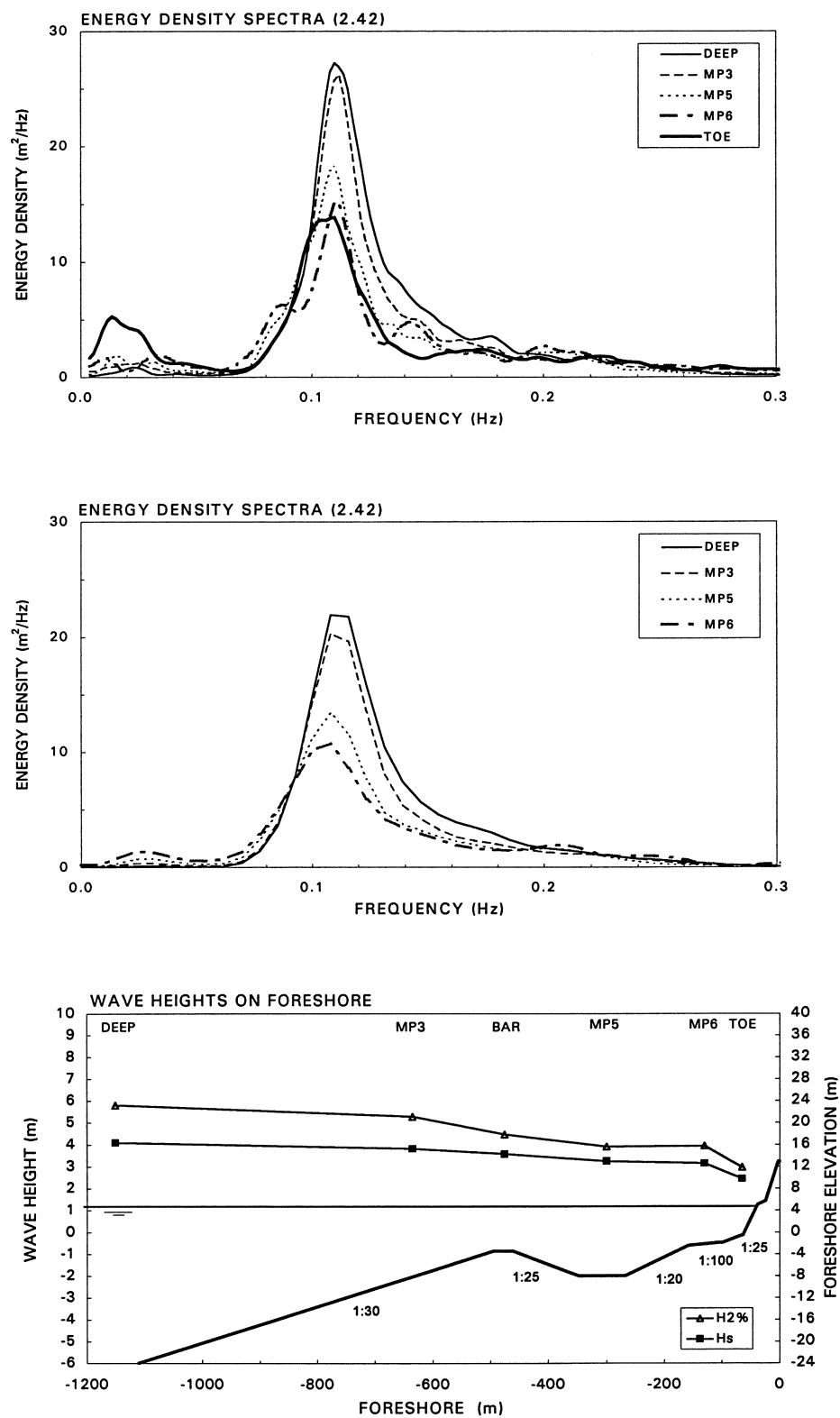


Figure F 2.42 Measured total wave energy spectra (upper), incident wave energy spectra (middle) and wave height evolution (lower).

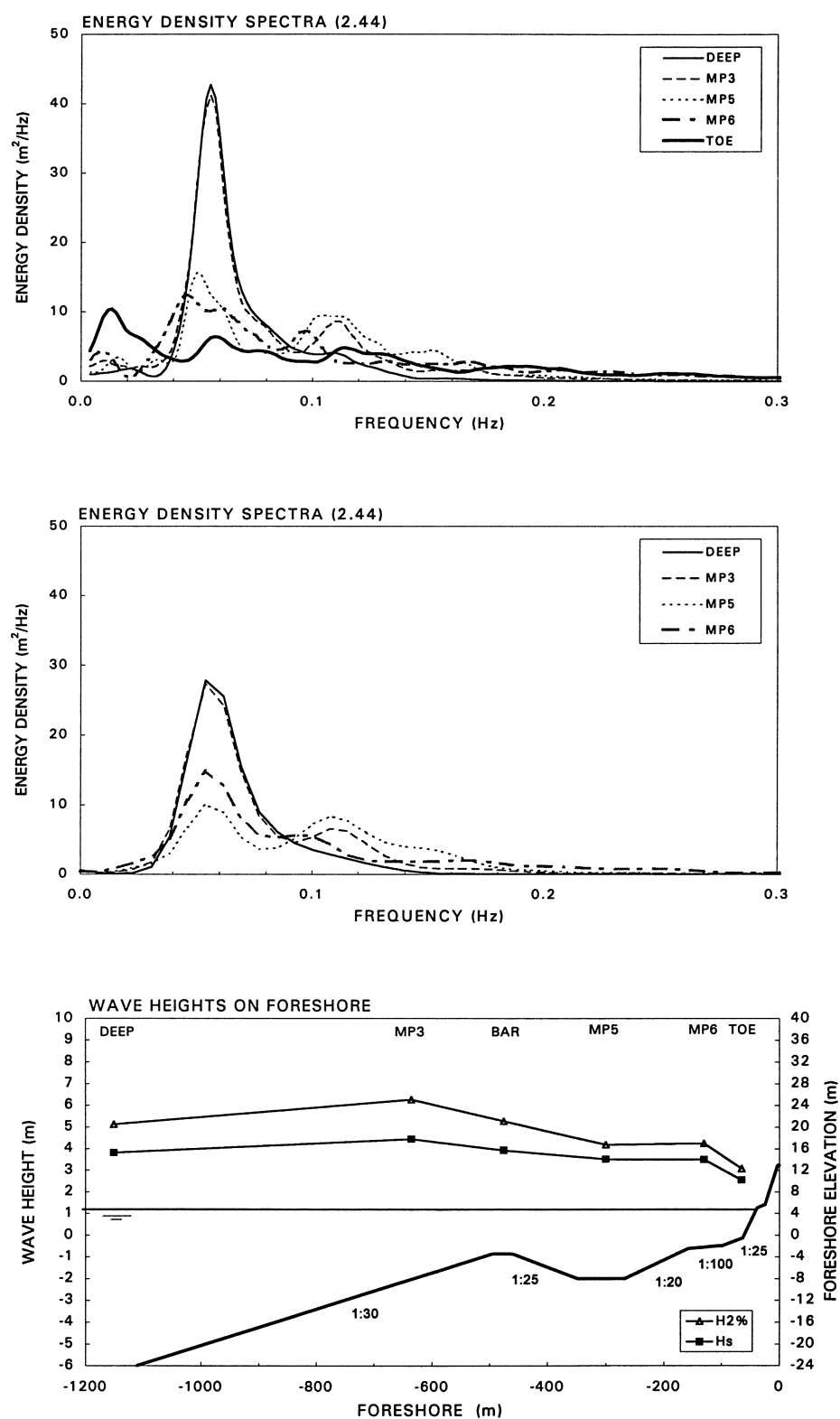


Figure F 2.44 Measured total wave energy spectra (upper), incident wave energy spectra (middle) and wave height evolution (lower).

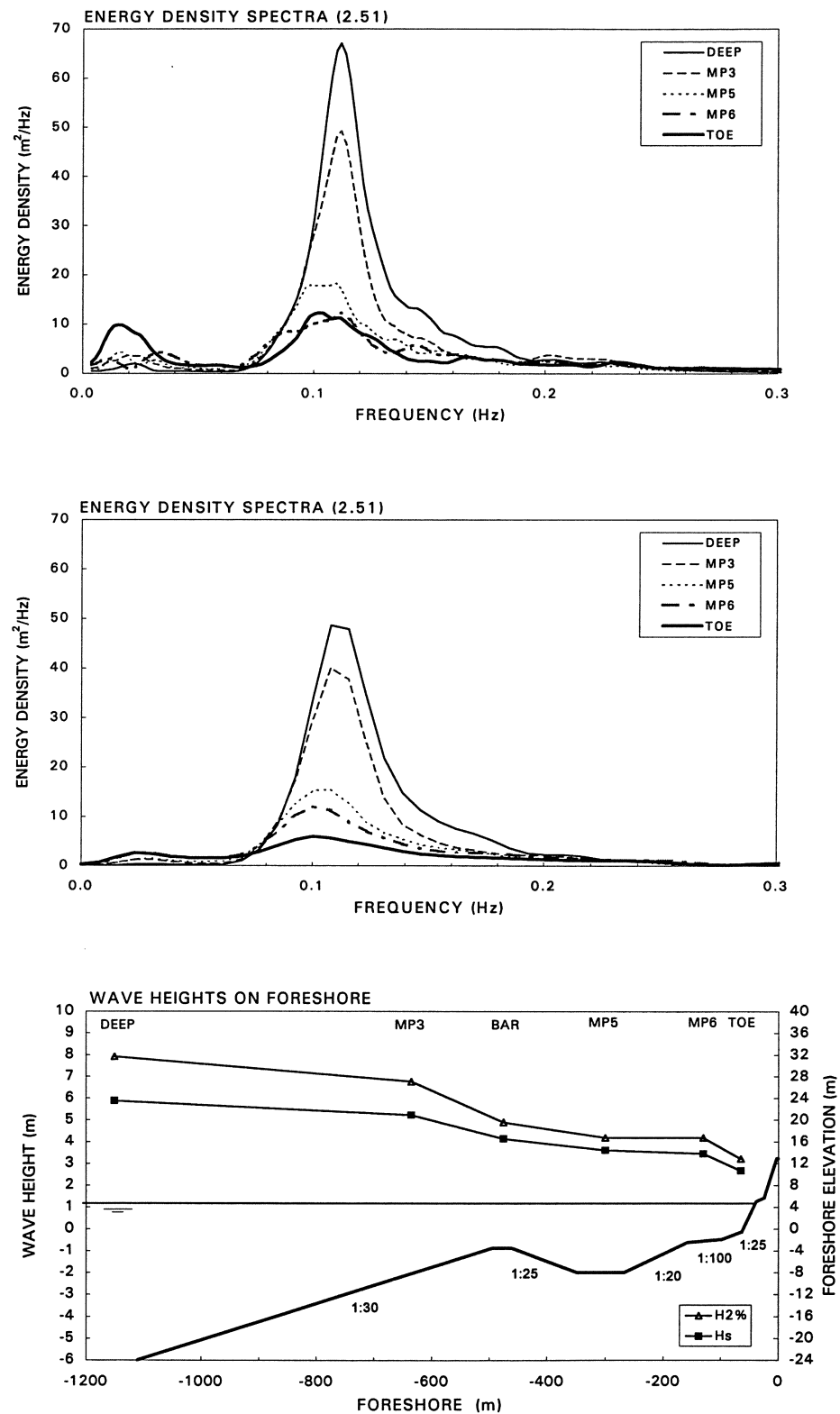


Figure F 2.51 Measured total wave energy spectra (upper), incident wave energy spectra (middle) and wave height evolution (lower).

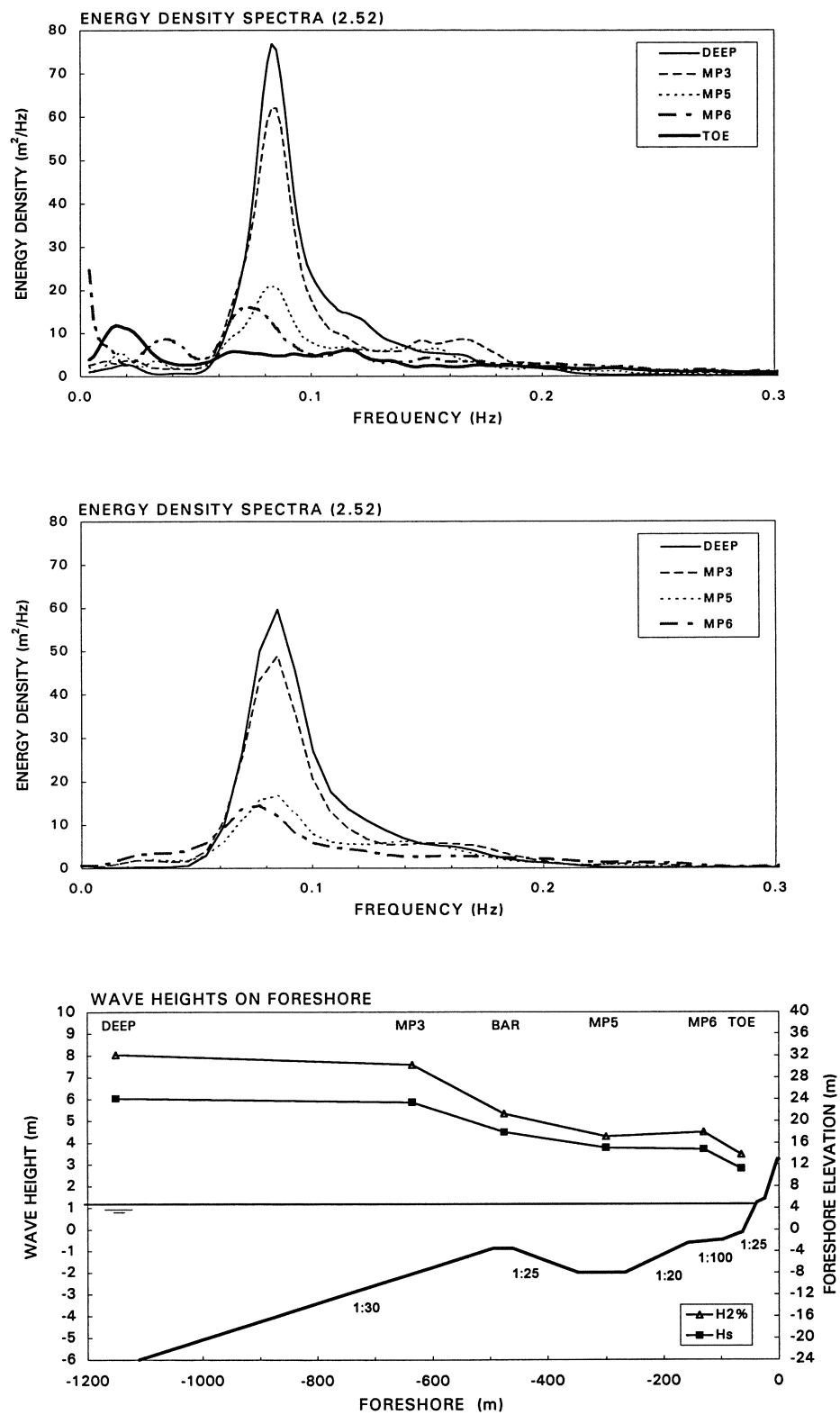


Figure F 2.52 Measured total wave energy spectra (upper), incident wave energy spectra (middle) and wave height evolution (lower).

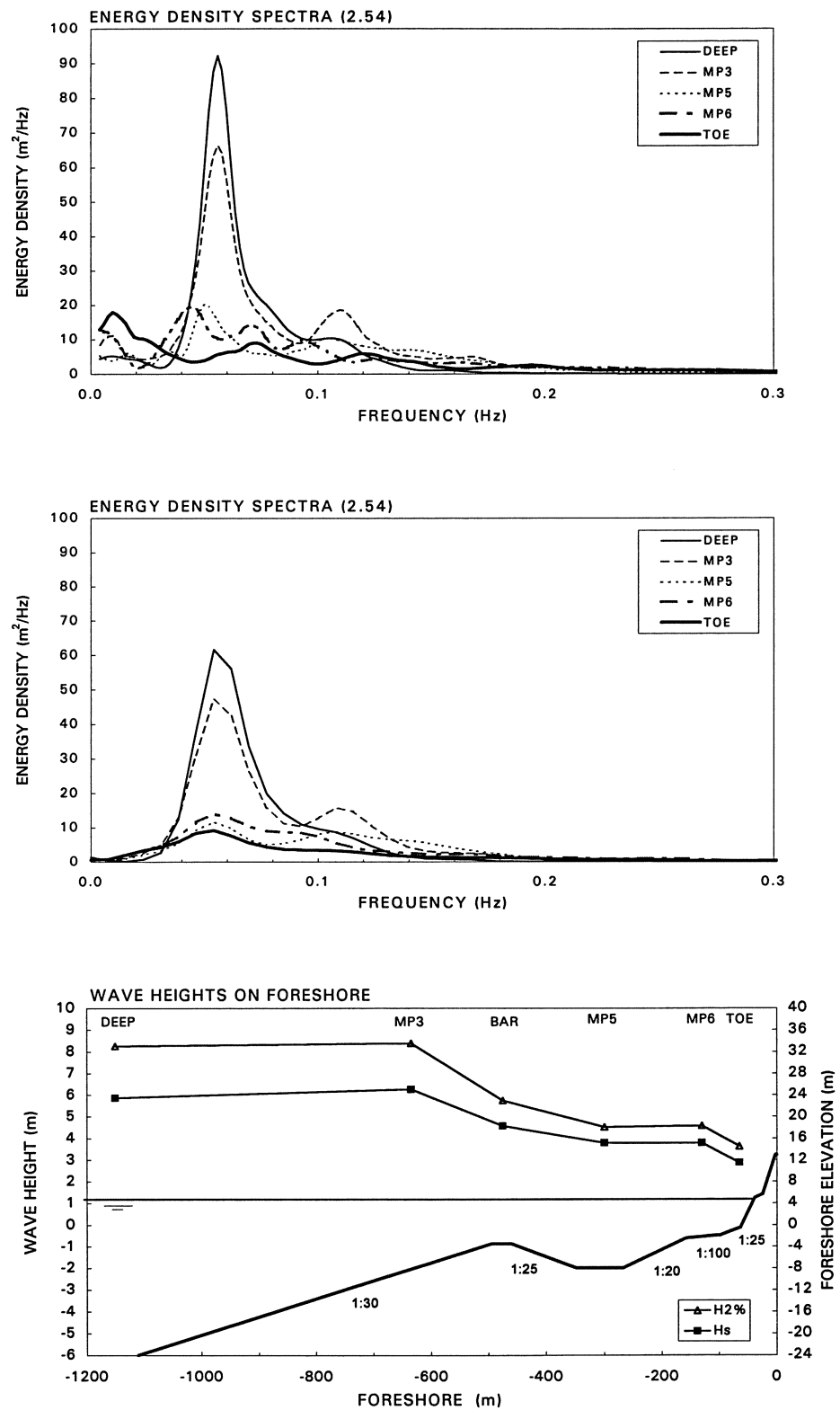


Figure F 2.54 Measured total wave energy spectra (upper), incident wave energy spectra (middle) and wave height evolution (lower).

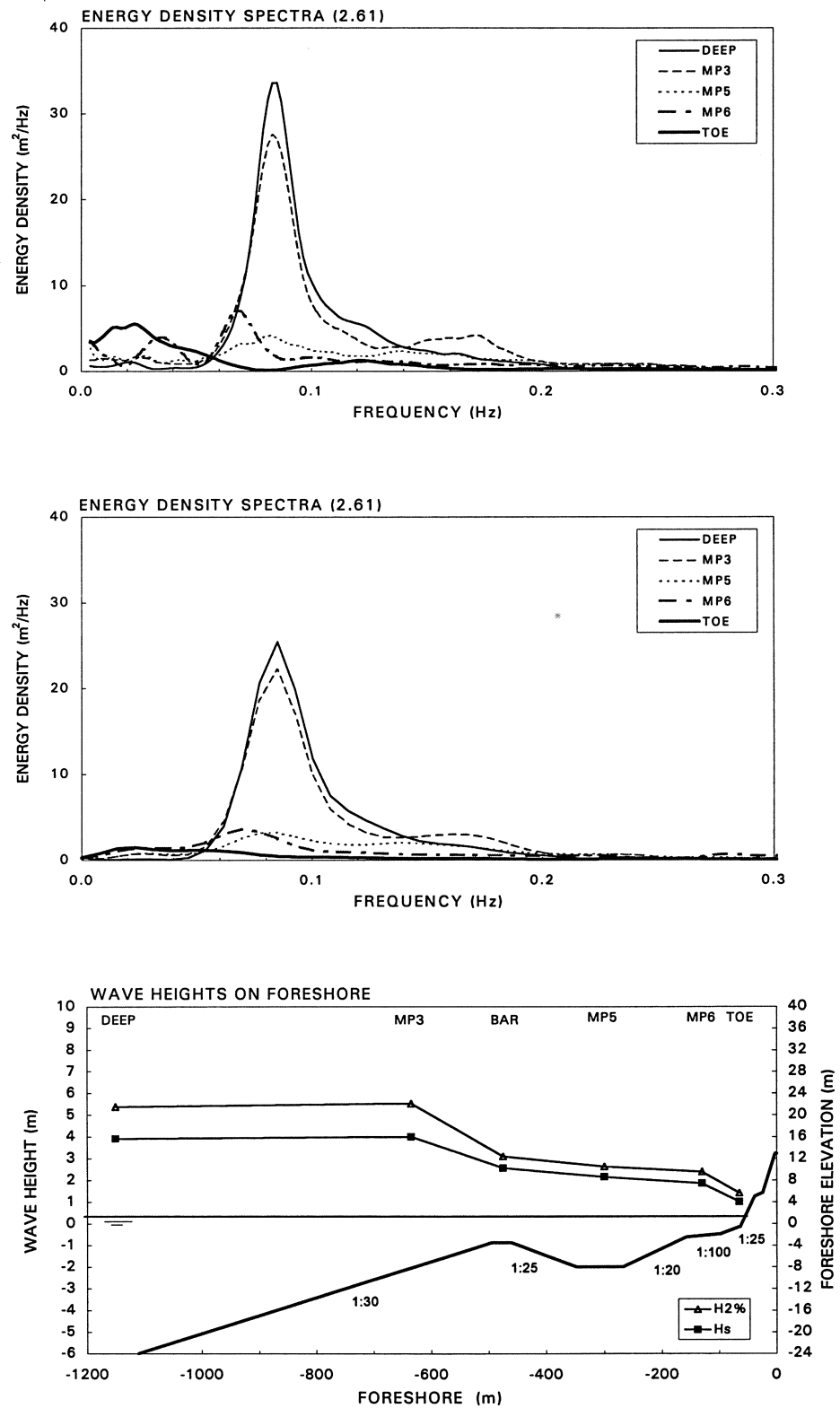


Figure F 2.61 Measured total wave energy spectra (upper), incident wave energy spectra (middle) and wave height evolution (lower).

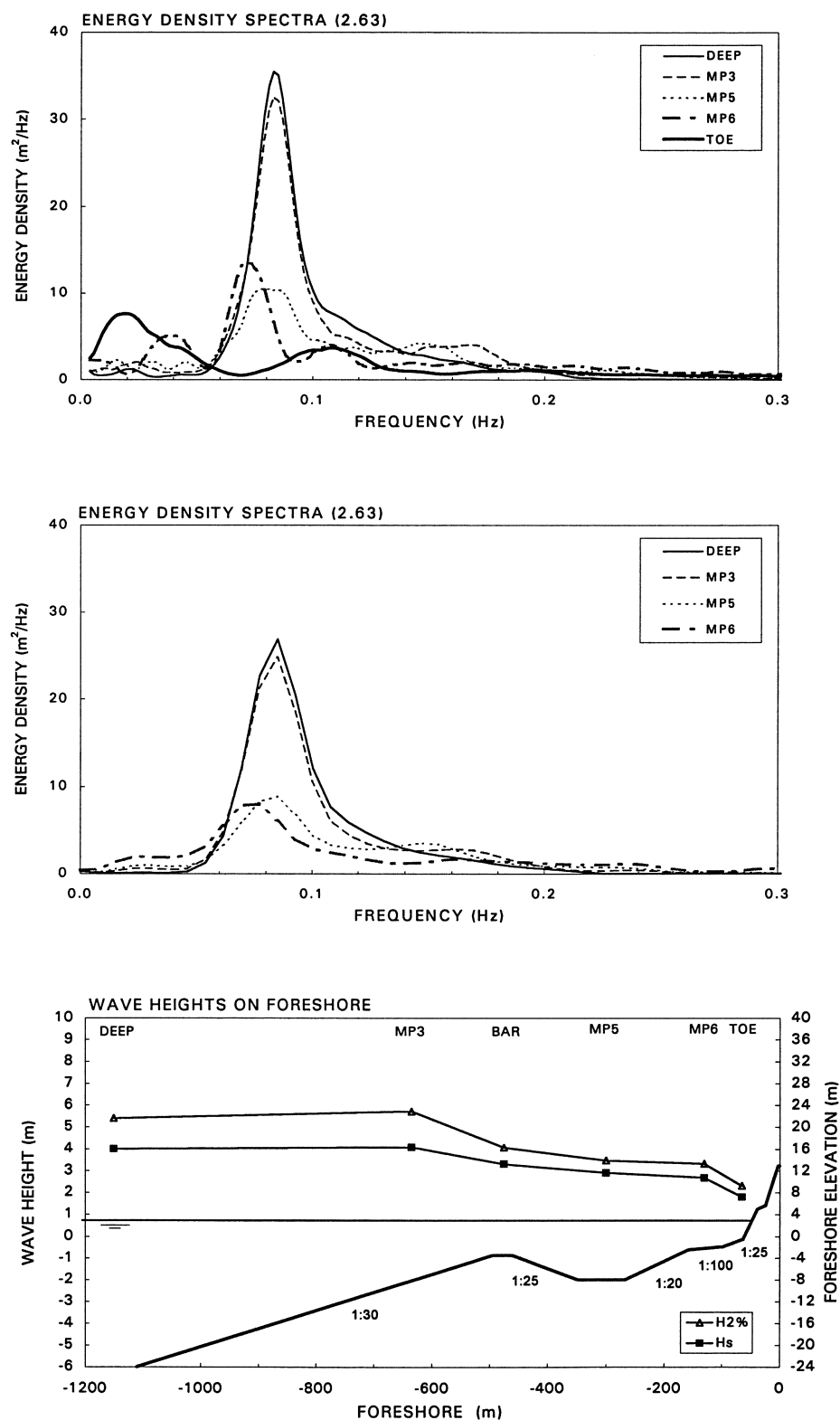


Figure F 2.63 Measured total wave energy spectra (upper), incident wave energy spectra (middle) and wave height evolution (lower).

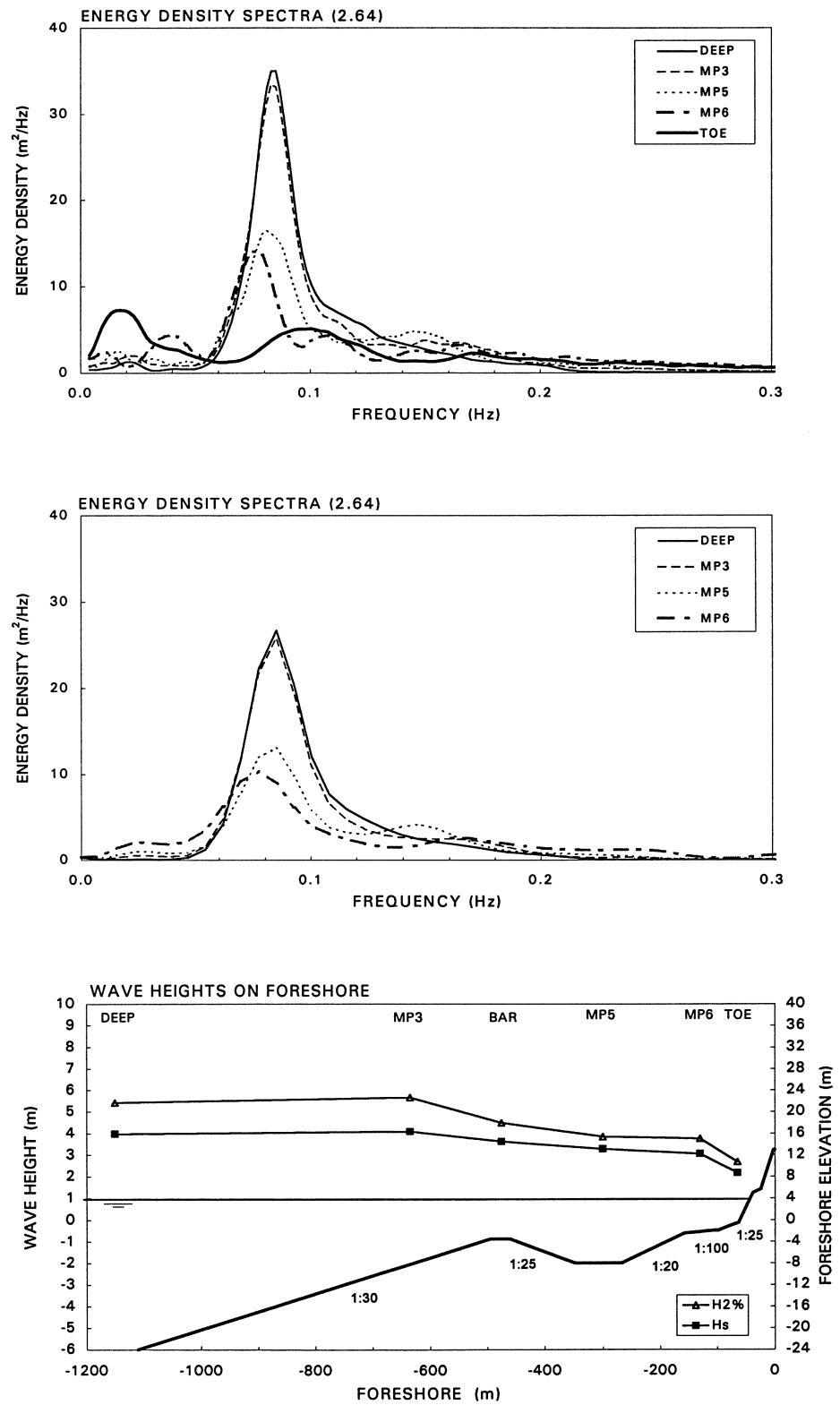


Figure F 2.64 Measured total wave energy spectra (upper), incident wave energy spectra (middle) and wave height evolution (lower).

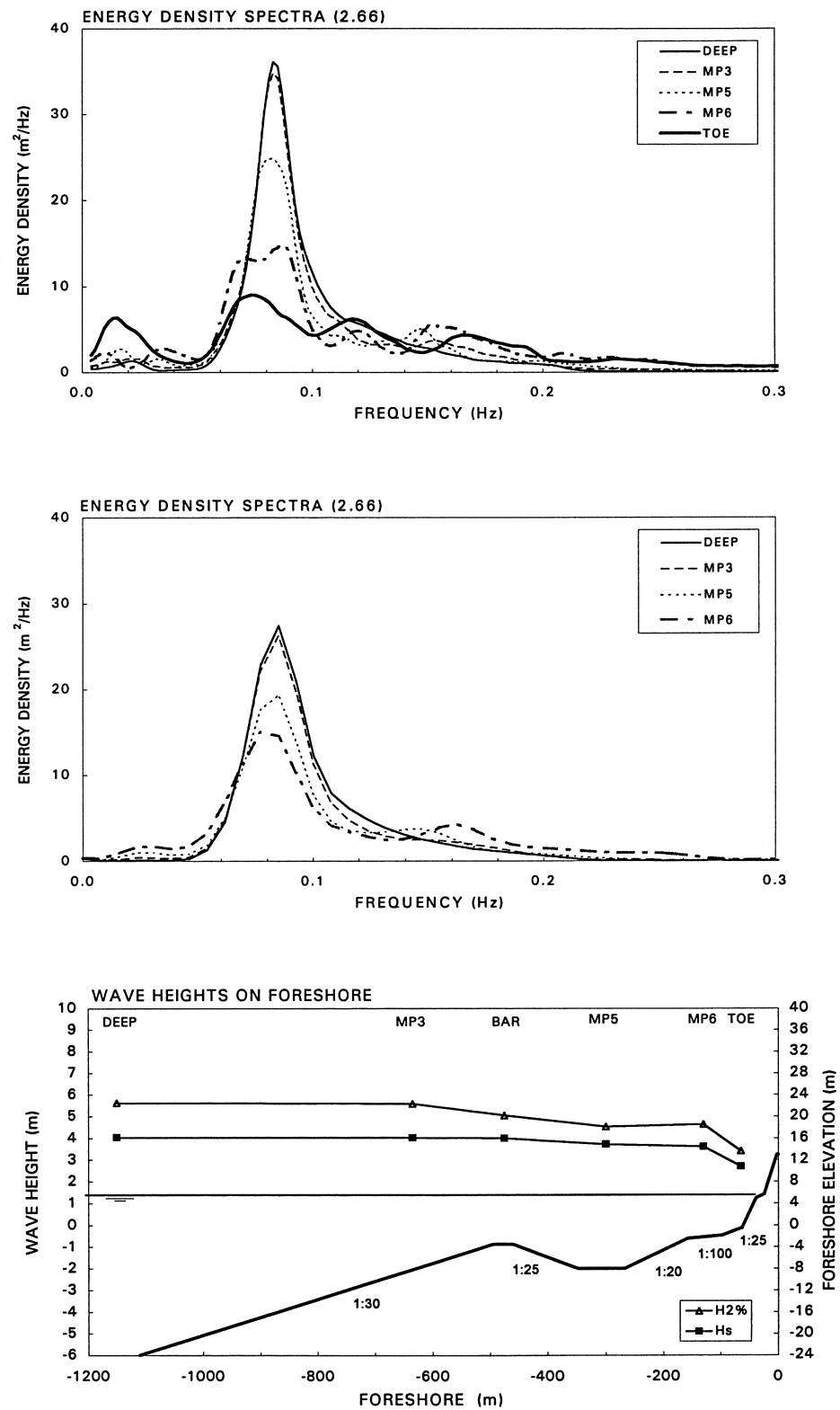


Figure F 2.66 Measured total wave energy spectra (upper), incident wave energy spectra (middle) and wave height evolution (lower).

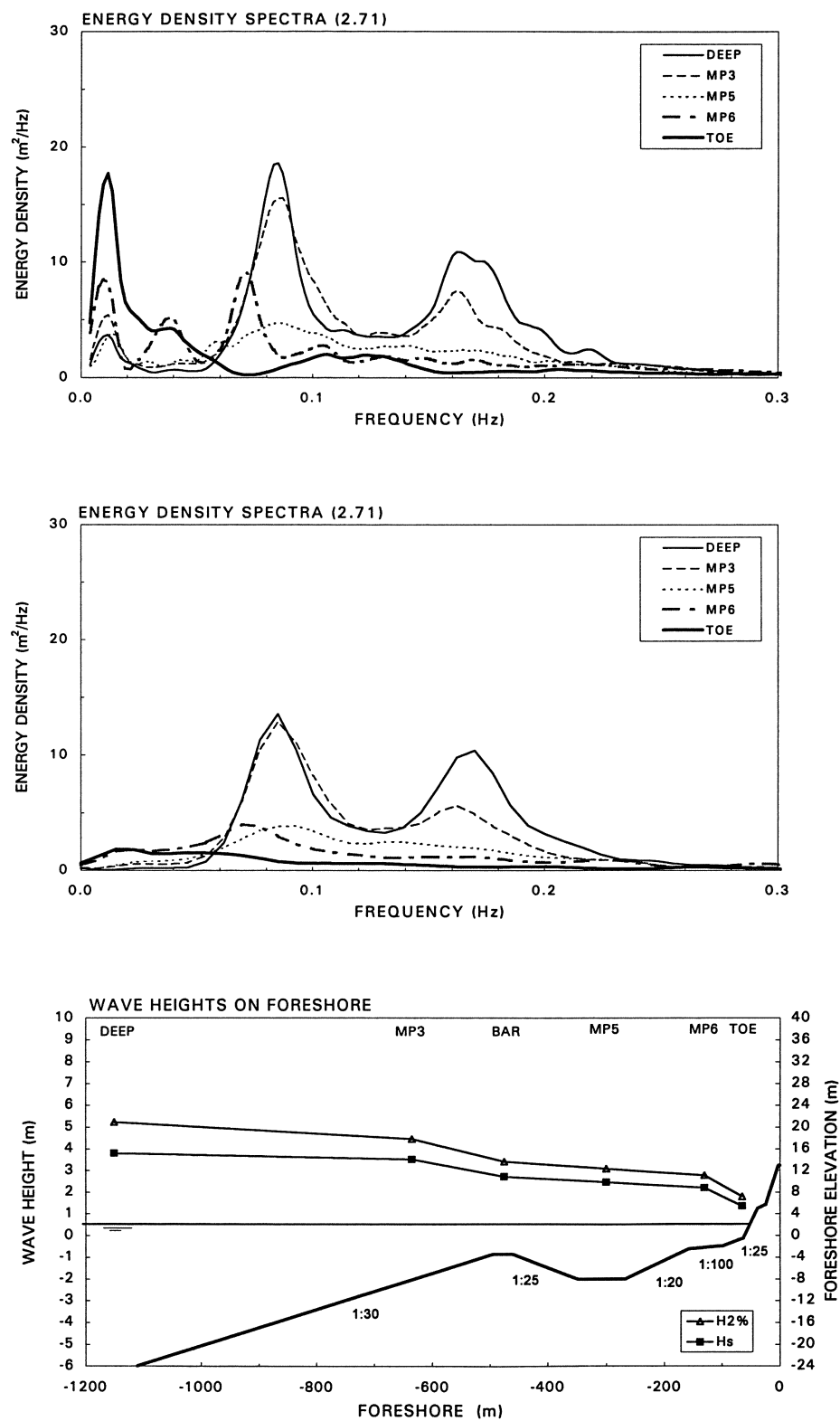


Figure F 2.71 Measured total wave energy spectra (upper), incident wave energy spectra (middle) and wave height evolution (lower).

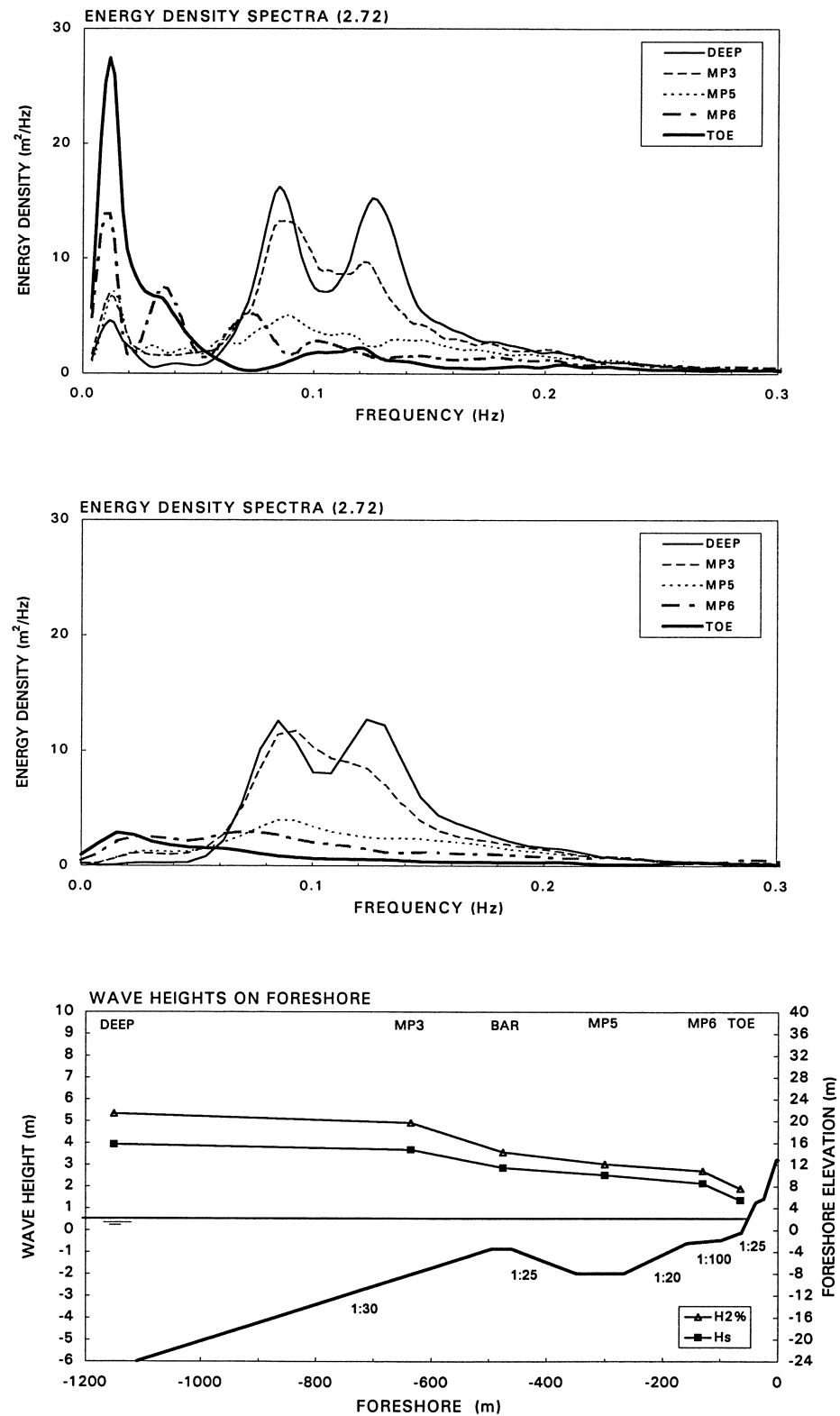


Figure F 2.72 Measured total wave energy spectra (upper), incident wave energy spectra (middle) and wave height evolution (lower).

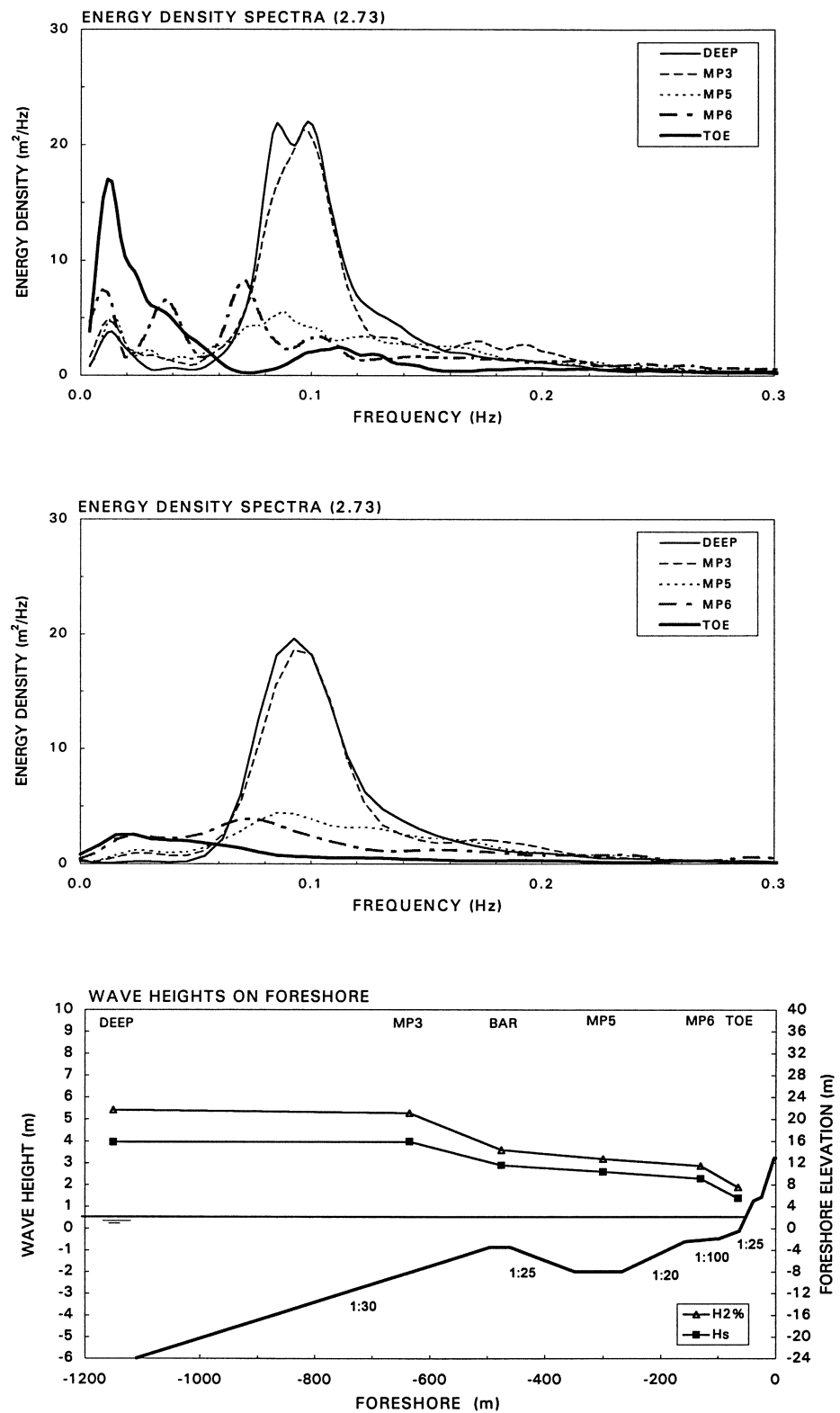


Figure F 2.73 Measured total wave energy spectra (upper), incident wave energy spectra (middle) and wave height evolution (lower).

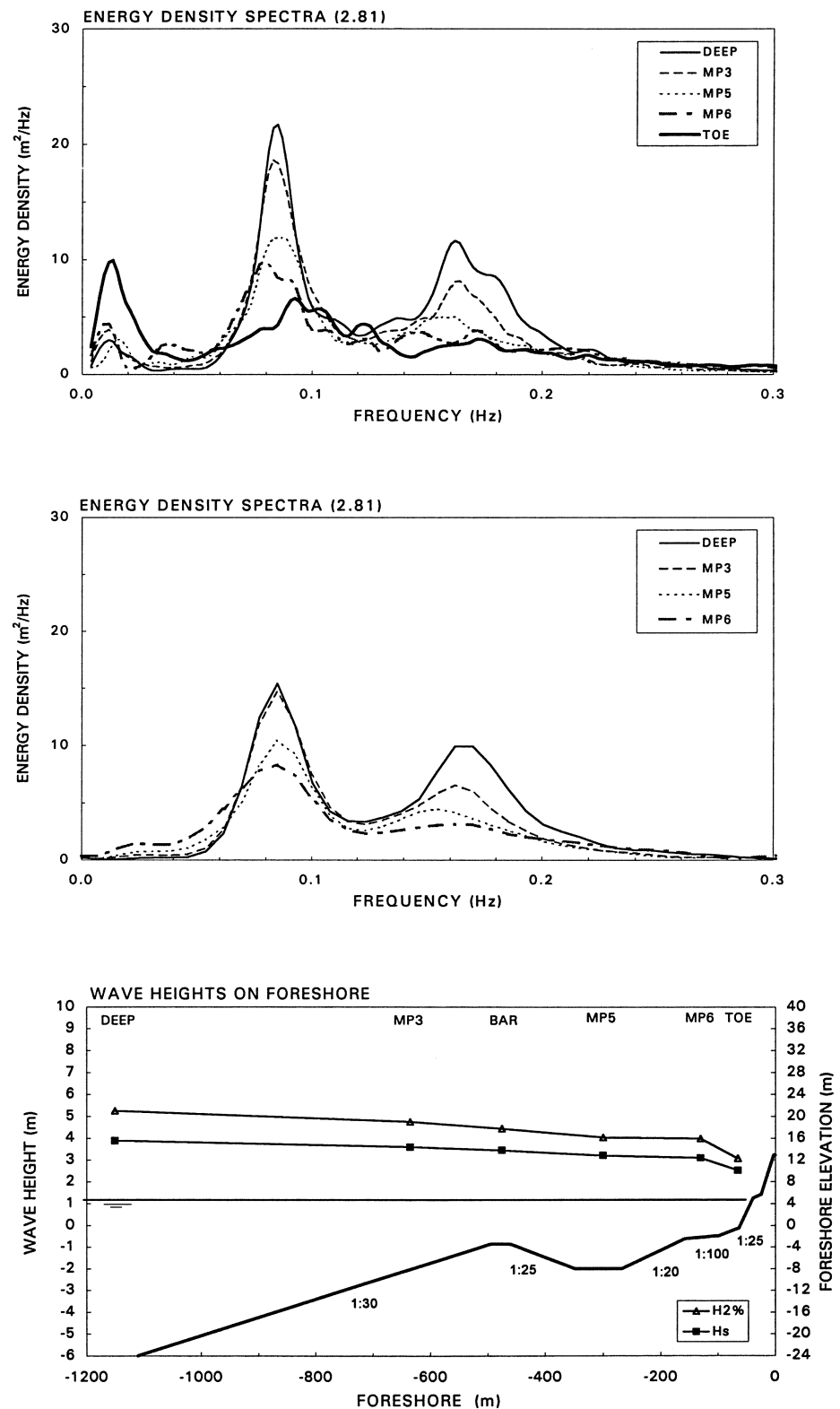


Figure F 2.81 Measured total wave energy spectra (upper), incident wave energy spectra (middle) and wave height evolution (lower).

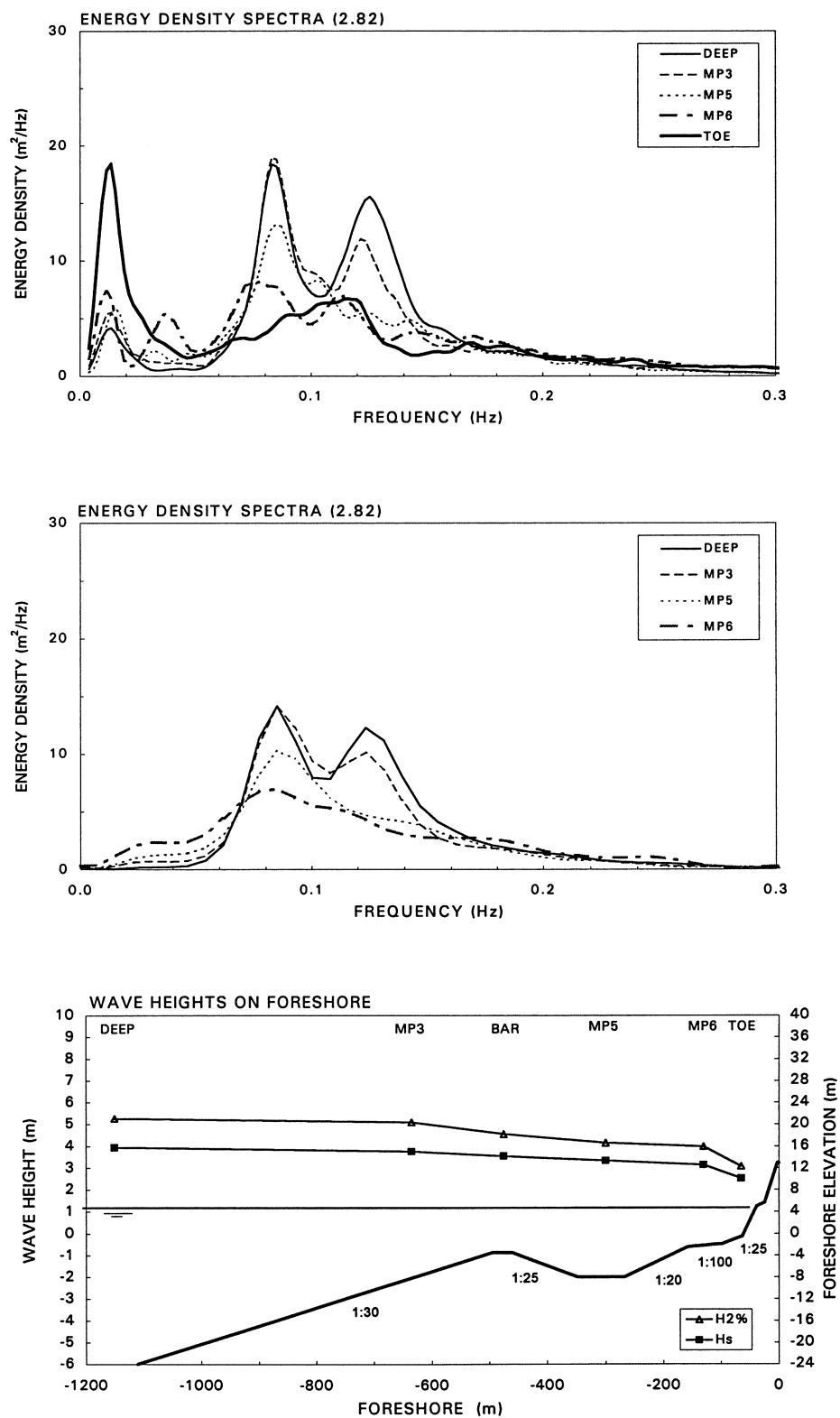


Figure F 2.82 Measured total wave energy spectra (upper), incident wave energy spectra (middle) and wave height evolution (lower).

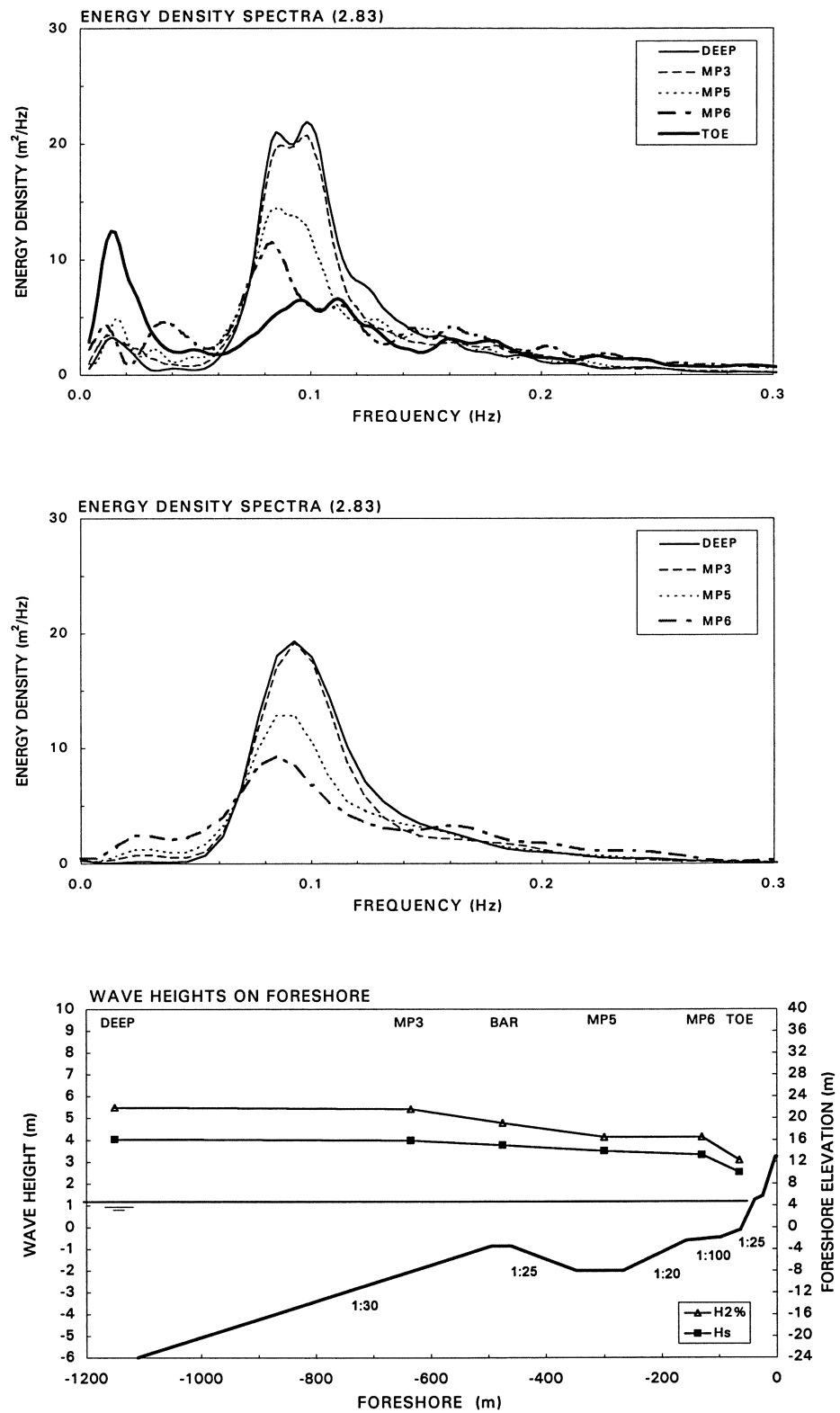


Figure F 2.83 Measured total wave energy spectra (upper), incident wave energy spectra (middle) and wave height evolution (lower).